THE EFFECT OF POLING STATE, SURFACE CHARGE, AND FREQUENCY OF VIBRATION OF PIEZOELECTRIC POLY (VINYLIDENE FLUORIDE) FILMS FOR BONE AND NEURAL TISSUE ENGINEERING APPLICATIONS

By

Rabab Chalaby

A dissertation submitted to the

School of Graduate Studies

Rutgers, The State University of New Jersey

In partial fulfillment of the requirements

For the degree of

Doctor of Philosophy

Graduate Program in Materials Science and Engineering

Written under the direction of

Dr. Ronke M. Olabisi

And approved by

_____

_____

_____

_____

New Brunswick, New Jersey

October 2018

ABSTRACT OF DISSERTATION

The Effect of Poling State, Surface Charge, and Frequency of Vibration of Piezoelectric Poly (Vinylidene Fluoride) Films for Bone and Neural Tissue Engineering Applications

BY RABAB CHALABY

Dissertation Director:

Ronke M. Olabisi

Novel paradigms for tissue engineering recognize the need for active or smart scaffolds in order to properly regenerate specific tissues. Electrical and electromechanical cues are the most relevant in promoting functionality in tissues such as nerve, muscle, and bone, among others. The existence of electrical phenomena within certain tissues may suggest the requirement of such phenomena (ie., electroactivity, piezoelectricity) during tissue regeneration. For instance, it has been shown that electrically charged surfaces can influence different aspects of cell behavior such as growth, adhesion, or morphology of different cell types, including osteoblast, neural, and muscular cells. Therefore, electroactive materials and, in particular, piezoelectric ones, show a strong potential for novel tissue engineering strategies. Piezoelectric materials have an interesting ability to vary surface charge when a mechanical load is applied, without the need for an external power source or connection wires, a feature that can be taken advantage of in novel tissue engineering strategies. Poly (vinylidene fluoride) (PVDF) is a semi-crystalline and biocompatible polymer with the largest piezoelectric response among piezoelectric polymers, mechanical properties appropriate for tissue engineering applications, and excellent electroactive properties such as piezo-, pyro and ferroelectricity. It was

hypothesized that by varying vibration frequencies in piezoelectric substrates, attached neuronal cells would respond with varying onsets of growth.

Since nerves innervate both bones and muscles, we further hypothesized that frequencies that promoted neural growth would also promote bone and muscle cell growth. The first aim of this study sought to investigate the effect of oscillating electric fields on a variety of mesenchymal tissues—human mesenchymal stem cells (hMSCs), bone (osteoblasts), and nerve cells by seeding them on poled and unpoled PVDF membranes and vibrating them at 20, 60, and 100 Hz. The results of this study indicated significant increases in osteogenic activity for both osteoblasts and hMSCs when subjected to mechanical vibration and the piezoelectric effect. Metabolic activity assays of hMSCs and osteoblasts verified that proliferation of both cell types was enhanced due to the piezoelectric effect of poled PVDF films but reduced in response to mechanical stimulation alone. Neurite imaging of undifferentiated and differentiated nerve cells revealed increases in neurite growth in response to mechanical and electrical stimulation.

Bone is itself piezoelectric, it follows that bone cells would respond to piezoelectric substrates. Nerves also come into direct contact with bone, thus it follows that the piezoelectric properties of bone also affect nerve cells. Therefore, the second hypothesis is that piezoelectric substrates with a surface charge most mimicking that of bone will promote increased adhesion and proliferation of bone and nerve cells. Thus, on the second aim of this dissertation is to examine the effect of stationary electric fields on a variety of mesenchymal tissues—human mesenchymal stem cells (hMSCs), bone, and nerve cells by seeding them on tissue culture polystyrene and three kinds of PVDF film surfaces: unpoled films with no surface charge, poled films with cells cultured on the positively charged side

of the sample, and poled films with cells cultured on the negatively charged side of the sample. The same methods that were used in investigating the effect of oscillating electric fields on cells were employed to observe how the stationary electric field affects cells differentiation and growth and at the same time points. The results showed a more homogeneous distribution of hMSCs and osteoblasts seeded on negatively poled PVDF films, but no osteogenesis. Metabolic activity assays of hMSCs and osteoblasts indicated that the highest number of viable hMSCs resulted on negatively poled PVDF films while the highest number of viable osteoblasts occurred on positively poled PVDF films. Finally, neurite imaging verified that charged piezoelectric PVDF membranes induce neurite outgrowth more than electrically neutral membranes in the absence of electrical stimulation.

The final goal of this study was to fully characterize the dynamics of the loading environment cells were subjected to, which has not been previously reported in PVDF cell studies, and to correlate the measurements to cell fate. Directly measuring PVDF and media displacement permitted calculation of the actual acceleration PVDF and cells were subjected to and illustrated that the cell culture media has a significant impact on the oscillating pressure imparted to the films and thus the piezoelectric output of the PVDF. From these measurements, it was possible to estimate the voltage output of the PVDF films, which for 100 Hz vibrations were in the physiological range of the action potentials that are experienced by excitable cells such as muscle and nerve. These results suggest a cause for the observed change in morphology of hMSCs towards neuronal cells. The results from this study may better define optimal stimulation parameters for desired cell fate and has already resulted in unexpected and new findings not yet reported in the literature.

DEDICATIONS

In life's journey, I got such an amazing gift, supporting me in my pain and my happiness. A handsome man called husband. To "Hamza", I am grateful to you forever, I love you…

To my kids, I am the luckiest woman to have wonderful boys who make me smile all the time and give me tremendous strength for their being in my life…

To my parents, the two persons who believe in me more than I believe in myself, you make my life fruitful…

To my angel, my brother, your pure smile awards me a big joy…

To my advisor, professor Olabisi, you were a sister to me through my time in the United States, the sister whom when I talk to, I get all the therapy that I need, I will miss you and keep you in my praying…

ACKNOWLEDGEMENTS

Working as a Ph.D. student at Rutgers was an unprecedented, magnificent, and challenging experience to me. For more than six years, I have met many people who were instrumental directly or indirectly in shaping up this project. First and foremost, my deep gratefulness and appreciation goes out to my awesome advisor Dr. Ronke M Olabisi. Thanks is not a sufficient word for all the guidance and support that you kindly awarded me, still and will, award. Thank you, professor, for making sure I am doing well while I am away from my family. I am super lucky to have the best supervisor that anybody can ask for. I always ask myself, how would my life be here, away from my family if I did not meet you?! I am also grateful to my other committee members Dr. Kimberly Cook-Chenault, Dr. Laura Fabris, Dr. Lisa Klein, Dr. Adrian Mann, big thanks for their advice, understanding and encouragement. I have to thank the Iraqi Government and the Department of Biomedical Engineering for their funding support, special thanks to Dr. David Shreiber, Dr. Joseph Freeman, and Mr. Lawrence Stromberg (Larry) for helping me successfully navigate through fellowships and administrative requirements. I am also thankful to the Materials Science and Engineering Department for their support and guidance. I am really grateful to the Olabisi lab members, past and present, for their endless support. Kristopher White, I will never forget how much time you spent on me, you are a big help. I would also like to thank Paulina Krzyszczyk, she was the first person after Dr. Olabisi to guide me in starting my first steps in the Olabisi lab.

My unique and lovely husband, thank you for supporting my dreams. Thank you for being patient with me, I know I gave you a hard time at moments, you are my hero.

PUBLIC PRESENTATIONS

A portion of this dissertation and related research has been presented at a scientific conference.

Conference presentation:

K Sheehan, R Chalaby, R Olabisi, "The Effect of Piezoelectricity on Human Mesenchymal Stem Cell Differentiation," The Biomedical Engineering Society Annual Meeting, Phoenix, AZ, Oct 11-14, 2017

TABLE OF CONTENTS

TABLE OF FIGURES

LIST OF ABBREVIATIONS

BMU	Basic Multicellular Unit
cAMP	Cyclic Adenosine Monophosphate
CNS	Central Nervous System
DNA	Deoxyribonucleic Acids
DRG	Dorsal Root Ganglions
FDA	Food and Drug Administration
hMSC	Human Mesenchymal Stem Cell
MSCs	Mesenchymal Stem Cells
NGF	Nerve Growth Factor
PEG	Poly (Ethylene Glycol)
PGA	Poly (Glycolic Acid)
PLA	Poly (Lactic Acid)
PLGA	Poly (Lactic-Co-Glycolic Acid
PNS	Peripheral Nervous System
PTFE	Poly (Tetra Fluoro Ethylene)
PVDF	Poly (Vinylidene Fluoride)
PVDF-TrFE	Poly (Vinylidene Fluoride Tri- Fluoroethylene
VDF- TrFE	Vinylidene Fluoride Tri- Fluoroethylene

CHAPTER 1: BACKGROUND AND INTRODUCTION

1.1 TISSUE ENGINEERING

Tissue engineering seek to replace or facilitate the regrowth of damaged or diseased tissue by applying a combination of biomaterials, cells and bioactive molecules [1]. Every day, thousands of clinical procedures are carried out to replace or repair tissues in the human body that have been damaged through trauma or disease. For instance, the current approach to reconstruct breast tissue due to cancer includes reconstructive surgery utilizing autologous tissue flaps, or implants of synthetic materials such as silicone. The damaged tissue is generally replaced by using donor graft tissues (autografts, allografts, or xenografts), but the main problems associated with this are a shortage of donors or autologous donor sites, transmission of disease, rejection of grafts, donor site pain and morbidity, the volume of donor tissue that can be safely harvested, and the possibility of harmful immune responses [2]. In contrast to replacing damaged tissues with grafts, tissue engineering, or regenerative medicine, aims to regenerate damaged tissues by developing biological substitutes

approach for breast reconstruction includes a combination of a patient's own cells with polymeric scaffolds [5]. Or in coronary artery disease, arteriosclerosis can occlude arteries to the point that they are no longer patent. The current standard is to harvest veins such as the saphenous vein to replace the blocked artery. Rather than harvest healthy vessels, blood vessel tissue engineering attempts to regrow vessels by seeding the lumen of scaffolds comprised of natural biologic and /or synthetic materials with endothelial cells [6]. The organs or tissues targeted for regeneration by tissue engineering and regenerative medicine

include breast for reconstruction blood vessel, heart valve, cornea, pancreas, liver, genitourinary tissue, bone, cartilage, tendon, ligament, periodontal and neural tissue for nerve regeneration. In the last two decades, the research and development among the scientific community in this emerging field of tissue engineering and regenerative medicine has progressed at a rapid rate [7].

Tissue engineering often relies on scaffolds for supporting cell differentiation and growth. Scaffolds optimized for tissue engineering should possess the following attributes:

1. Mechanical properties that are sufficient to shield cells from tensile forces without inhibiting biomechanical cues;
2. The desired volume, shape, and mechanical strength [8];
3. Acceptable biocompatibility;
4. A highly porous and well-interconnected open pore structure to allow high cell seeding density and tissue in-growth;
5. Bioadsorption at predetermined time periods;
6. Biocompatible chemical compositions of both the materials and their degradation products, causing minimal immune or inflammatory responses [9]; and
7. A physical structure to support cell adhesion and proliferation, facilitating cell–cell contact and cell migration [10]

Tissue engineering technologies involve the successful interaction between three components: (1) the scaffold that holds the cells together to create the tissue's physical form; (2) the cells that create the tissue; and (3) the biological signaling molecules, such as

growth factors, that direct the cells to express the desired tissue phenotype (Figure 1.1) [11].

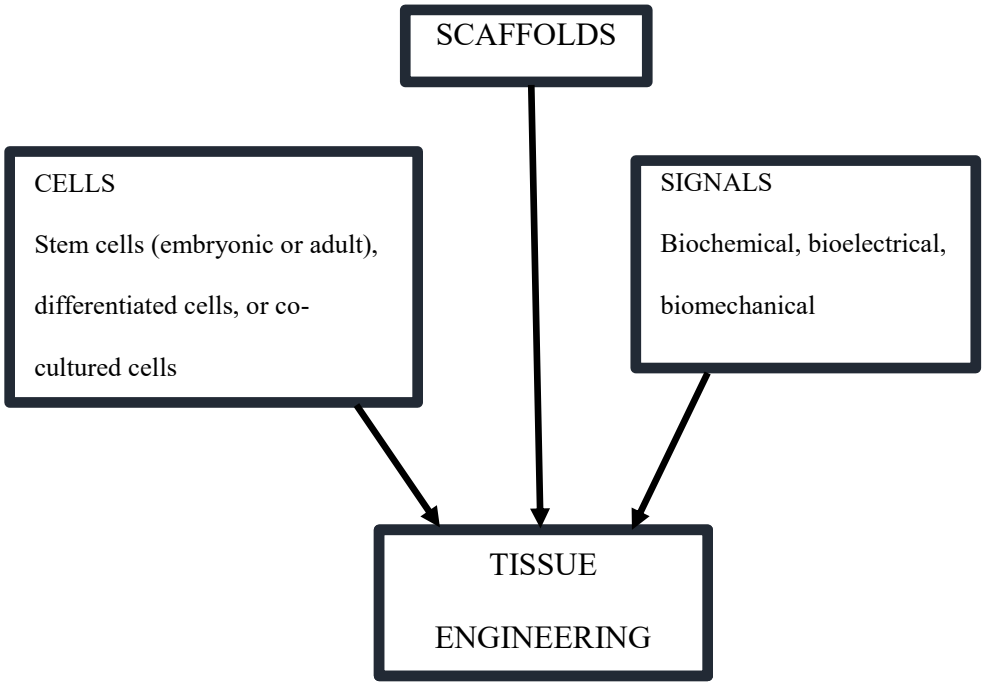

Figure 1.1: The tissue engineering paradigm [11].

Much of the research surrounding tissue engineering approaches is focused on the materials that serve as the scaffolds. Biodegradable polymers provide a surface for the adhesion of cells in a three-dimensional structure, which plays an important role in cell interaction and tissue specific gene expression. Their porous structure allows delivery of sufficient nutrient, waste removal and gas exchange, and ingrowth of host tissue [12]. Scaffolds have been fabricated from naturally derived materials, synthetic polymers, and cellular tissue matrices [13, 14]. Often, the scaffold material can be selected to direct the differentiation of mesenchymal stem cells, which are often used in tissue engineering applications. This approach has been met with varying success, depending on the tissue.

A particular challenge for regenerative medicine and tissue engineering strategies is the damaged nervous system applications. After transection of nerves due to traumatic injury, the axon distal to the lesion becomes disconnected from its neuronal cell body and degenerates in a manner called Wallerian degeneration. This occurs in both the central nervous system (CNS) and peripheral nervous system (PNS). After spinal cord injury, spinal cord parenchyma involving glial and neuronal cells is lost. Long descending projection axons from the motor cortex (corticospinal tract) and subcortical regions, ascending sensory projections, and projections spanning a shorter distance may be transected completely, depending on the lesion severity. Ultimately a cystic lesion defect will develop at the site of injury. The spinal cord lacks the intrinsic capacity to replace organotypic tissue and instead produces nonfunctioning scar, which, besides a concomitant expression of growth inhibitory factors and a lack of growth promoting factors, represents the major factor contributing to the failure of CNS axons to regenerate [15]. Substantial progress in replacing the lesion defect and subsequently promoting axonal regeneration has been achieved through cell transplantation strategies. Specific primary cell populations replace lost spinal cord parenchyma and provide a growth permissive substrate for regenerating axons [16]. Despite initial promising results, cell transplantation approaches either do not promote axon regeneration in a directed rostro-caudal, or superior-inferior, fashion for proper reconnection of disrupted axon pathways.

Electrical and electromechanical cues are the most relevant in promoting functionality in certain tissues such as nerve, muscle, and bone. Novel paradigms for tissue engineering recognize the need for active or smart scaffolds in order to properly regenerate specific

tissues. The existence of electrical phenomena within certain tissues may suggest the requirement of such phenomena (ie., electroactivity, piezoelectricity) during tissue regeneration [1]. For instance, it has been shown that electrically charged surfaces can influence different aspects of cell behavior such as growth, adhesion, or morphology of different cell types, including osteoblast, neural, and cardiac cells. Therefore, electroactive materials and, in particular, piezoelectric ones, show strong potential for innovative tissue engineering approaches. Piezoelectric materials have an interesting ability to vary surface charge when a mechanical load is applied, without the need for an external power source or connection wires, a property that can be taken advantage of in novel tissue engineering strategies [17].

1.2 PIEZOELECTRIC EFFECT IN THE HUMAN BODY

Bio-piezoelectricity can be thought of as an extended property of living tissue, where it plays a significant role in several physiological phenomena [2]. Piezoelectricity can thus be found in different parts of the human body such as bone, tendon, ligaments, cartilage, skin, dentin, collagen, deoxyribonucleic acids (DNA), and conceivably, in cell membranes [2,6]. The first study proposing the piezoelectric property of bone was in 1955 [4]. A few years later, electric currents in bone and the generation of electric potentials when bone is mechanically stressed were verified [7,18]. This phenomenon, recognized as piezoelectricity, is independent of cell viability. According to Wolff's law, mechanical stress produces electrical signals and these signals act as the stimulus that promotes bone growth and remodeling [19]. Mechanotransduction describes the cellular action of converting mechanical stimuli into electrochemical responses. It has been hypothesized

that piezoelectricity plays a role in certain types of mechanotransduction. It has also been suggested that the action of piezoelectric signals may function to alter the chemistry of pertinent macromolecules, such as collagen, or to influence cellular activity directly [20]. The influence of electrical stimulation on bone healing has been studied *in vitro* [21, 22] and *in vivo* [23, 24] and it has been demonstrated that the application of such electrical stimuli can enhance and stimulate osteogenic activity. Wolff's law demonstrates that mechanical stimuli do the same. Thus, osteoblasts are directed by both electrical and mechanical signals to deposit bone tissue [25, 26], reflecting both the piezoelectric nature of bone and the mechanotransduction of these signals.

1.3 POLYMERS FOR TISSUE ENGINEERING

Piezoelectric polymeric materials have been considered in tissue engineering applications. These materials generate transient surface charges in response to tiny mechanical deformations of the material under minute mechanical strain and do not require additional energy sources or electrodes. Poly (vinylidenefluoride) (PVDF) is a synthetic, semicrystalline polymer with piezoelectric properties that generates transient surface charges due to its unique molecular structure [27]. Studies exploring the use of piezoelectric polymers for tissue engineering applications are mostly devoted to bone, muscle and neural regeneration (Table 1.1).

Table 1.1: PVDF scaffold designs and cells used for different biomedical applications.

Applications	Material type	Scaffold design	Cell types used
Bone tissue engineering	PVDF and copolymer	Films	MC3T3-E1 [28]; Goat marrow stromal cells into osteoblast [17,29]
		Fibers	Human mesenchymal stem cells (MSCs) [30]
		Blends membranes (porous)	NIH3T3 mouse fibroblast [31]
Muscle regeneration	PVDF	Films	C2C12 myoblast [32]
		Fibers	C2C12 myoblast [32]
		Fibers, meshes	In vivo study in rabbits [33,34]
Neural regeneration	PVDF	Films	Mouse neuroblastoma cells (Nb2a) [35] Spinal cord neurons [36]
		Blends membranes (porous)	Dense and microporous membranes: neuronal cells [37]
		Channels/Tubes	Nerve guidance channels: in vivo assay: mouse sciatic nerve model [38]; Tube containing nerve growth factor (NGF) and Collagen gel: in vivo assay: Wistar rats [39].

Damaraju et al. examined piezoelectric scaffolds for bone tissue engineering applications. PVDF fibers were produced and their effect on biological function was studied with seeded human mesenchymal stem cells (hMSCs) [40]. They established that the cells attach to the PVDF fibers and result in higher alkaline phosphatase activity (a marker of osteogenic activity) and early mineralization when compared with controls, showing the potential for the use of PVDF scaffolds for bone tissue engineering applications. Using MC3T3-E1 cells (an immortalized murine preosteoblast line), it has been demonstrated that the charge surface of PVDF influences cell viability and proliferation, with increases of both when

seeded on poled (larger net surface charge) than on non-poled films (where the charge distribution is not homogeneous) [17]. In another study, the influence of polarization and morphology of electroactive PVDF on the adhesion and morphology of myoblasts was examined [41]. It was shown that negatively charged surfaces improve cell adhesion and proliferation and that directional growth of the myoblasts could be achieved by culturing these cells on aligned fibers.

When nerve regeneration was investigated with poly (vinylidene fluoride trifluoroethylene) (PVDF-TrFE), neurites attached and extended radially on the randomly aligned fibers, whereas the aligned fibers directed aligned neurite outgrowth, demonstrating the potential of this material for neural tissue engineering [42, 43]. Microporous PVDF membranes were fabricated for neural tissue engineering by covalently immobilizing L-lysine on the surface of the membranes. PC12 cells (a cell line containing a mixture of neuroblastic cells and eosinophilic cells derived from a pheochromocytoma of the rat adrenal medulla with an embryonic origin from the neural crest) cultured on these L-lysine/PVDF membranes showed good cell adhesion and proliferation, suggesting the membrane's usefulness in the development of strategies to promote the regrowth and regeneration of nervous tissue [44]. Piezoelectric nerve guidance channels were fabricated using PVDF and evaluated in a transected mouse sciatic nerve model. The results showed that these nerve channels enhanced peripheral nerve regeneration and served as a tool to investigate the influence of electrical activity on nerve regeneration [45]. In yet another study, researchers developed tubular nerve guides using a vinylidenefluoride–trifluoroethylene (VDF-TrFE) copolymer synthesized by a melt–erosion process.

Piezoelectrically active VDF-TrFE copolymer tubes were found to significantly enhance the nerve regeneration process [46]. Enhanced neurite outgrowth has been attributed to the presence of piezoelectric surface charges and transient charge generation [47].

1.4 POLY (VINYLIDENE FLUORIDE) POLYMER

Poly (vinylidene fluoride) (PVDF) and its copolymers have unique electrical and physicochemical properties, making them the most commonly used fluorinated polymers for an increasing number of advanced applications [48, 49]. PVDF is an extremely non-reactive, semi-crystalline polymer specified by long chain macromolecules, and consists of approximately 59 wt.% fluorine and 3 wt.% hydrogen, obtained through the polymerization of the monomer vinylidene fluoride. The backbone of PVDF, the vinylidene fluoride monomer, CH2═CF2, was first synthesized in 1901 by Swarts [68]. Vinylidene fluoride is relatively stable, no inhibitor is needed to prevent spontaneous polymerization. More reactive fluorocarbon monomers such as trifluorethylene and tetrafluoroethylene are normally stored and handled in the presence of inhibitors. Vinylidene fluoride is a member of the fluorinated ethylene series and includes the following [69]:

CH2═CH2 Ethylene

CHF═CH2 Fluoroethylene (vinyl fluoride)

CH2═CF2 Difluoroethylene (vinylede fluoride)

CHF═CF2 Trifuoroethylene

CF2═CF2 Tetrafluoroethylene

Different conformational structures of PVDF can be obtained depending on polymerization reaction and crystallization conditions. The temperature at which the reaction occurs is recognized as a key factor in the process, influencing the content of head-to-head chains in the polymer and its crystallinity [50, 51]. At least five polymorphic modifications can be found in the PVDF crystalline phase (identified as α, β, γ, δ, and ε), which are distinguished by the conformational structure of the chains and the macromolecule packing in the unit cells of their crystallites. The different chain conformations are designated as all trans (TTT) planar zigzag for the β-phase, TGTG' (trans-gauche-trans-gauche) for the α- and δ-phases, and T3GT3G' for the γ- and ε-phases [52, 53]. As illustrated in Figure 1.2, in which the most investigated and used PVDF phases are depicted, the position of the fluorine atoms in the molecular chain instructs the phase of the polymer. The high electronegativity of fluorine atoms generates a strong electrical dipole moment of the monomer unit [54, 55]. The β- and γ-phases have the highest dipolar moment per unit cell and therefore are known to possess piezoelectricity, while the other three phases (α, δ, and ε) are apolar due to antiparallel packing of dipoles within the unit cell [56]. The α-phase of PVDF can be transformed into the β-phase and, thus, into the electroactive phase by an additional treatment such as stretching, high pressure or polarization, while melt crystallization may lead back to the formation of the polar α-phase [57].

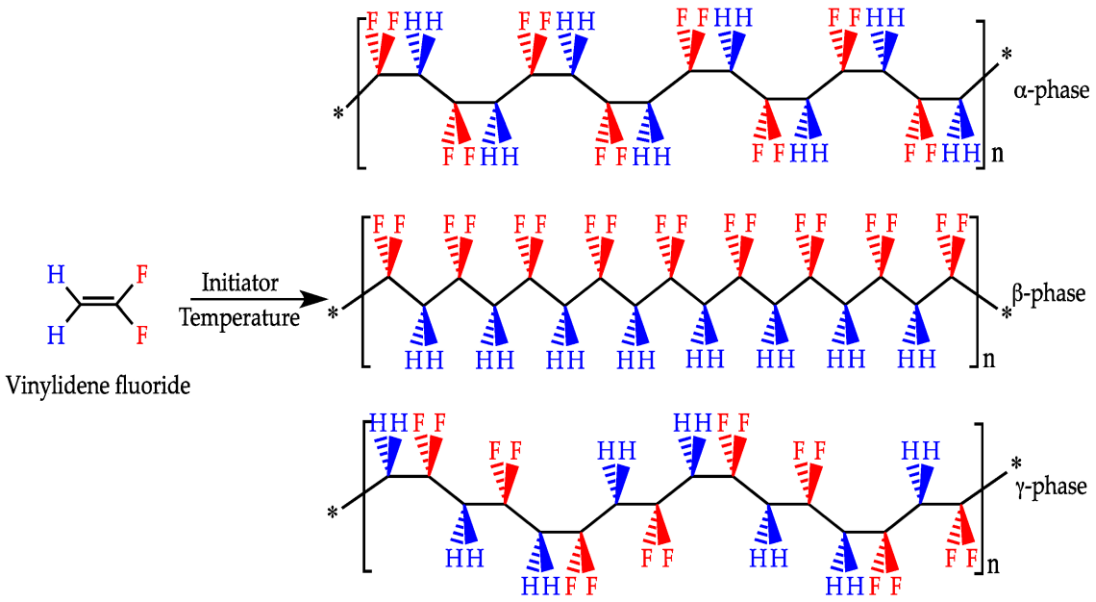

Figure 1.2: Schematic representation of the chain conformations of the α, β, and γ phases of PVDF [58].

Each phase of PVDF gives different properties to the polymer but other characteristics such as the molecular weight, molecular weight distribution, and extent of irregularities along the polymer chain also play an important role in polymer properties. The most widely investigated properties of PVDF are its piezoelectricity, its large dielectric constant, and its pyroelectric and ferroelectric effect. Properties such as improved mechanical strength, creep resistance, and wear resistance when compared with other fluorinated polymers such as PTFE, have also been investigated [59]. These properties are very important when considering the development of smart materials for advanced applications [60, 61]. Piezoelectric materials can react to changes in their environment, converting electrical energy to mechanical energy, and vice versa. This means that under mechanical impulses the charge at the surface of a piezoelectric material varies without the need for an additional

energy source or electrodes [62]. This strategy has been applied in tissue engineering applications for the development of scaffolds that support the growth, proliferation, and differentiation of different cell types such as osteoblasts, myoblasts and fibroblasts [63, 64]. PVDF also shows pyroelectricity that indicates the capability of PVDF to generate electricity in response to the application of heat or vice versa. As a ferroelectric material, PVDF also shows a spontaneous electric polarization that can be switched by the application of an external electric field, resulting in a polarization-field hysteresis loop [65]. Due to their robust electroactive properties, materials comprising the β- and γ-phases of PVDF are the most sought after for advanced applications; the higher the piezoelectric response, the better for many applications, thus, strategies to improve this response have been widely investigated. One of the approaches to improve the piezoelectric response involves the development of PVDF copolymers. Though the fact that copolymer unit structures are less polar than those of pure PVDF, some copolymers show a higher crystallinity, resulting in higher overall piezoelectric responses [66]. Other properties, such as glass transition temperature, melting point, stability, elasticity, permeability, and chemical reactivity may also be changed as a result of copolymerization [67].

1.5 BONE

Bone is a specialized form of connective tissue that functions both as a tissue and an organ system, being the component of the skeleton that is committed with the protection, support and motion of the entire organism. Bone is a natural composite, with hard mineral elements and compliant protein components. The mineral/organic combination imparts a stiffness and toughness that allows for the protection of vital organs, e.g. skeletal components of the

rib cage and vertebrae protect the heart, lungs and other organs and/or tissues in the thoracic cavity. Bone's stiffness also contributes to the maintenance of the structural support and mechanical action of muscles and tendons, which are broadly responsible for movement. At the cellular level, bone is a productive and metabolically active biological entity, i.e. bone is continually undergoing turnover to repair microstructural damage incurred through normal daily activities. Further, bone marrow lies within the trabeculae of cancellous bone and is a major locus of cell proliferation and differentiation, including hematopoietic processes. In addition to its structural functions and biological activities, bone serves a critical role in homeostatic regulation by acting as a reservoir for calcium and phosphate ions.

By weight, bone contains approximately 70% mineral, 8% water, and about 22% collagenous matrix, and the interactions of these constituents play major roles in determining the mechanical behavior of bone [70]. At the macroscopic level, mature bone can be classified into two architectural forms: trabecular (cancellous or spongy) and cortical (compact), Figure 1.3 [71]. The trabecular bone is commonly found in the vertebral bodies and the epiphyses of long bones, covered by cortical bone. Cortical bone is the predominant bone in the body and is found in long, short, and flat bones [72].

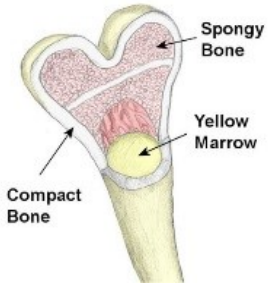

Figure 1.3: Bone at a macroscopic level.

1.5.1 Bone Cells

Several cell types comprise and maintain bone, including osteoblasts, osteoclasts, bone lining cells, and osteocytes. Together these cells play essential role in bone formation, maintenance, and remodeling, and are illustrated in Figure 1.4.

Osteoblasts, osteocytes and bone lining cells originate from mesenchymal stem cells (MSCs), whereas osteoclasts originate from hemopoietic stem cells. Osteoblasts are fully differentiated cells and their function is to synthesize the organic component of bone matrix and to regulate the formation of hydroxyapatite crystals in the newly formed bone. Osteocytes are mature osteoblasts trapped in the lacunae within the bone matrix. These cells are thought to communicate with neighboring osteocytes information about the stress state of the surrounding bone, and are thereby responsible for the matrix maintenance, build-up, and breakdown. Bone lining cells cover the bone surfaces that are not undergoing bone formation nor remodeling. Similarly, to osteocytes, they have less cytoplasm and fewer organelles than osteoblasts. These cells regulate the transport in and out of the bone. Beyond transport functions, the role of these cells still remains relatively unclear, although it is accepted that they, together with the osteocytes, sense the mechanical load in the bone, which leads to bone remodeling. Osteoclasts are large, multinucleated cells, which carry out the resorption of bone by dissolving the minerals and digesting the bone matrix through osteocytic osteolysis. Osteoclasts are the agents that release calcium and phosphate ions from the bone to maintain homeostasis of these ions in the blood. Bone resorption occurs at a specialized osteoclastic cell membrane called the ruffled membrane. This forms a

sealing zone between the bone and the osteoclast into which degradation products are released [73].

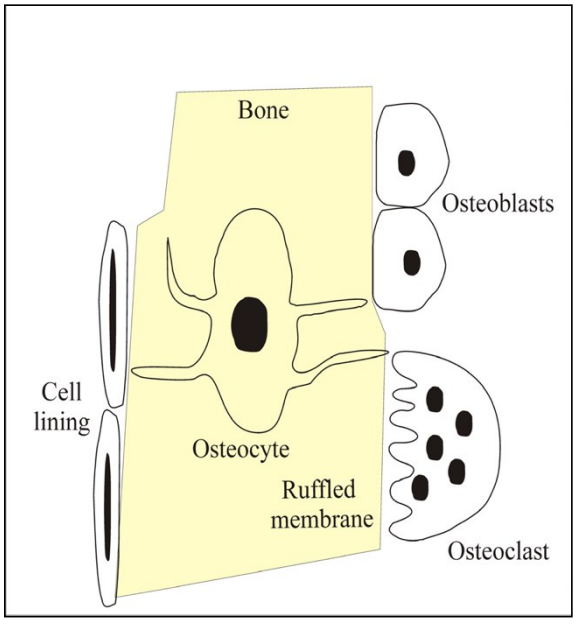

Figure 1.4: Schematic illustration of the different types of cells present in bone: osteoblasts, osteoclasts, osteocytes and bone lining cells [73].

1.5.2 Bone Modeling and Remodeling

Throughout life, bone undergoes a highly dynamic and complex process involving two important mechanisms, bone modeling and remodeling. Bone modeling is crucial for growth and adaptation of the skeleton to mechanical forces and stresses. During bone modeling, bone formation and resorption occur independently at distinct anatomical sites [74, 75]. It is a process that takes place less often in adults than bone remodeling [76]. Bone remodeling is the process by which old and damaged bone is removed and repaired [77]; it plays an important role in maintaining bone strength and mineral homeostasis. This process undergoes four sequential steps in a well-organized cycle as indicated in

Figure 1.5: (1) Activation which initiates the recruitment and activation of mononuclear osteoclast precursors, (2) resorption through osteoclasts activation, (3) reversal in which resorption transits to formation and (4) formation of bone through osteoblast activation. The temporary anatomical structure, which results of the coordination between osteoclast, osteoblasts, osteocytes and bone lining cells, is called the basic multicellular unit (BMU) [74, 75].

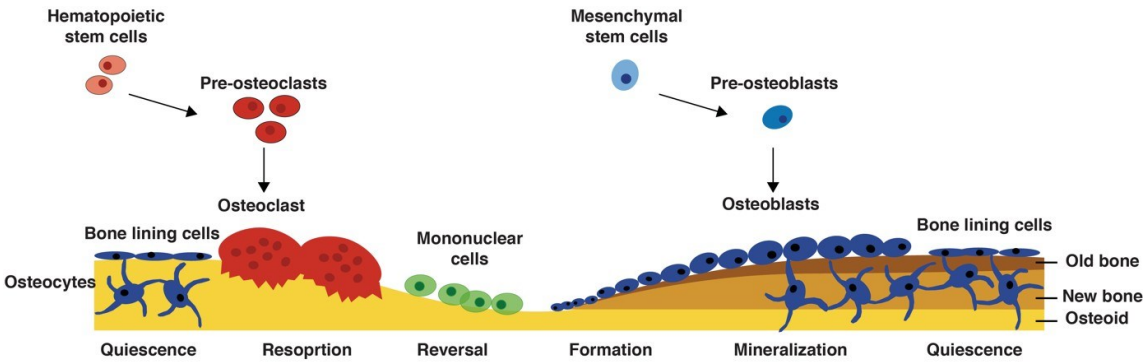

Figure 1.5: The bone remodeling process [78].

1.5.3 Cells for Bone Tissue Engineering

The outcome of bone tissue engineering is influenced not only by the scaffolding but also by the type of cell selected for bone regeneration. The ideal cell source should be easily expandable to higher passages, non-immunogenic and have a protein expression pattern similar to the tissue to be regenerated. Use of autologous cells circumvents the risks of immunological incompatibility and transmission of infection. The stem cells located in the bone marrow, known as mesenchymal stem cells (MSCs), have been used in experimental BTE. Besides their differentiation potential, MSCs have other important properties and can be expanded extensively *in vitro* [79]. They are the body's repair cells and express a variety

of growth factors. As well as bone-marrow derived MSCs, other osteogenic cells with potential application for bone include mesenchymal cells derived from the periosteum or adipose tissue, and fully differentiated osteoblasts [80]. Experimentally sourcing osteogenic cells from alveolar bone obtained during routine surgery offers two important advantages: first the cells are readily harvested by biopsy and second the procedure causes minimal damage at the donor site.

1.6 NERVOUS SYSTEM

The nervous system is divided into two parts, the central nervous system (CNS) which contains the brain, spinal cord, optic, olfactory and auditory systems and the peripheral nervous system (PNS) which is a collective term for the nervous system structures that do not lie within the CNS.

1.6.1 Neural Cells

Neurons are the basic structural and functional elements of the nervous system and consist of a cell body, termed soma, and its extensions, the axons and dendrites. Neurons send signals to other cells as electrochemical waves travelling along thin fibers called axons, which cause chemicals called neurotransmitters to be released at junctions called synapses (Figure 1.6). A cell that receives a synaptic signal may be excited, inhibited, or otherwise modulated. Sensory neurons are activated by physical stimuli impinging on them and send signals that inform the central nervous system of the state of the body and the external environment. Motor neurons situated either in the central nervous system or in peripheral ganglia connect the nervous system to muscles or other effector organs.

Central neurons, which in vertebrates greatly outnumber the other cell types, only connect to other neurons. Neurons can be distinguished from other cells in a number of ways; their communication with other cells via synapses is a fundamental feature, in addition to rapid transmission of electrical and chemical signals via membranes. Many types of neurons possess an axon, a protoplasmic protrusion that can extend to distant parts of the body and make thousands of synaptic contacts. In the body axons frequently travel in bundles called nerves. These nerves include sensory and motor neurons that transfer physical stimuli into neural signal and neural signal into activity respectively. The neurons receive their input from other neurons and give their output to other neurons.

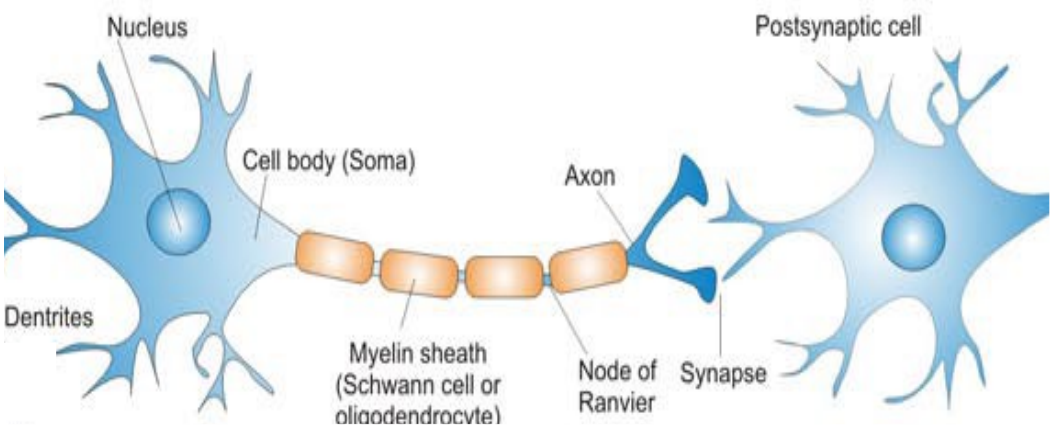

Figure 1.6: Schematic drawing of a neuron and its connection to a postsynaptic cell [81].

1.6.2 Response of PNS and CNS to Injury

Traumatic injury, as well as degenerative diseases, can considerably alter the architecture and function of peripheral and central nerves. Though neurons and glia function similarly to propagate electrochemical signals in the PNS and CNS, these cells possess dramatically different regenerative responses after injury that depends on their environment. Though

CNS neurons were previously believed to be incapable of regeneration, it was shown that neuronal sprouting occurred from an injured spinal cord into a peripheral nerve graft, therefore indicating the role of environment in CNS regeneration [82]. Increasing evidence supports the observation that the regenerative ability of the nerve is highly influenced by permissive and non-permissive cues in the environment. The different abilities of the CNS and PNS to promote growth may be attributed to the following: 1) in the PNS, the role of Schwann cells in providing trophic factors; 2) in the CNS, the presence of myelin and myelin-associated inhibitors [83]; 3) the suppression of apoptotic pathways and activation of anti-apoptotic proteins [84]; and 4) the effect of the glial scar in spinal cord injury.

A myriad of neural cell-types, as well as cells of the inflammatory system, are involved in responses after PNS injury. Upon transection of a nerve, the distal portion of the nerve begins to degenerate due to protease activity and separation from the cell body or soma (Figure 1.7). The proximal portion may also undergo apoptosis, depending on the neuron's age, type, and distance of axotomy from the proximal end [85]. Several hours after injury, growth-related molecules are upregulated, inducing axons and growth cones to sprout from the nodes of Ranvier and the soma. During this time, Schwann cells play a key role in regeneration by increasing their proliferation to form Bands of Bünger and by secreting neurotrophic and chemotactic factors that influence growing axons, adjacent Schwann cells, and macrophages. Schwann cells are also able to expedite the elimination of myelin, which inhibits axonal regrowth, by degrading their own myelin, phagocytosing extracellular myelin, and presenting myelin to macrophages. Two to three days after injury, macrophages infiltrate the site to clear it of cell debris and myelin, which may persist for

up to 2 weeks post-injury. While small nerve gaps can be repaired by the human body, the regeneration of large nerve defects (greater than 3 mm) is more difficult. Greater control over the direction of axon sprouting toward the distal nerve is desired since inappropriate reconnections lead to neuropathic pain. The direction and rate of axonal re-growth is affected by the presence of substrate or soluble cues that may be growth-permissive or repulsive. Effective spatiotemporal presentation of these cues may be used to better guide the growth cone.

In addition to axonal re-growth, improving the myelination of the sprouted axons is also likely to improve functional recovery. This is a challenge since longer denervation of the remaining Schwann cells further reduces their capacity to support regeneration. Currently, there is no treatment that enables complete functional recovery after spinal cord injury, likely due to significant cell death and the presence of a growth inhibitory environment. The spinal cord is incapable of regeneration without intervention. Within thirty minutes of axotomy, the proximal and distal axons degenerate, reducing their length by hundreds of microns (Figure 1.8). Axons that are not damaged by the initial injury will also degenerate from secondary events. The loss of axonal contact causes oligodendrocytes to undergo apoptosis 4-8 days after injury. Surviving oligodendrocytes revert to quiescence and, unlike their Schwann cell counterpart, contribute little to clearing myelin and axonal debris. Myelin and myelin-associated components are inhibitors of axon growth in vitro. Due to the blood-spine barrier and limited access to the injury site, macrophages do not play an appreciable role in myelin clearance. Microglia, which play a role in CNS immune responses, increase proliferation 4-6 days post-injury but fail to develop into fully

phagocytic cells. Therefore, myelin can still be found several years after degeneration of the nerve.

In addition to myelin, glial scarring at the lesion is another growth-inhibitory barrier that prevents regeneration. The main inhibitory component of glial scars is chondroitin sulfate proteoglycans, molecules that are secreted by reactive astrocytes and are characterized by a protein core to which highly sulfated glycosaminoglycans are attached. Chondroitin sulfate proteoglycan synthesis can be strongly increased and may be expressed as soon as 24 hours post-injury. Therefore, most investigations into CNS nerve regeneration focus on increasing cell survival and creating a growth-permissive environment. In addition, increasing the axonal elongation rate, directing axonal sprouting, and improving the myelination of newly sprouted and surviving axons are also highly relevant goals for achieving functional recovery in CNS repair [86].

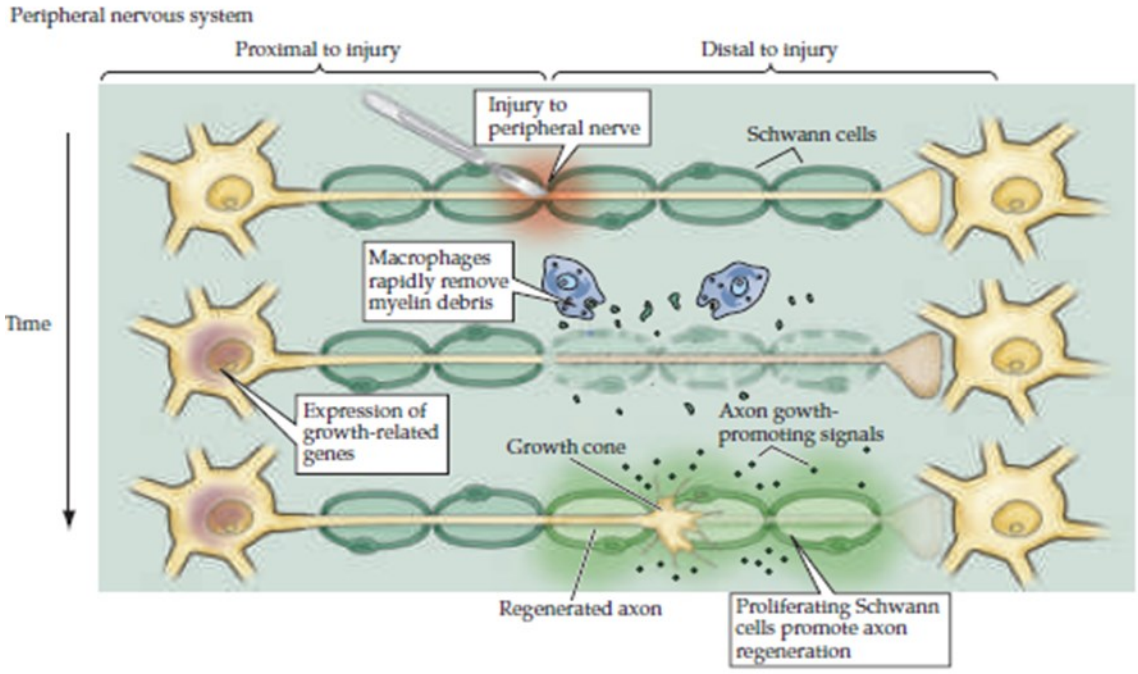

Figure 1.7: Response after injury in the peripheral nervous system [86]. (a) A damage happens in a peripheral nerve leads to series of cellular responses which is generally called (Wallerian degeneration). Distal to the site of injury, axons start disconnecting from the cell bodies and degenerate, then the cellular debris is removed by invading macrophages. Schwann cells which formerly ensheathe the axons proliferate align to form longitudinal arrays increasing their production of neurotrophic factors that can enhance generation of axon. Surfaces of Schwann cells and their extracellular matrix also provide a favorable substratum for regenerating axons extension.

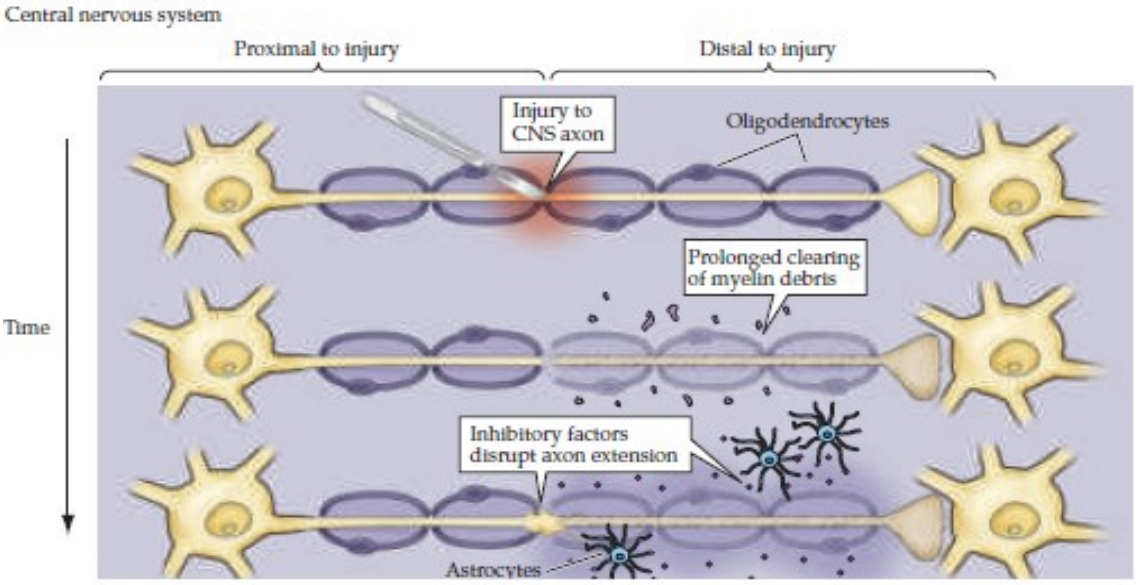

Figure 1.8: Response after injury in the central nervous system [86]. For the CNS, the myelin debris removal is relatively slow, also the myelin membranes produce inhibitory molecules that can block the growth of axon. At the site of injury, astrocytes also interfere with regeneration. At the proximal site of the injury, neuron bodies react to peripheral nerve injury by inducing growth- related genes expression that include those for major components of axonal growth cones. Following CNS injury, however neurons identically fail to activate these growth- associated genes.

1.7 CELL RESPONSES TO ELECTRICAL STIMULATION

In addition to piezoelectricity and streaming potentials in bone and other fibrous tissues, endogenous electric fields up to 500 mV/mm have been reported in many living tissue types [87]. The transport of ionic species and macromolecules related with endogenous electric fields play critical roles in embryonic development [88], wound healing [89], and neural regeneration [90]. There exists a difference in concentrations of intracellular and

extracellular ions, resulting in a transmembrane potential of 10 to 90 mV in different cell types. Shifts in transmembrane potential are known to change cellular proliferation and differentiation [91] and exciting the resting transmembrane potential of neurons can trigger self-propagation of action potentials along the axon [92].

This necessary role of electricity in living systems has created numerous studies to either mimic biological piezoelectricity and endogenous electric fields or manipulate transmembrane potentials by external electrical stimulation to promote cellular differentiation and growth. Neural regeneration investigation has focused on repairing injuries of peripheral nerves through improvement of neural differentiation and directional outgrowth of neurites. Direct electric fields as low as 70 mV/mm have been shown to encourage the outgrowth of the neurites of embryonic chick dorsal root ganglions (DRG) toward the stimulating cathode [93]. A direct electric field of 250 mV/mm or higher when applied on Xenopus neurons resulted in more neurite-bearing cells and longer neurites directed towards the cathode and contracted neurites on the anode side (Figure 1.9) [94]. Such promising findings are not just limited to neurons; a study on the effect of electrical stimulation on bone formation mentioned that implanting insulated batteries into the medullary canal of canine femora resulted in substantial formation of endosteum near the cathode in a 14–21day period [95], which is a significant result, since in bone resorption typically occurs on surface of endosteal whereas formation happens on surface of periosteal. Even in the absence of external electrical stimulation, implantation of poled sintered hydroxyapatite disks in canine compact bone resulted in the filling of a 0.2 mm gap between the negatively charged hydroxyapatite surface and the compact bone in 14

days, while no bone formation happened using the unpoled hydroxyapatite before day 28 [96].

Electrical stimulation can be delivered through the substrate or the cell culture media. Electrical stimulation through media has a distinguished effect on Schwann cells: while DC electrical stimulation aligns the Schwann cells perpendicular to the direction of the electric field, AC electrical stimulation alters the cellular morphology from bipolar spindles to flat and spread with more processes [96].

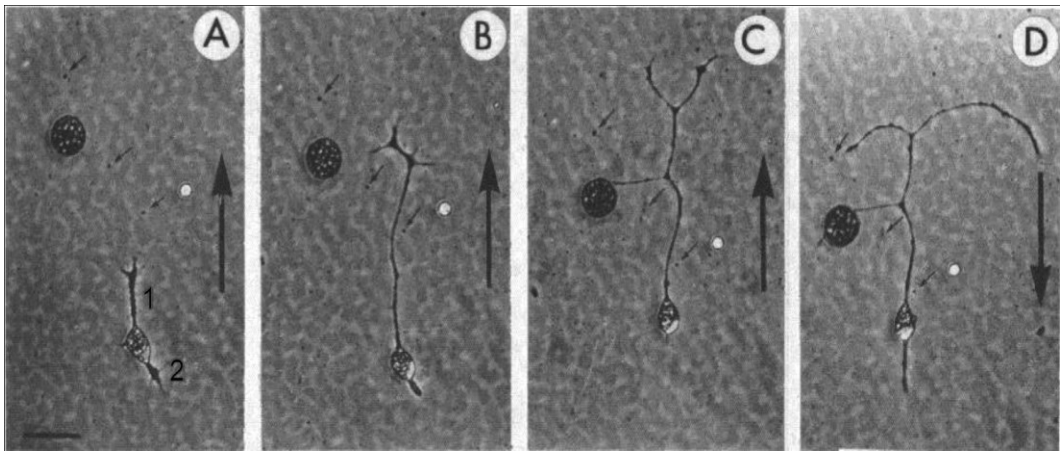

Figure 1.9: Direction and outgrowth of the neurites (labeled 1 and 2) of a bipolar neuron as a result of stimulation by a 500 mV/mm electric field. The black arrow shows the direction of the electric field. The neuron at the beginning of the electrical stimulation (A); after 2 h of exposure to the electric field, neurite 1 has noticeably grown towards the cathode (B); 4 h of stimulation in the same direction resulted in further extension of neurite 1 as well as its branching, while neurite 2 has almost diminished (C); 2 h after changing the direction of the electric field, the tips of neurite 1 curved and neurite 2 grew towards the new cathode (D) [94].

Alternating electric fields additionally have been shown to lead to morphological changes and increased number of processes in Schwann cells, but did not cause directional outgrowth [97]. Since endogenous electric fields and transmembrane potentials are direct rather than alternating, a lot of neural studies use direct electrical stimulation. On the contrary, the periodic nature of the stress that is applied to bone has inspired studies in bone repair to focus on alternating electric fields to promote osteoblast proliferation and activity. In order to avoid electrode implantation and consequently electrolytic byproducts, noninvasive stimulation for bone fracture healing drew great attention. Noninvasive bone growth stimulators are approved by the U.S. Food and Drug Administration (FDA) [98, 99], and are recently marketed for healing fractures and nonunion. Present research techniques performed on osteogenic electrical stimulation varies from capacitively coupled stimulation [100, 101], to applying electromagnetic waves using Helmholtz [102, 103] and solenoid coils [104, 105]. Capacitively-coupled electrical stimulation has been proven to notably increase the proliferation [100] and matrix mineralization of osteoblast-like cells [101].

The mechanisms through which electrical stimulation leads to cellular migration and changes proliferation and differentiation are not yet fully understood. It is expected that the effect of electric is either direct by intracellular components such as ions, growth factors and receptors, or indirect by agglomeration or conformational change of extracellular ions and proteins [94, 106]. Free calcium cations (Ca^{2+}) are observed to be a major factor in both direct and indirect mechanisms of electrical stimulation. Electric fields cause redistribution of Ca^{2+} in the extracellular matrix or on the substrate [97]. In addition,

intracellular Ca^{2+} concentrations are also reported to increase due to electrical stimulation [107]. The effect of electrical stimulation on improved bone formation was initially based on the indirect-stimulation hypothesis; i.e., piezoelectric bone produced electric fields that aggregated charged ions and macromolecules in the bone interstitial fluid, that resulted in enhancement of osteoblast activity [108]. Now it is assumed that direct electric fields mobilize Ca^{2+} and Mg^{2+} towards the cathode or negatively charged surface and cause apatite formation, which can become a scaffold for bone formation by osteoblasts [96].

Figure 1.10 shows an adaptation of cellular galvanotaxis, or electrically-driven cell movement, as reviewed by Mycielska et al. [87]. Direct electric fields depolarize the cathodal side of the cell and hyperpolarize the anodal side. This causes the diffusion of extracellular Ca^{2+} through the anodal side into the cell. Increases in the Ca^{2+} may cause actin depolymerization and contraction on the anodal side, which drive the cell forward and thus makes the cathodal side of the cell protrude [87]. This could describe the phenomenon observed by Patel and Poo [94] as illustrated in Figure 1.9, e.g., the outgrowth of the neurites on the cathodal side of the cell and the diminishing of the neurites on the anodal side. Patel and Poo additionally mentioned that neither blocking Na^{+} channels nor nullifying intercellular Ca^{2+} gradient stopped directional neurite outgrowth in cells exposed to direct electric fields [94]. However, there was a larger distribution of concanavalin A receptors on the cathodal side of the cell than on the anodal side, which caused the authors to conclude that the effect of electrical stimulation on the neurons directional growth could be resulted by preferential migration of membrane receptors [94]. Schmidt et al. showed that electrical stimulation could be caused in more favorable conformational changes in

fibronectin, which enhance the adsorption of more proteins onto the biomaterial [109]. Since some extracellular matrix proteins play crucial roles in cellular attachment, more adhered proteins on the surface of biomaterials could promote cells adhesion and outgrowth.

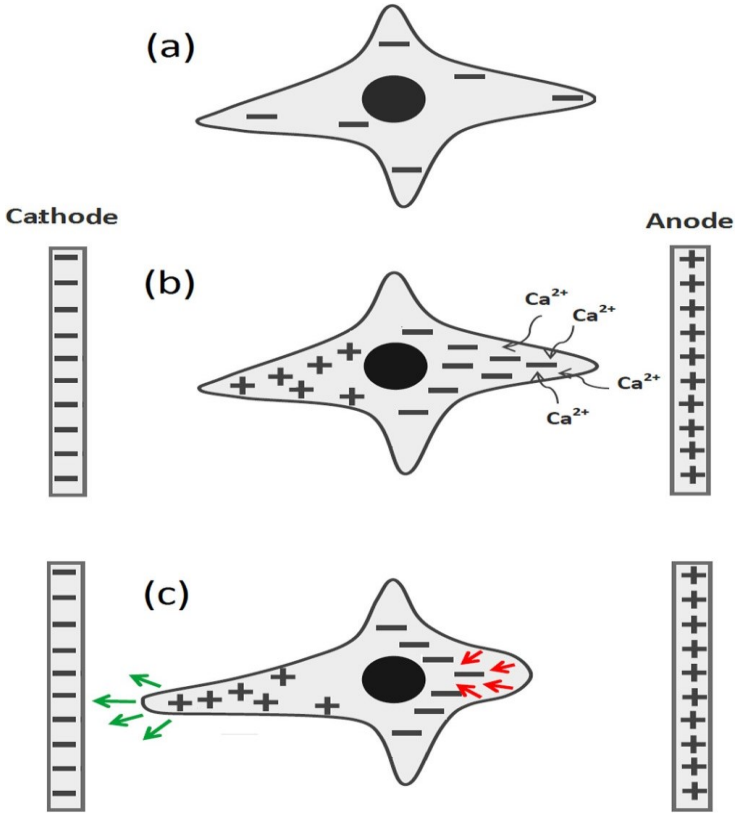

Figure 1.10: A cell with insignificant voltage-gated Ca^{2+} channels at resting transmembrane potential (a); application of an electric field causing direct effects: the field redistributes the intracellular charges resulting in the depolarization and hyperpolarization of the cathodal and anodal sides of the cell, respectively. Extracellular Ca^{2+} is consequently diffused through the anodal side (b). The increase in the intracellular Ca^{2+} on the anodal side depolymerizes actin. The result is the contraction of the anodal side and protrusion of the cathodal side (c) [87].

REFERENCES

1. Ribeiro, C., Sencadas, V., Correia, D. M. & Lanceros-Méndez, S., Piezoelectric polymers as biomaterials for tissue engineering applications. Colloids and Surfaces B: Biointerfaces, 2015, 136, 46-55.
2. M. H. Shamos; L. S. Lavine, Nature 1967, 213, 267-&. DOI 10.1038/213267a0.
3. D. E. Ingber, Scientific American 1998, 278, 48-57.
4. I. Yasuda; K. Noguchi; T. Sato, Journal of bone and joint surgery 1955, 37, 1292-1293.
5. Kim BS, and Mooney DJ. Development of biocompatible synthetic extracellular matrices for tissue engineering. Trends Biotechnol 1998; 16:224-30.
6. Herring MB, Gardner AL, and Glover JA. Single-staged technique for seeding vascular grafts with autogenous endothelium. Surgery 1987; 84:498-502.
7. E. Fukada; I. Yasuda, Journal of the Physical Society of Japan, 1957, 12, 1158-1162. DOI 10.1143/ jpsj.12.1158.
8. Hutmacher DW. Scaffolds in tissue engineering bone and cartilage. Biomaterials. 2000; 21:2529–43.
9. Peter SJ, Miller MJ, Yasko AW, Yaszemski MJ, Mikos AG. Polymer concepts in tissue engineering. J Biomed Mater Res. 1998; 43:422–7.
10. Chung HJ, Park TG. Surface engineered and drug releasing pre-fabricated scaffolds for tissue engineering. Adv Drug Deliv Rev. 2007; 59:249–59.
11. Lyons F, Partap S, O'Brien FJ. Part 1: scaffolds and surfaces. Technol Health Care. 2008; 16:305–17.
12. Vacanti CA, Vacanti JP, and Langer R. Tissue engineering using synthetic biodegradable polymers. In polymers of biological and biomedical significance. W. Shalaby, Am Chem Soc Washignton DC: vol.540, pp.16-34;1994.
13. Atala A. Tissue engineering for the replacement of organ function in the genitourinary system. Am J Transplant 2004;4 Suppl 6:58-73.
14. Atala A, Freeman MR, Vacanti JP, Shepard J, and Retik AB. Implantation in vivo and retrival of artificial structures consisting of rabbit and human urothelium and human bladder muscle. J Urol 1993; 150:608-12.
15. Tuszynski MH, Kordower J. CNS Regeneration. San Diego: Academic Press;1999.
16. Reier PJ. Cellular transplantation strategies for spinal cord injury and translational neurobiology. Neuro Rx 2004; 1:424-51.
17. C. Ribeiro, J. A. Panadero, V. Sencadas, S. Lanceros-Me´ndez, M. N. Taman˜o, D. Moratal, M. Salmero´n-Sa´nchez and J. L. G. Ribelles, Enhanced proliferation of pre-osteoblastic cells by dynamic piezoelectric Stimulation,Biomed. Mater., 2012, 7, 035004.
18. C. A. L. Bassett; R. O. Becker, Science 1962, 137, 1063-&. DO 10.1126/ science.137.3535.1063.
19. H. M. Frost, The Angle Orthodontist 1994, 64, 175-188. DOI 10.1043/0003-3219(1994)064<0175: wlabsa>2.0.co;2.
20. A. A. Marino; R. O. Becker, Nature 1970, 228, 473-&. DOI 10.1038/228473a0.
21. J. Ferrier; S. M. Ross; J. Kanehisa; J. E. Aubin, Journal of Cellular Physiology 1986, 129, 283-288. DOI 10.1002/jcp.1041290303.

22. S. D. McCullen; J. P. McQuilling; R. M. Grossfeld; J. L. Lubischer; L. I. Clarke; E. G. Loboa, Tissue Engineering - Part C: Methods 2010, 16, 1377-1386.
23. M. Akai; Y. Shirasaki; T. Tateishi, Archives of Physical Medicine and Rehabilitation 1997, 78, 405-409. DOI http:/ /dx.doi.org/10.1016/S0003-9993(97)90233-1.
24. K. Yonemori; S. Matsunaga; Y. Ishidou; S. Maeda; H. Yoshida, Bone 1996, 19, 173-180. DOI http://dx.doi.org/10.1016/8756 3282(96)00169X.
25. K. Anselme, Biomaterials 2000, 21, 667-681. DOI 10.1016/s0142 9612(99)00242-2.
26. B. Miara; E. Rohan; M. Zidi; B. Labat, Journal of the Mechanics and Physics of Solids 2005, 53, 2529-2556. DOI 10.1016/ j. jmps.2005.05.006.
27. Valentini RF, Vargo TG, Gardella JA Jr, et al. 1992; Electrically charged polymeric substrates enhance nerve fibre outgrowth in vivo. Biomaterials 13: 183–190.
28.C. Frias; J. Reis; F. Capela e Silva; J. Potes; J. Simões; A. T. Marques, Journal of Biomechanics 2010, 43, 1061-1066. DOI http://dx.doi.org/10.1016/ j. jbiomech.2009.12.010.
29. M. T. Rodrigues; M. E. Gomes; J. F. Mano; R. L. Reis, beta-PVDF Membranes Induce Cellular Proliferation and Differentiation in Static and Dynamic Conditions. In Advanced Materials Forum Iv, Marques, A. T.; Silva, A. F.; Baptista, A. P. M.; Sa, C.; Alves, F.; Malheiros, L. F.; Vieira, M., Eds. 2008; Vol. 587-588, pp 72-76.
30. S. M. Damaraju; S. Wu; M. Jaffe; T. L. Arinzeh, Biomedical Materials 2013, 8. DOI 045007, 10.1088/1748-6041/8/4/045007.
31. L. Marques; L. A. Holgado; R. D. Simoes; J. Pereira; J. F. Floriano; L. Mota; C. F. O. Graeff; C. J. L. Constantino; M. A. Rodriguez-Perez; M. Matsumoto; A. Kinoshita, Journal of Biomedical Materials Research Part B-Applied Biomaterials 2013, 101, 1284-1293. DOI 10.1002/ jbm.b.32941.
32. P. M. Martins; S. Ribeiro; C. Ribeiro; V. Sencadas; A. C.; F. M. Gama; S. Lanceros-Mendez, Rsc Advances 2013, 3, 17938-17944. DOI 10.1039/ c3ra43499k.
33. P. L. Jansen; U. Klinge; M. Anurov; S. Titkova; P. R. Mertens; M. Jansen, European Surgical Research 2004, 36, 104-111. DOI 10.1159/000076650.
34. A. Inui; T. Kokubu; T. Makino; I. Nagura; N. Toyokawa; R. Sakata; M. Kotera; T. Nishino; H. Fujioka; M. Kurosaka, International Orthopaedics 2010, 34, 1327-1332. DOI10.1007/ s00264-009-0917-8.
35. R. F. Valentini; T. G. Vargo; J. A. Gardella; P. Aebischer, Journal of Biomaterials Science, Polymer Edition 1994, 5, 13-36. DOI 10.1163/156856294x00626.
36. N. Royo-Gascon; M. Wininger; J. I. Scheinbeim; B. L. Firestein; W. Craelius, Annals of Biomedical Engineering 2013, 41, 112-122.
37. T.-H. Young; H.-H. Chang; D.-J. Lin; L.-P. Cheng, Journal of Membrane Science 2010, 350, 32-41. DOI 10.1016/j.memsci.2009.12.009.
38. P. Aebischer; R. F. Valentini; P. Dario; C. Domenici; P. M. Galletti, Brain Research 1987, 436, 165-168.
39. H. Delaviz; A. Faghihi; A. A. Delshad; M. H. Bahadori; J. Mohamadi; A. Roozbehi, Cell Journal 2011, 13, 137-142.
40. S. M. Damaraju; S. Wu; M. Jaffe; T. L. Arinzeh, Biomedical Materials 2013, 8. DOI 045007 10.1088/1748-6041/8/4/045007.

41. P. M. Martins, S. Ribeiroa C. Ribeiro, V. Sencadas, A. C. Gomes, F. M. Gama and S. Lanceros-Me´ndez, Effect of poling state and morphology of piezoelectric poly (vinylidene fluoride) membranes for skeletal muscle tissue engineering, 2013.
42. Y. S. Lee; T. L. Arinzeh, Tissue Engineering - Part A 2012, 18, 2063-2072.
43. Y. S. Lee; G. Collins; T. Livingston Arinzeh, Acta Biomaterialia 2011, 7, 3877-3886.
44. Young TH, Lu JN, Lin DJ, et al. 2008; Immobilization of L-lysine on dense and porous poly (vinylidene fluoride) surfaces for neuron culture. Desalination 234: 134–143.
45. Aebischer P, Valentini RF, Dario P, et al. 1987; Piezoelectric guidance channels enhance regeneration in the mouse sciatic nerve after axotomy. Brain Res 436: 165–168.
46. Fine EG, Valentini RF, Bellamkonda R, et al. 1991; Improved nerve regeneration through piezoelectric vinylidenefluoride– trifluoroethylene copolymer guidance channels. Biomaterials 12: 775–780.
47. Schmidt CE, Shastri VR, Vacanti JP, et al. 1997; Stimulation of neurite outgrowth using an electrically conducting polymer. Proc Natl Acad Sci USA 94: 8948–8953.
48. Kepler, R.G.; Anderson, R.A. Ferroelectric polymers. Adv. Phys. 1992, 41, 1–57.
49. Pukada, E. History and recent progress in piezoelectric polymers. IEEE Trans. Ultrason. Ferroelectr. Freq. Control 2000, 47, 1277–1290.
50. Lando, J.B.; Doll, W.W. The polymorphism of poly (vinylidene fluoride). I. The effect of head-to-head structure. J. Macromol. Sci. B 1968, 2, 205–218.
51. Pierre, U. Pvdf piezoelectric polymer. Sens. Rev. 2001, 21, 118–126.
52. Dmitriev, I.Y.; Lavrentyev, V.K.; Elyashevich, G.K. Polymorphic transformations in poly (vinylidene fluoride) films during orientation. Polym. Sci. Ser. A 2006, 48, 272–277.
53. Martins, P.; Lopes, A.C.; Lanceros-Mendez, S. Electroactive phases of poly (vinylidene fluoride): Determination, processing and applications. Prog. Polym. Sci. 2014, 39, 683–706.
54. Salimi, A.; Yousefi, A.A. Ftir studies of _-phase crystal formation in stretched PVDF films. Polym. Test. 2003, 22, 699–704.
55. Gandini, A.; Botaro, V.; Zeno, E.; Bach, S. Semi-crystalline fluorinated polymers. Polym. Int. 2001, 50, 10–26.
56. Correia, H.M.G.; Ramos, M.M.D. Quantum modelling of poly (vinylidene fluoride). Comput. Mater. Sci. 2005, 33, 224–229.
57. Sajkiewicz, P.; Wasiak, A.; Goclowski, Z. Phase transitions during stretching of poly (vinylidene fluoride). Eur. Polym. J. 1999, 35, 423–429.
58. Vanessa F. Cardoso, Daniela M. Correia, Clarisse Ribeiro, Margarida M. Fernandes and Senentxu Lanceros-Méndez, Fluorinated Polymers as Smart Materials for Advanced Biomedical Applications, Portugal, 2018.
59. Teng, H.X. Overview of the development of the fluoropolymer industry. Appl. Sci. (Basel) 2012, 2, 496–512.
60. Rabuni, M.F.; Sulaiman, N.M.N.; Aroua, M.K.; Chee, C.Y.; Hashim, N.A. Impact of in situ physical and chemical cleaning on PVDF membrane properties and performances. Chem. Eng. Sci. 2015, 122, 426–435.

61. Rabuni, M.F.; Sulaiman, N.M.N.; Aroua, M.K.; Hashim, N.A. Effects of alkaline environments at mild conditions on the stability of pvdf membrane: An experimental study. Ind. Eng. Chem. Res. 2013, 52, 15874–15882.
62. Lovinger, A.J. Developments in Crystalline Polymers; Springer: London, UK, 1982; pp. 559–560.
63. Costa, R.; Ribeiro, C.; Lopes, A.C.; Martins, P.; Sencadas, V.; Soares, R.; Lanceros-Mendez, S. Osteoblast, fibroblast and in vivo biological response to poly (vinylidene fluoride) based composite materials. J. Mater. Sci. Mater. Med. 2013, 24, 395–403.
64. Parssinen, J.; Hammarén, H.; Rahikainen, R.; Sencadas, V.; Ribeiro, C.; Vanhatupa, S.; Miettinen, S.; Lanceros-Méndez, S.; Hytönen, V.P. Enhancement of adhesion and promotion of osteogenic differentiation of human adipose stem cells by poled electroactive poly (vinylidene fluoride). J. Biomed. Mater. Res. A 2015, 103, 919–928.
65. Li, J.Y.; Liu, Y.M.; Zhang, Y.H.; Cai, H.L.; Xiong, R.G. Molecular ferroelectrics: Where electronics meet biology. Phys. Chem. Chem. Phys. 2013, 15, 20786–20796.
66. Nix, E.L.; Ward, I.M. The measurement of the shear piezoelectric coefficients of polyvinylidene fluoride. Ferroelectrics 1986, 67, 137–141.
67. Ameduri, B. From vinylidene fluoride (VDF) to the applications of vdf-containing polymers and copolymers: Recent developments and future trends. Chem. Rev. 2009, 109, 6632–6686.
68. F. Swarts, Bull. Acad. Roy. Belg. (1901) 383.
69. T. T. Wang, J. M. Herbert, The applications of ferroelectric polymers, 1988.
70. Cullinane, D. M. & Einhorn, T. A. (2002) Biomechanics of bone, in principles of bone biology, second edition 1 (eds: Bilezikian, j, raisz, l, and rodan, g.), academic press., San Diego, Califonia, USA.
71. Marks, S. C. & Odgren, P. R. (2002) Structure and development of the skeleton, in principles of bone biology, second edition 1 (eds: Bilezikian, j, raisz, l, and rodan, g.), academic press., San Diego, Califonia, USA
72. Rho, J. Y., Kuhn-Spearing, L. & Zioupos, P. (1998) Mechanical properties and the hierarchical structure of bone. Med Eng Phys 20: 92-102.
73. Maria Persson (2014), 3D WOVEN SCAFFOLDS FOR BONE TISSUE ENGINEERING, University of Oulu, Finland.
74. Clarke, B., 2008. Normal bone anatomy and physiology. Clinical Journal of the American Society of Nephrology, 3 Suppl 3(Supplement 3), pp. S131-9.
75. Florencio-Silva, R. et al., 2015. Biology of bone tissue: Structure, function, and factors that influence bone cells. Biomed Research International, 2015, pp.1-17.
76. Kobayashi, S. et al., 2003. Trabecular minimodeling in human iliac bone. Bone, 32(2), pp.163-169.
77. Seeman, E., 2009. Bone modeling and remodeling. Critical Reviews in Eukaryotic Gene Expression, 19(3}, pp.219-233.
78. Kapinas K. et al. 2011 and Biomedical Tissue Research, University of York).
79. Salgado, A. J., Coutinho, O. P. & Reis, R. L. (2004) Bone tissue engineering: State of the art and future trends. Macromol Biosci 4: 743-765.

80. Coelho, M. J., Cabral, A. T. & Fernande, M. H. (2000) Human bone cell cultures in biocompatibility testing. Part i: Osteoblastic differentiation of serially passaged human bone marrow cells cultured in alpha-mem and in dmem. Biomaterials 21: 1087-1094.
81. Kiran Chandrakantrao Pawar, in vitro and in vivo characterization of alginate based anisotropic capillary hydrogels to guide directed axon regeneration,Regensburg, 2010.
82. David, S. & Aguayo, A.J., Axonal elongation into peripheral nervous system "bridges" after central nervous system injury in adult rats. Science 214 (4523), 931-933 (1981).
83. Filbin, M.T., Myelin-associated inhibitors of axonal regeneration in the adult mammalian CNS. Nature Reviews Neuroscience 4 (9), 703-713 (2003).
84. Hughes, P.E. et al., Activity and injury-dependent expression of inducible transcription factors, growth factors and apoptosis-related genes within the central nervous system. Progress in Neurobiology 57 (4), 421-450 (1999).
85. Vargas, M.E. & Barres, B.A., Why is Wallerian degeneration in the CNS so slow? Annu Rev Neurosci 30, 153-179 (2007).
86. Purves, D. et al., Neuroscience, 3rd ed. (Sinauer Associates, Inc., Sunderland, 2004).
87. M.E. Mycielska, M.B. Djamgoz, Cellular mechanisms of direct-current electric field effects: galvanotaxis and metastatic disease, J. Cell Sci. 117 (2004)1631–1639.
88. R. Nuccitelli, Endogenous electric fields in embryos during development, regeneration and wound healing, Radiat. Prot. Dosimetry 106 (2003)375–383.
89. R. Nuccitelli, A role for endogenous electric fields in wound healing, Curr. Top. Dev. Biol. (2003) 1–26. Academic Press.
90. C.D. McCaig, A.M. Rajnicek, B. Song, M. Zhao, has electrical growth cone guidance found its potential? Trends Neurosci 25 (2002) 354–359.
91. S. Sundelacruz, M. Levin, D.L. Kaplan, Role of membrane potential in the regulation of cell proliferation and differentiation, Stem Cell Rev. 5 (2009) 231–246.
92. D.A. McCormick, Chapter 12 – Membrane potential and action potential, in: J.H. Byrne, R. Heidelberger, M.N. Waxham (Eds.), From Molecules to Networks, third ed., Academic Press, Boston, 2014, pp. 351–376.
93 L.F. Jaffe, M.-M. Poo, Neurites grow faster towards the cathode than the anode in a steady field, J. Exp. Zool. 209 (1979) 115–127.
94. N. Patel, M.M. Poo, Orientation of neurite growth by extracellular electric fields, J. Neurosci. 2 (1982) 483–496.
95. C.A.L. Bassett, R.J. Pawluk, R.O. Becker, Effects of electric currents on bone in vivo, Nature 204 (1964) 652–654.
96. T. Kobayashi, S. Nakamura, K. Yamashita, Enhanced osteobonding by negative surface charges of electrically polarized hydroxyapatite, J. Biomed. Mater. Res. 57 (2001) 477–484.
97. H.T. Nguyen, C. Wei, J.K. Chow, L. Nguy, H.K. Nguyen, C.E. Schmidt, Electric field stimulation through a substrate influences Schwann cell and extracellular matrix structure, J. Neural Eng. 10 (2013) 1741–2560.
98. FDA, Premarket Approval, 1986.
99. FDA, Premarket Approval, 1999.
100. H. Zhuang, W. Wang, R.M. Seldes, A.D. Tahernia, H. Fan, C.T. Brighton, Electrical stimulation induces the level of TGF-b1 mRNA in osteoblastic cells by a mechanism

involving calcium/calmodulin pathway, Biochem. Biophys. Res. Commun. 237 (1997) 225–229.
101. H.-P. Wiesmann, M. Hartig, U. Stratmann, U. Meyer, U. Joos, Electrical stimulation influences mineral formation of osteoblast-like cells in vitro. Biochimica et Biophysica Acta (BBA) - Molecular, Cell Res. 1538 (2001) 28–37.
102. V. Cane, P. Botti, S. Soana, pulsed magnetic fields improve osteoblast activity during the repair of an experimental osseous defect, J. Orthop. Res. 11 (1993) 664–670.
103. T. Bodamyali, B. Bhatt, F.J. Hughes, V.R. Winrow, J.M. Kanczler, B. Simon, et al., Pulsed electromagnetic fields simultaneously induce osteogenesis and upregulate transcription of bone morphogenetic proteins 2 and 4 in rat osteoblasts in vitro, Biochem. Biophys. Res. Commun. 250 (1998) 458–461.
104. T. Takano-Yamamoto, M. Kawakami, M. Sakuda, Effect of a pulsing electromagnetic field on demineralized bone-matrix-induced bone formation in a bony defect in the premaxilla of rats, J. Dent. Res. 71 (1992) 1920–1925.
105. W.H.-S. Chang, L.-T. Chen, J.-S. Sun, F.-H. Lin, Effect of pulse-burst electromagnetic field stimulation on osteoblast cell activities, Bioelectromagnetics 25 (2004) 457–465.
106. C.E. Schmidt, V.R. Shastri, J.P. Vacanti, R. Langer, Stimulation of neurite outgrowth using an electrically conducting polymer, Proc. Natl. Acad. Sci. 94 (1997) 8948–8953.
107. E.K. Onuma, S.W. Hui, Electric field-directed cell shape changes, displacement, and cytoskeletal reorganization are calcium dependent, J. Cell Biol. 106 (1988) 2067–2075.
108. C.A.L. Bassett, Biologic significance of piezoelectricity, Calcif. Tissue Int. 1 (1967) 252–272.
109. A. Kotwal, C.E. Schmidt, Electrical stimulation alters protein adsorption and nerve cell interactions with electrically conducting biomaterials, Biomaterials 22 (2001) 1055–1064.

CHAPTER 2: THE EFFECT OF OSCILLATING ELECTRIC FIELDS ON CELLS

2.1 INTRODUCTION

The ability of biomaterials to support cell adhesion is necessary for their use in tissue regeneration and tissue engineering, particularly for adherent cell types. Typically, the materials should not be merely tolerated passively by the cells; rather, the materials should actively provide an appropriate environment to facilitate cellular contacts and signaling, allowing the cells to perform their role effectively [1]. Poly (vinylidene fluoride) (PVDF) is used in a variety of disciplines ranging from aerospace and medical applications to common household applications. This polymer as indicated before, can be manufactured in four different crystalline phases, known as α, β, γ, and δ depending on the processing conditions. The all-trans planar zig-zag conformation, TTT, confers to the β-phase the highest resulting permanent dipole and consequently the best electroactive properties. These properties can be found in the γ- and δ -phases too, but to a lesser extent [2]. To enhance polymer piezoelectric response, an electric poling procedure is applied to the polymer that induces the dipole alignment in the direction of the applied electric field [3]. The α-PVDF crystallizes in a trans-gauche (TGTG') conformation, which causes the consecutive permanent dipoles of the monomer to orient in opposite directions, resulting in non-polar crystals [4]. Figure 2.1 illustrates how the electroactive polymers respond to electrical stimulation.

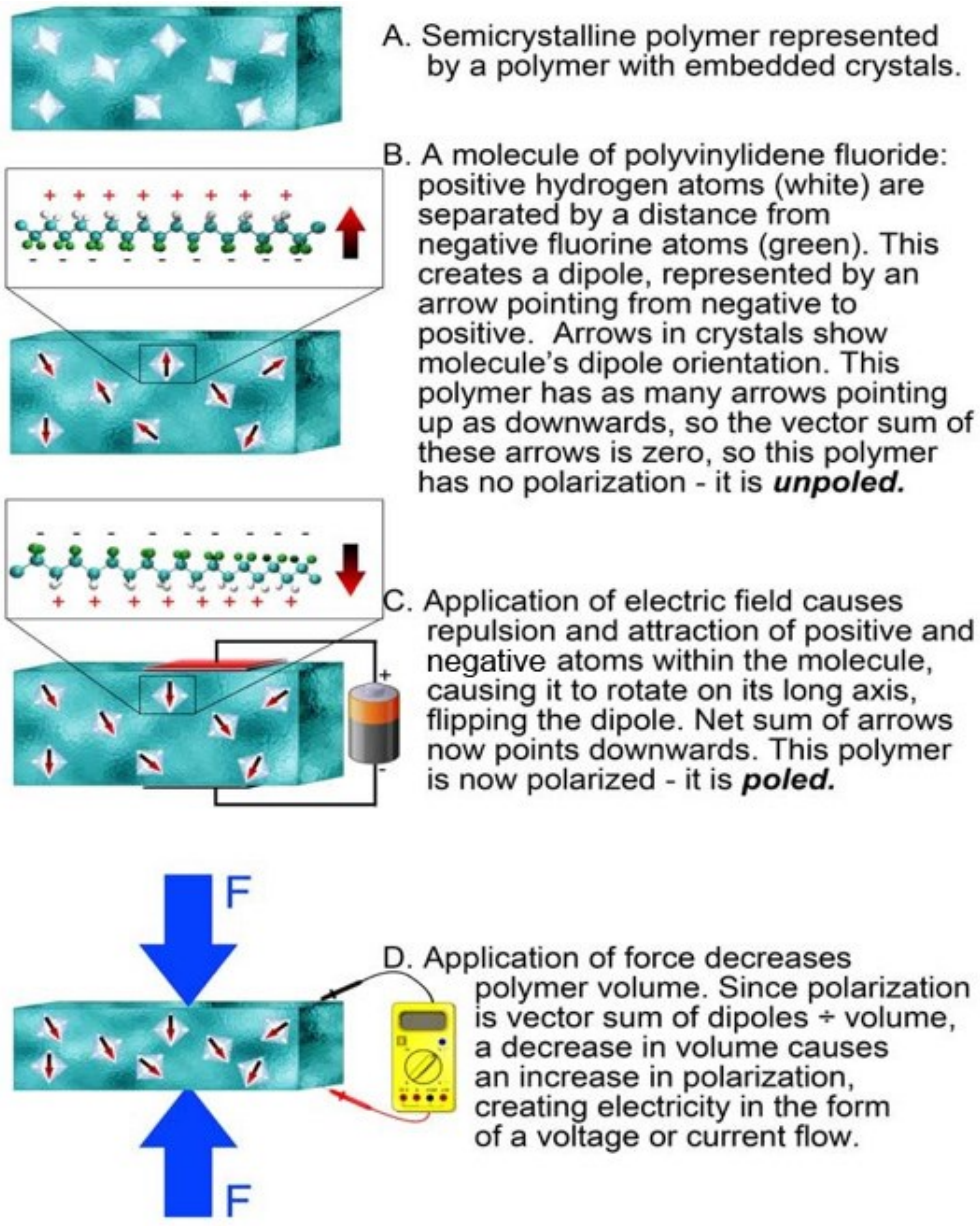

Figure 2.1: Response of electroactive polymers to electrical stimulation.

The electrical charge on a piezoelectric substrate may be an important cue for the cells. Numerous studies have demonstrated that electrically charged surfaces can influence different aspects of cell behavior such as growth, adhesion, or morphology of different cell types, like osteoblast, nervous, and muscular cells [5, 6, 7], but there are no studies

exploring the fact that these tissues are interconnected. Nerves innervate both bone and muscles. Further, it has been shown that when a limb is denervated, fracture repair is adversely impacted [8]. Additionally, fractures heal more slowly when soft tissues such as muscle are injured [9]. This seemingly symbiotic relationship between bone, nerves, and muscles form the basis of the hypothesis for this chapter. The central hypothesis of the present chapter was that frequencies that promoted the growth of neural cells would also promote the growth of bone and muscle cells. Since bone is itself piezoelectric, it follows that bone cells would respond to piezoelectric substrates. This chapter further hypothesized that by varying vibration frequencies in piezoelectric substrates, attached neuronal cells would respond with varying onsets of growth. Muscle progenitors reside within bone, while nerves come into direct contact with bone, thus it also follows that the piezoelectric properties of bone also affect muscle and nerve cells.

In order to isolate the effect of oscillating electric fields on cell response, piezoelectric substrates were seeded with cells and vibrated at different frequencies. Poled and unpoled PVDF films were seeded with mouse preosteoblasts, hMSCs, and rat neurons, then vibrated at 20, 60, and 100 Hz. Cell proliferation was assessed with MTS assays. Bone formation was assessed with Alizarin Red staining, and nerve cells were evaluated with neurite imaging, see Figure 2.2.

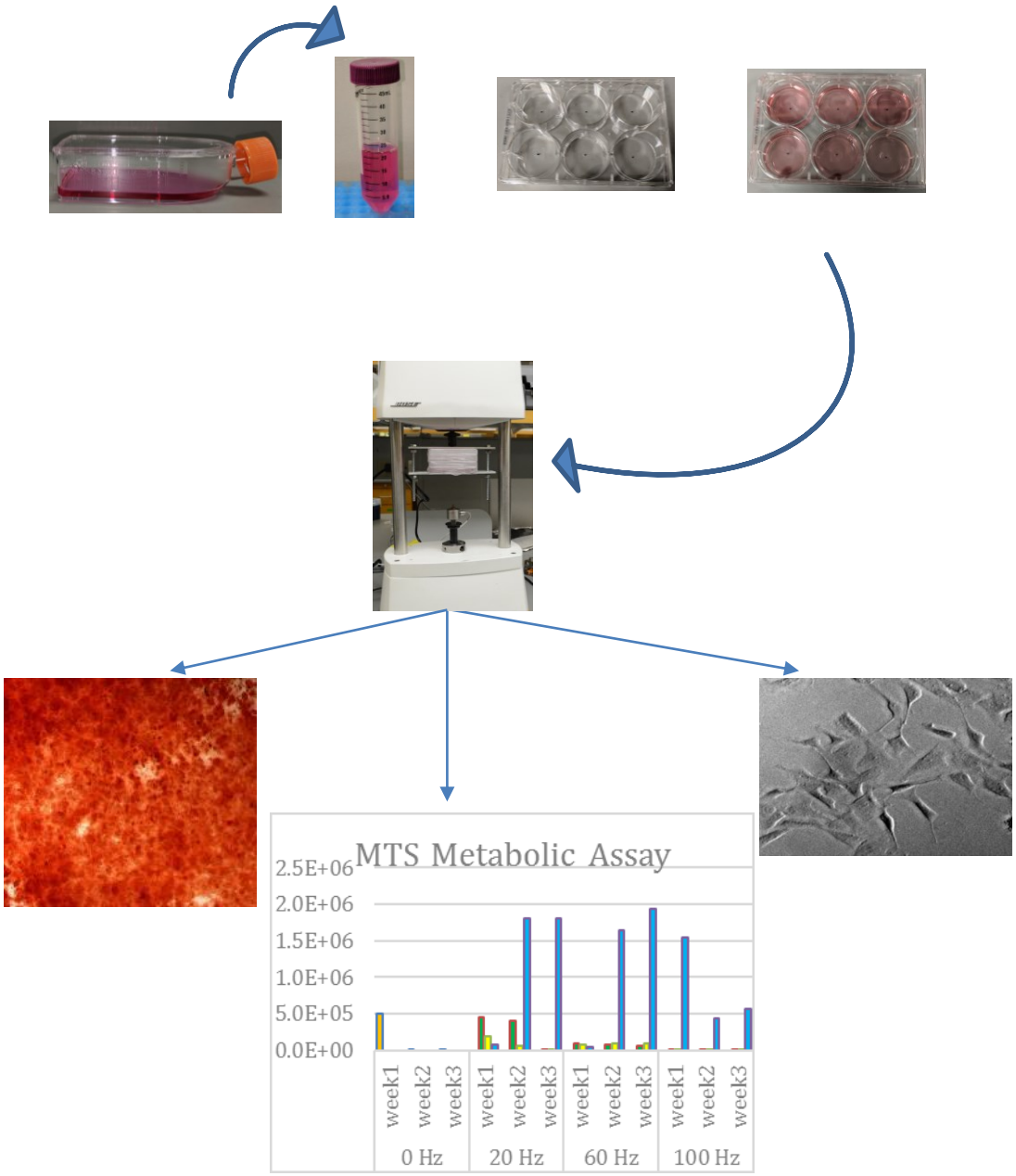

Figure 2.2: Schematic of the chapter experiments**.**

2.2 MATERIALS AND METHODS

2.2.1 Tissue Culture

Human mesenchymal stem cells (hMSCs isolated from normal adult human bone marrow and reported to differentiate down many different lineages including chondrogenic, osteogenic, adipogenic and neural [10] and MC3T3-E1 pre-osteoblasts (an established mouse (Mus musculus) calvaria preosteoblast cell line, commonly used for studies concerning bone differentiation and development) were obtained from American Type Culture Collection (ATCC, Manassas, VA). hMSCs and MC3T3-E1 were cultured in Minimum Essential Medium (MEM alpha nucleosides) (was obtained from Thermofisher Scientific company) with 15% Fetal Bovine Serum (FBS) and 1% Penicillin/Streptomycin (P/S) (were obtained from Sigma Aldrich company) (growth media), at 37ºC in humidified air containing 5% CO_2. The media was changed three times a week.

RN33B (a neuronal cell line derived from medullary raphe cells that retain many properties of mature CNS neurons) spindle-shaped cells were also obtained from ATCC and cultured in Dulbecco's Modified Eagle's Medium (DMEM)/Nutrient Mixture F-12 Ham (obtained from Sigma Aldrich) with 10% Fetal Bovine Serum (FBS) and 1% Penicillin/Streptomycin (P/S), at 33ºC in 95% humidified air containing 5% CO. The medium was changed three times a week. For RN33B cells to be differentiated into neurite-shaped, a 175 cm^2 tissue culture flask of 75% confluent cells were incubated at 37ºC in humidified air containing 5% CO_2. The cells require about 2 weeks in these conditions to be differentiated (Figure 2.3).

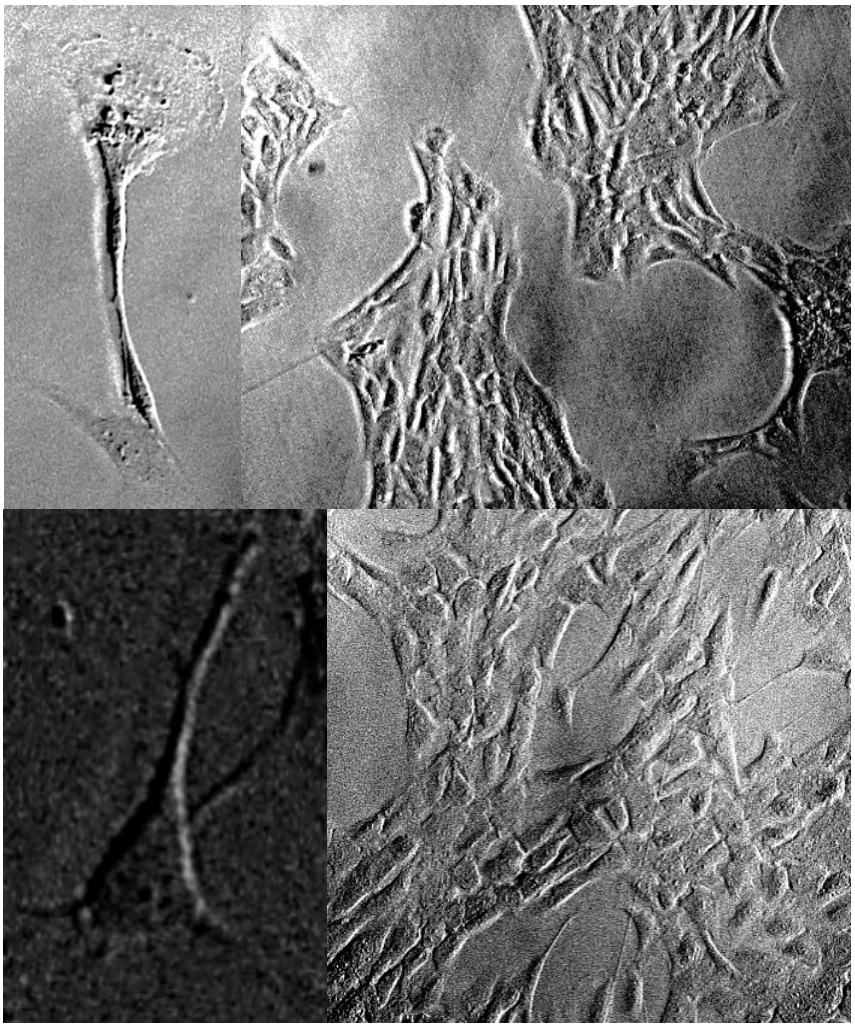

Figure 2.3: A, B Undifferentiated RN33B cells. C, D: Differentiated RN33B cells. 20x magnification [11].

Undifferentiated RN33B cells will remain undifferentiated at 33ºC and these cells have a spindle-shaped morphology. Warming RB33B cells to 37ºC induces their differentiation, when they develop a neurite-shaped morphology.

2.2.2 Poly (vinylidene fluoride) PVDF Film Preparation

PVDF films (unpoled and poled) were obtained from Goodfellow company with a thickness of 0.03-0.05 mm and cut into small square sheets (1 cm x 1 cm) then sterilized by immersing 3 times in fresh 70% ethanol for 30 min. Afterwards, the samples were washed 5 times for 5 min in sterile phosphate- buffered saline (PBS) to eliminate any residual ethanol. Finally, the samples were exposed to (UV) light for 2 hrs. (1 hr. each side). The film samples were glued to 6-well tissue culture polystyrene plate (TPCS) by using liquid tissue adhesion glue, Vetbond (Figure 2.4).

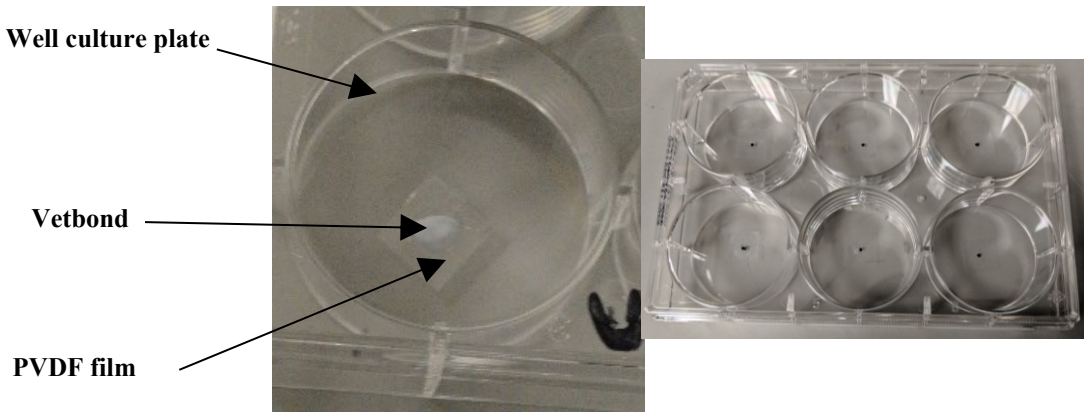

Figure 2.4: PVDF film glued onto the tissue culture polystyrene (TCPS) of a 6-well plate**.**

hMSCs, MC3T3-E1, and RN33B (spindle, or undifferentiated, and neurite-shaped, or differentiated) cells were seeded directly onto well plates, or onto poled or unpoled PVDF films at seeding densities of $2x10^3$ cells/cm^2, $25x10^3$ cells/cm^2 and $1x10^4$ cells/cm^2 for each cell type respectively, then incubated for 24-36 hrs.

2.2.3 Stimulation Protocol

First, the six well culture plates were wrapped in sterile parafilm. Next, wells were clamped between custom made clamps that were mounted into a material testing device capable of applying tensile loading or vibration (Bose Electroforce 3100, shown in Figure 2.5). Then the well plates were subjected to vibration for 24 hrs. starting on the second day after seeding. Three vibration frequencies (20, 60, 100) Hz at a fixed vibration acceleration of approximately 0.3 g were used in the stimulation protocol. This corresponded to peak-to-peak amplitudes of 0.37, 0.04, and 0.014 mm, respectively.

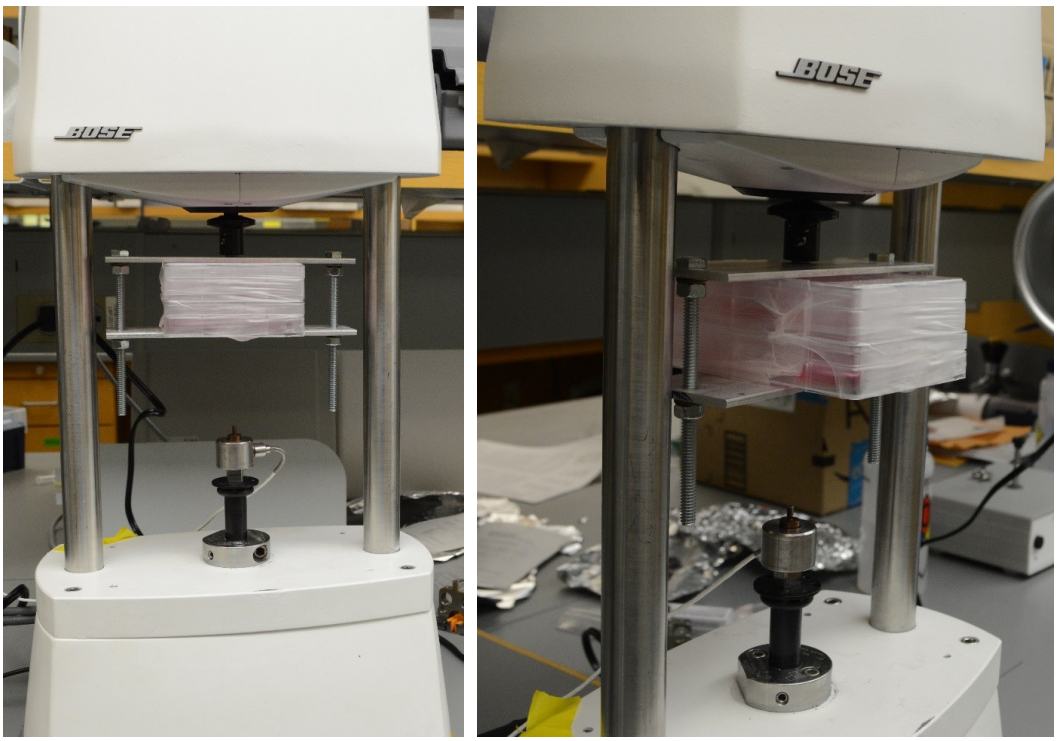

Figure 2.5: Set-up of the Electro Force Instrument (Bose-3100) used in the stimulation protocol. Well plates are stacked, wrapped with parafilm to prevent infection.

2.2.4 Alizarin Red Staining

To determine whether hMSCs and MC3T3-E1 cells differentiate into osteoblasts due to the electrical stimulation, an Alizarin red staining (ARS) assay was used. Alizarin red is an anthraquinone dye (obtained from Sigma Aldrich company) and has been widely used to evaluate calcium deposits in cell culture. The ARS staining is quite versatile because the dye can be extracted from the stained monolayer of cells and readily assayed. Since cells that have differentiated into osteoblasts form calcium deposits as a precursor to bone, positive Alizarin red staining is a marker of osteogenic differentiation. Following vibration, cells were returned to incubators. The cells were evaluated at Week 1, Week 2 and Week 3 after vibration. hMSC or MC3T3-E1 monolayers in 6-well plates (9 cm^2/well) were washed with 1.0 mL PBS and fixed in 10% (v/v) formalin (obtained from Sigma Aldrich) at room temperature for 15 min. The monolayers were then washed twice with excess dH_2O prior to the addition of 1 mL of 40 mM ARS (pH 4.2) per well. The plates were incubated at room temperature for 20 min with gentle shaking. After aspiration of the unincorporated dye, the wells were washed four times with 1 mL dH_2O for 5 min each time. The plates were then left at an angle for 2 min to facilitate removal of excess water. Stained monolayers were visualized by phase microscopy. The cells were fixed for staining at time points: Week 1, Week 2, and Week 3.

2.2.5 MTS Assays

To determine the effect of the electrical stimulation on the proliferation of hMSCs and MC3T3-E1 cells, these cells were seeded in 6-well culture plates with PVDF films and subjected to vibration for 24 hours. Following vibration, cells were returned to incubators.

The cells were evaluated at Week 1, Week 2 and Week 3 after vibration. MTS (3-(4,5-dymethylthiazol-2-yl)-5-(3-carboxymethoxyphenyl)-2(4-sulfopheny)-2Htetrazolium) assay (CellTiter 96TM Aqueous One Solution Cell Proliferation Assay, Promega) was carried out in order to quantify cell proliferation. Assays are performed by adding CellTiter 96 ® Aqueous One Solution Reagent (1:5 v/v) directly to well cultures, incubating for 1–4 hours and then recording the absorbance at 492 nm with a 96-well plate reader (DTX 880 Multimode Detector).

2.2.6 Neurite Imaging

Neurons (RN33B rat neurons) were vibrated as described for hMSCs and MC3T3-E1 cells, but these were also maintained at 33ºC or 37ºC to promote undifferentiated and differentiated states, respectively. When undifferentiated, the cells are spindle-shaped, while differentiated RN33B cells are neurite-shaped. Temperatures were achieved with 2 heat lamps directed at the Electroforce instrument, an overview of the experimental set-up is indicated in Figure 2.6. A uniform temperature at the location of the well plates was confirmed with thermometers. After a week of vibration, RN33B cells (spindle-shaped and neurite-shaped) were imaged on tissue culture polystyrene (TCPS) or on PVDF films (poled and unpoled), using a phase contrast microscopy. Cells were evaluated for potential neurite formation.

Figure 2.6: Set-up of the Electro Force Instrument (Bose-3100) used in the stimulation protocol for RN33B cells. Well plates are stacked, wrapped with parafilm to prevent infection, and the neurons were maintained at (33 and 37) ºC due to their sensitivity to temperature.

NIH ImageJ was used to measure average neurite length. Figure 2.7.

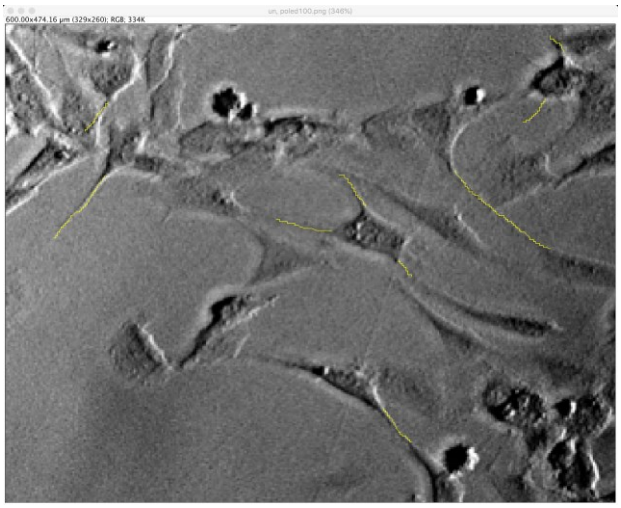

Figure 2.7: RN33B neurites with their extensions traced in NIH ImageJ.

2.2.7 Statistical Analysis

Cellular metabolic activity and neurite extension were compared between the different vibration frequencies using an analysis of variance (ANOVA). *p*-Values less than 0.05 were considered significant. Pairwise comparison between groups was performed after ANOVA using the least significant difference (LSD) method. All analyses were conducted using Microsoft Excel. Statistical significance is denoted in the figures, which are reported as mean ± standard deviation.

2.3 RESULTS

2.3.1 Alizarin Red Staining of hMSCs and MC3T3-E1 Cells

Images of ARS stained hMSCs and MC3T3-E1 cells seeded with PVDF membranes in 6-well plates at Week 1, Week 2 and Week 3 are presented in Figures (2.8-2.13). The images of cells seeded on unpoled PVDF show a less mineralization than images of cells seeded on poled PVDF. Both unpoled and poled PVDF induced and higher mineralization levels than TCPS images, which were negative for Alizarin red stain.

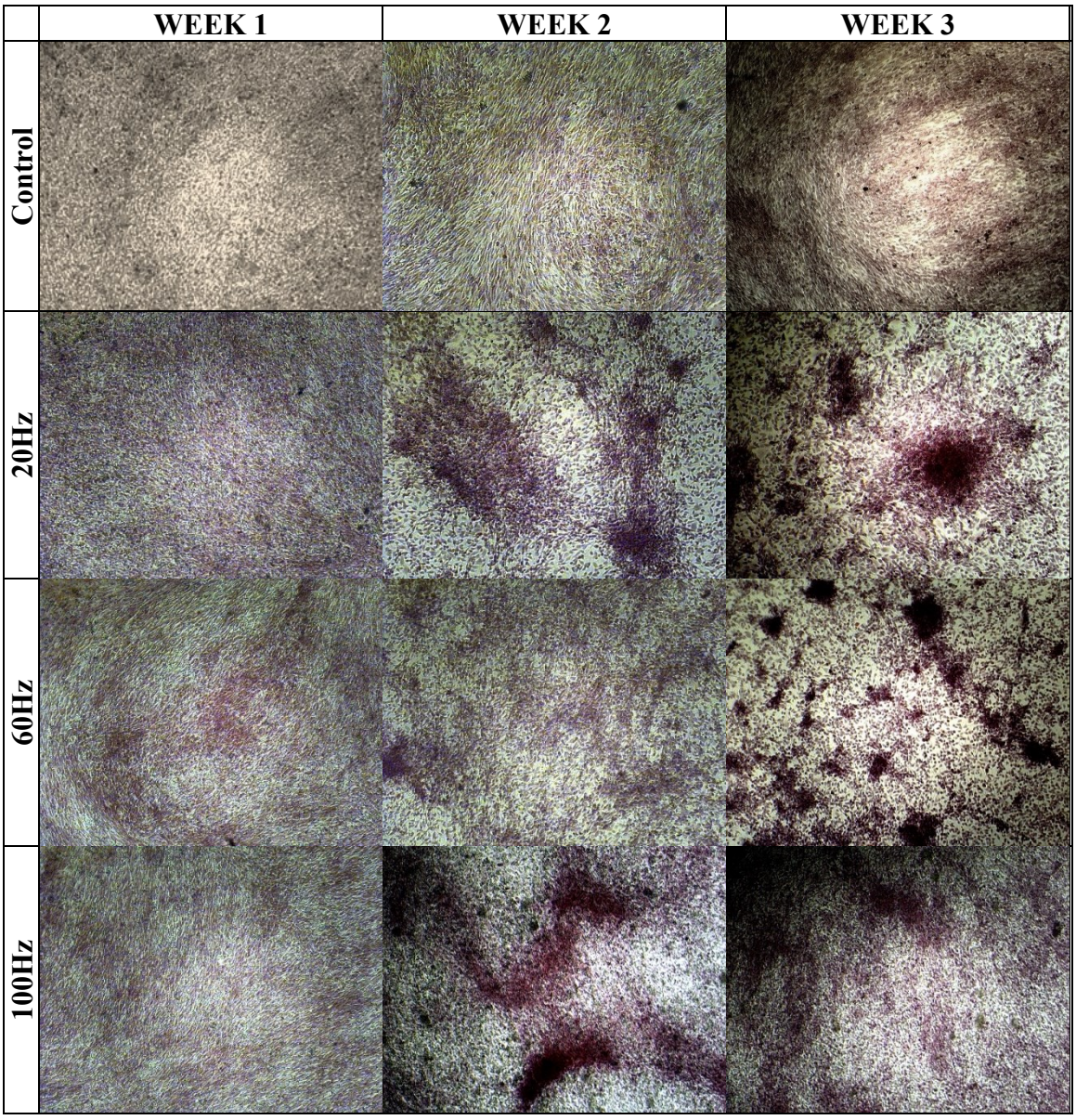

Figure 2.8: Alizarin red staining to assay bone formation of hMSCs seeded on TCPS in 6-well plates and subjected to vibration for 24 hours. The cells were stained at Week 1, Week 2 and Week 3 after vibration. The absence of red stain indicates that this is a negative result. Dense clusters are likely excess extracellular matrix.

Week 2 resulted in a greater mineralization staining than both Week 1 and Week 3 for all vibration frequencies. All cells seeded on PVDF and subjected to vibration exhibited enhanced mineralization. Vibrated hMSCs seeded on TCPS did not form mineralization, while vibration promoted mineralization in all MC3T3-E1 cells, regardless of substrate.

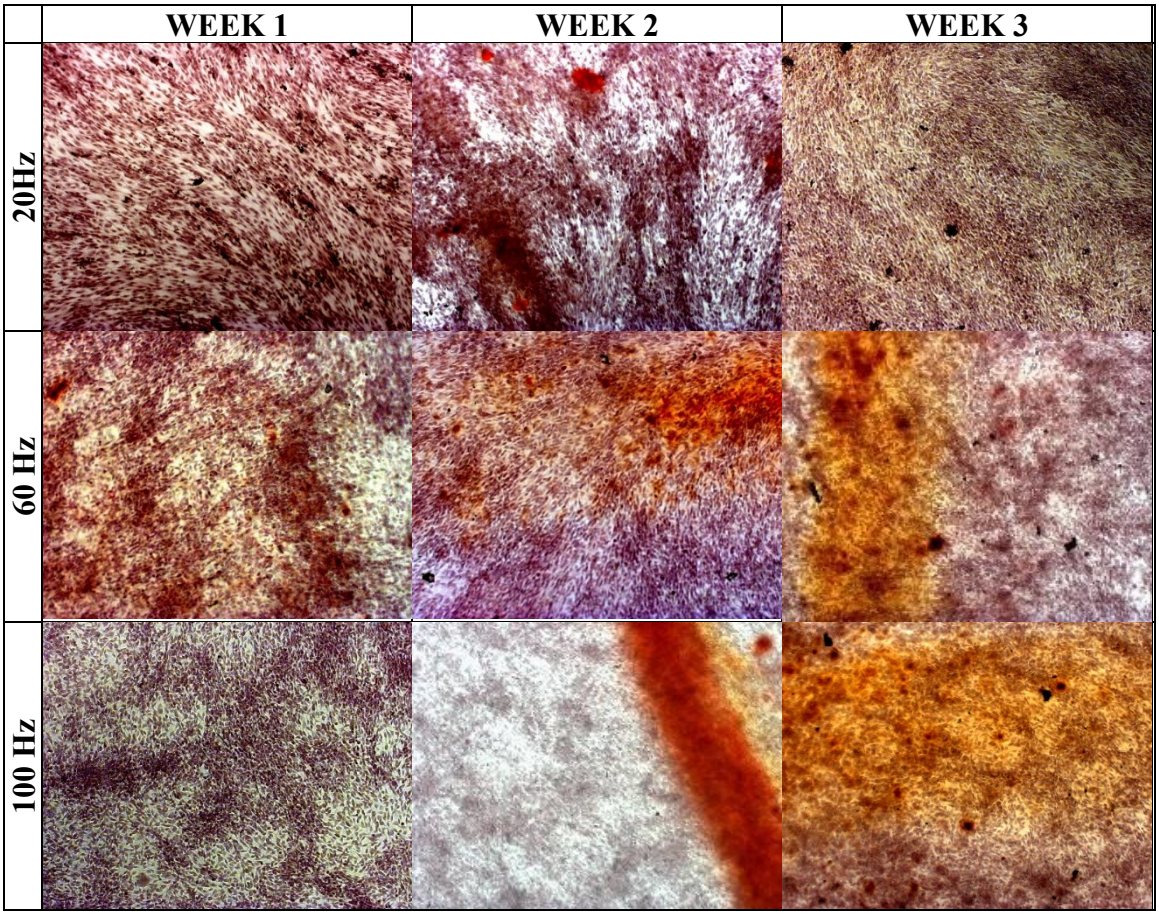

Figure 2.9: Alizarin Red Staining to assay bone formation of hMSCs seeded on unpoled PVDF films in 6-well plates and subjected to vibration for 24 hours. The cells were stained at Week 1, Week 2 and Week 3 after vibration. Red staining indicates positive Alizarin red result.

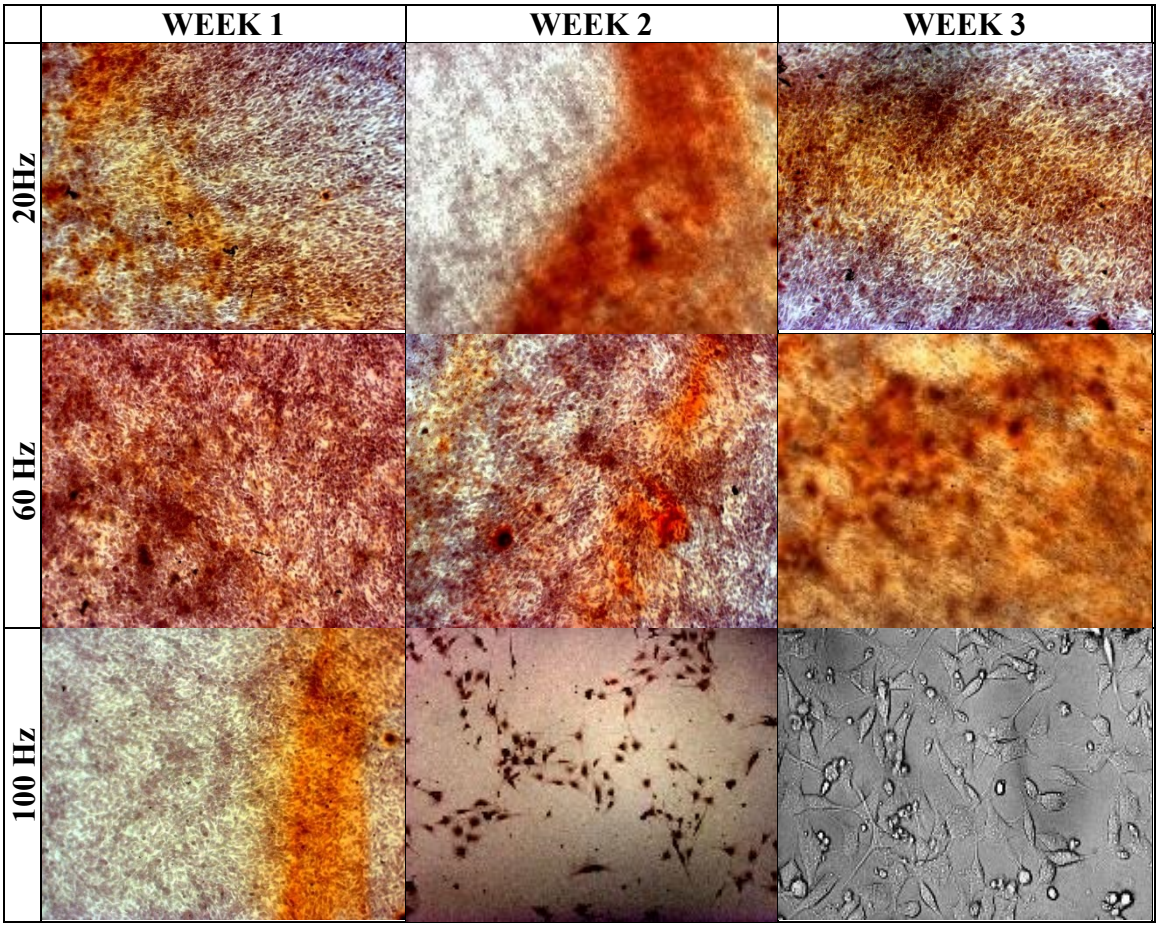

Figure 2.10: Alizarin Red Staining to assay bone formation of hMSCs seeded on poled PVDF films in 6- well plates and subjected to vibration for 24 hours. The cells were stained at Week 1, Week 2, and Week 3 after vibration. Red staining indicates positive Alizarin red result. Weeks 2 and 3 at 100 Hz showed marked change in morphology very similar to neuronal cells.

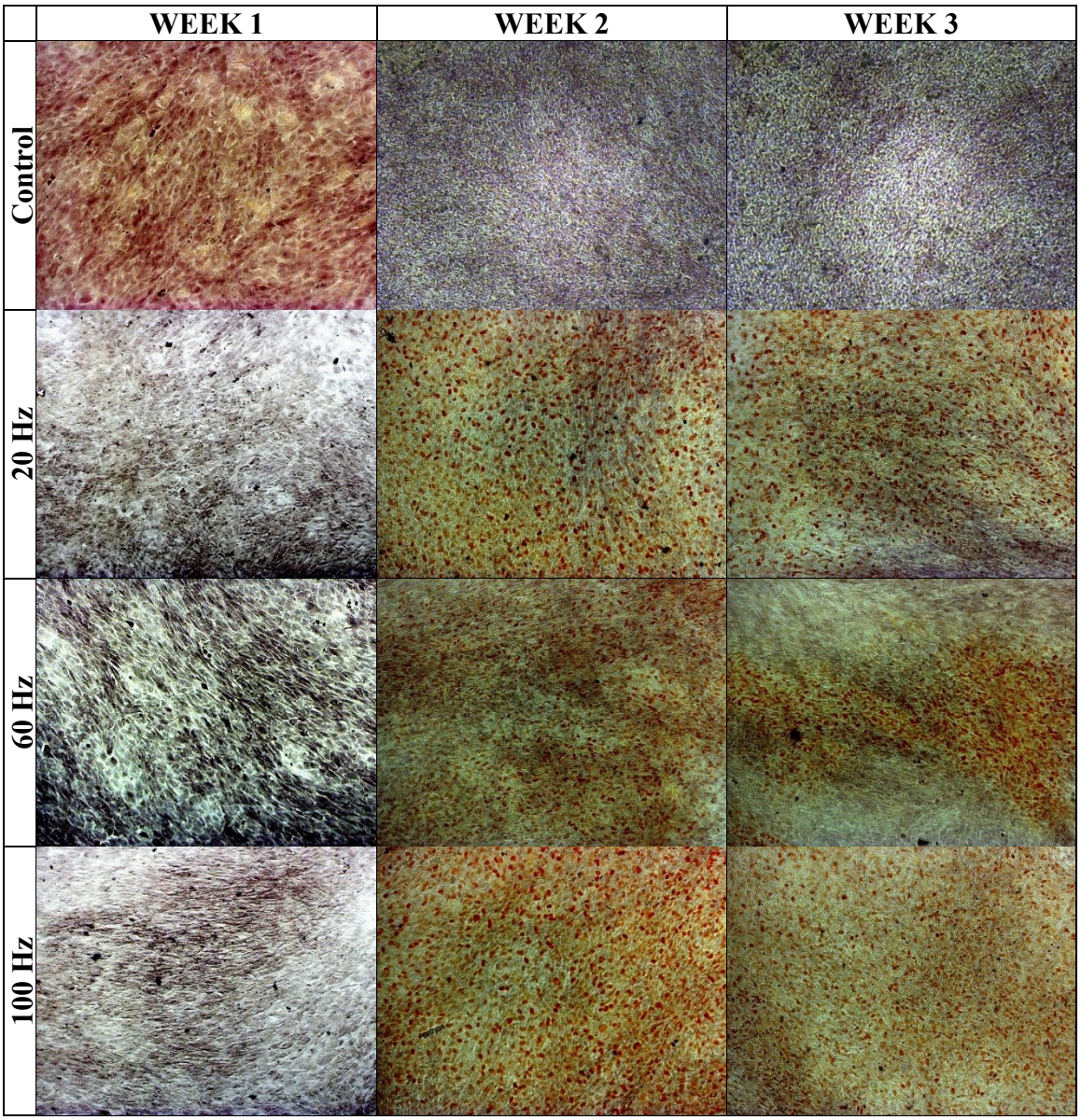

Figure 2.11: Alizarin Red Staining to assay bone formation of MC3T3-E1 osteoblasts seeded on TCPS in 6- well plates and subjected to vibration for 24 hours. The cells were stained at Week 1, Week 2, and Week 3 after vibration. Red staining indicates positive Alizarin red result.

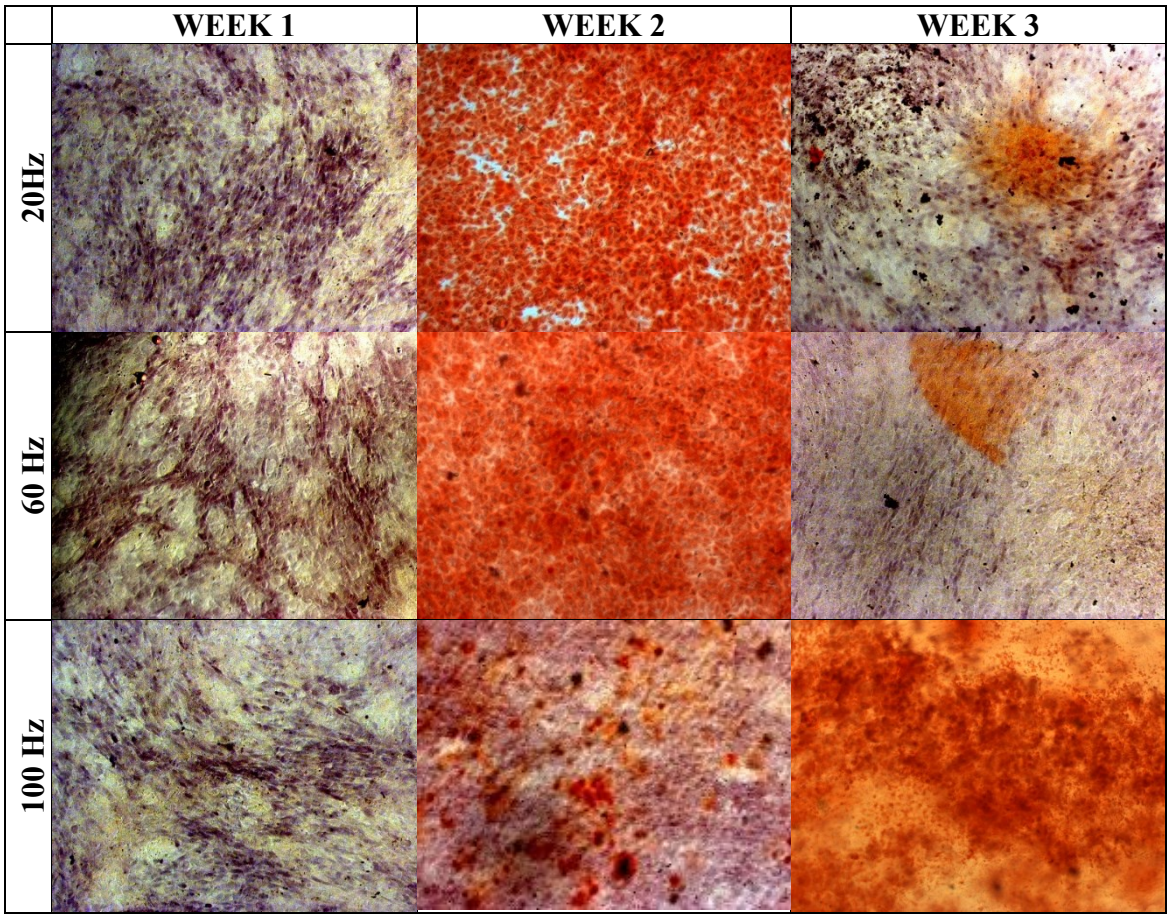

Figure 2.12: Alizarin Red Staining to assay bone formation of MC3T3-E1 osteoblasts seeded on unpoled PVDF films in 6-well plates and subjected to vibration for 24 hours. The cells were stained at Week 1, Week 2, and Week 3 after vibration. Red staining indicates positive Alizarin red result.

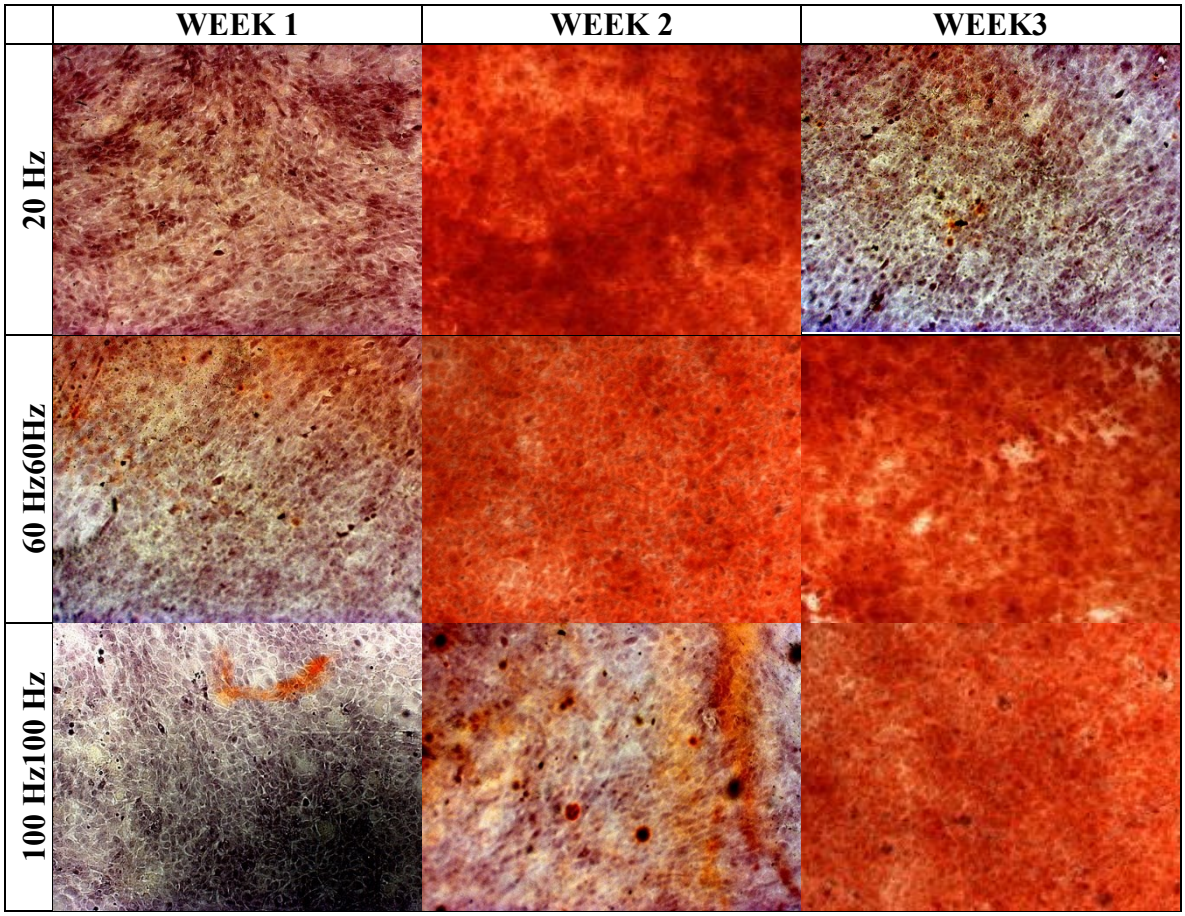

Figure 2.13: Alizarin Red Staining to assay bone formation of MC3T3-E1 osteoblasts seeded on poled PVDF films in 6-well plates and subjected to vibration for 24 hours. The cells were stained at Week 1, and Week 2 after vibration. Red staining indicates positive

2.3.2 MTS Assays of hMSCs and MC3T3-E1 Cells

hMSCs and MC3T3-E1 cells when seeded on PVDF membranes, attached a few hours afterwards and proliferated very rapidly, completely covering the PVDF surface within one week of culture. When qualitatively evaluated under an optical microscope, the proliferation rate of both cell types appeared unaffected by substrate, whether TCPS or PVDF membrane. The reduction of the MTS tetrazolium compound by viable cells produces a colored dye is a measure of cell metabolic activity that can be quantified to

assess cell proliferation, cell viability, and cytotoxicity. Cell proliferation was quantified using MTS assays and is reported for hMSCs and MC3T3-E1 cells seeded on TCPS, and non-piezoelectric and piezoelectric PVDF films at Week 1, Week 2, and Week 3 after vibration (Figures 2.14 and 2.15 respectively).

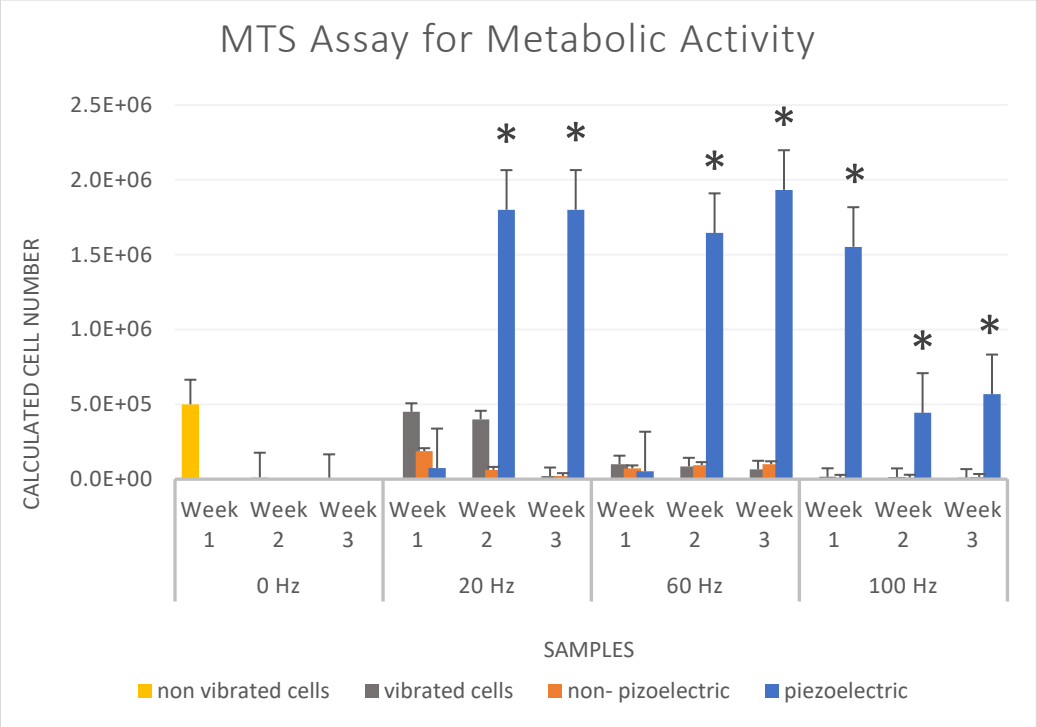

Figure 2.14: Cell proliferation of hMSCs seeded on tissue culture polystyrene (non-vibrated—yellow or vibrated—grey), non-piezoelectric, and piezoelectric PVDF films at Week 1, Week 2, and Week 3 after vibration. Asterisks show statistically significant differences ($p < 0.05$) compared to all other groups. For non-vibrated cells, TCPS at week 1 had statistically greater metabolic activity than all other groups. For vibrated cells, piezoelectric PVDF films show statistically significant increases in metabolic activity ($p < 0.05$) compared to all other groups on corresponding days. Error bars show standard deviation.

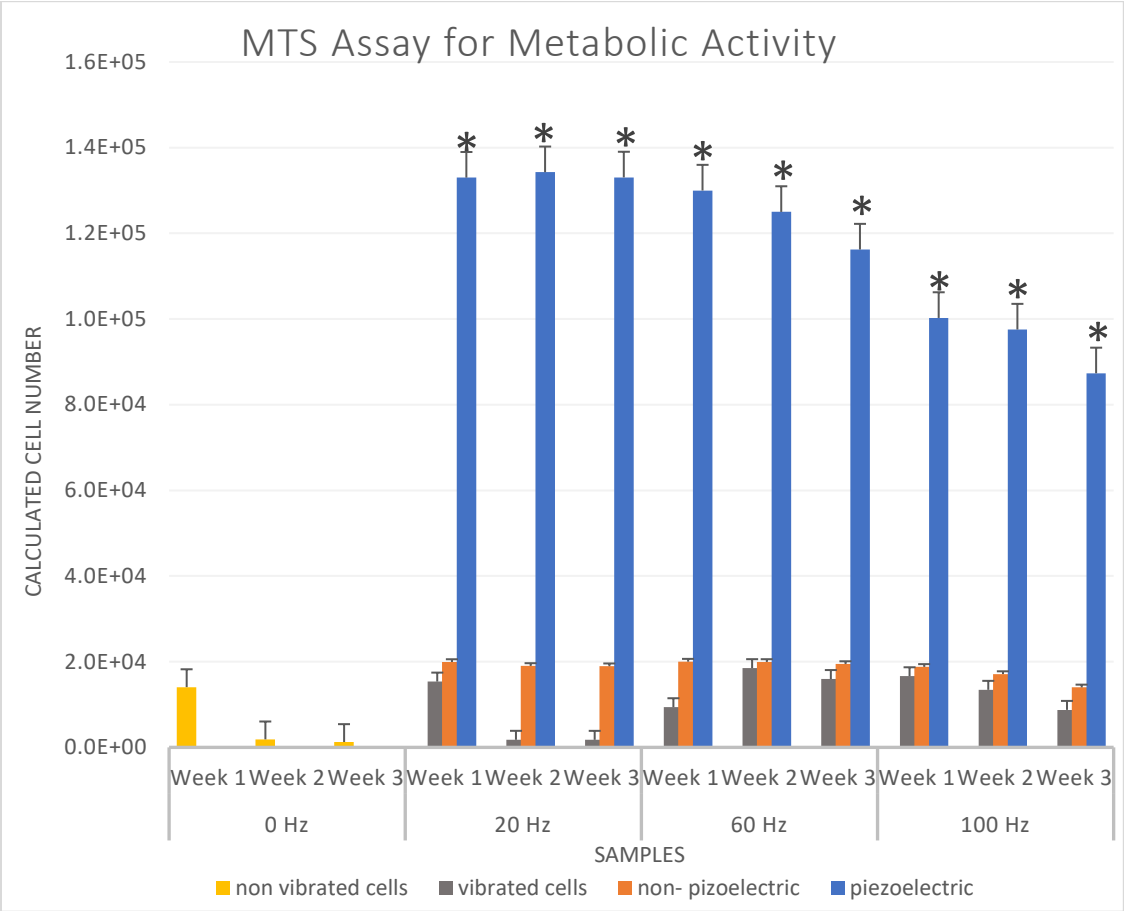

Figure 2.15: Cell proliferation of MC3T3-E1 seeded on tissue culture plastic (non-vibrated—yellow or vibrated—grey), non-piezoelectric, and piezoelectric PVDF films at Week 1, Week 2, Week 3 after vibration. Piezoelectric PVDF films show statistically significant increases ($p < 0.05$) over all groups at all timepoints. Asterisks indicate statistical significance. Error bars show standard deviation.

Figure 2.14 shows that for the vibration frequencies 20 and 60 Hz, the highest number of viable hMSCs were seeded on poled PVDF films at Week 2 and Week 3 ($p < 0.05$). At 100 Hz, the number of viable cells initially decreased at Week 2 and slightly started to increase

at Week 3. Figure 2.15 shows that the highest number of viable MC3T3-E1 cells is obtained when seeded on poled PVDF films at all frequencies of vibration.

2.3.3 Neurite Imaging

When comparing images of neurites in Figure 2.16, which shows undifferentiated RN33B (spindle-shaped cells) in three different conditions: cells that are 1) vibrated on TCPS; 2) vibrated on unpoled PVDF films; or 3) vibrated on poled PVDF films; differences can be observed between the cells without and with electrical stimulation. This indicates that differentiation was induced in these neural cells without raising the temperature of the cells. This is important because increased temperature is a necessary condition of differentiation in these cells. The figure shows that there is a change in cell morphology with some dendrites growing in vibrated cells.

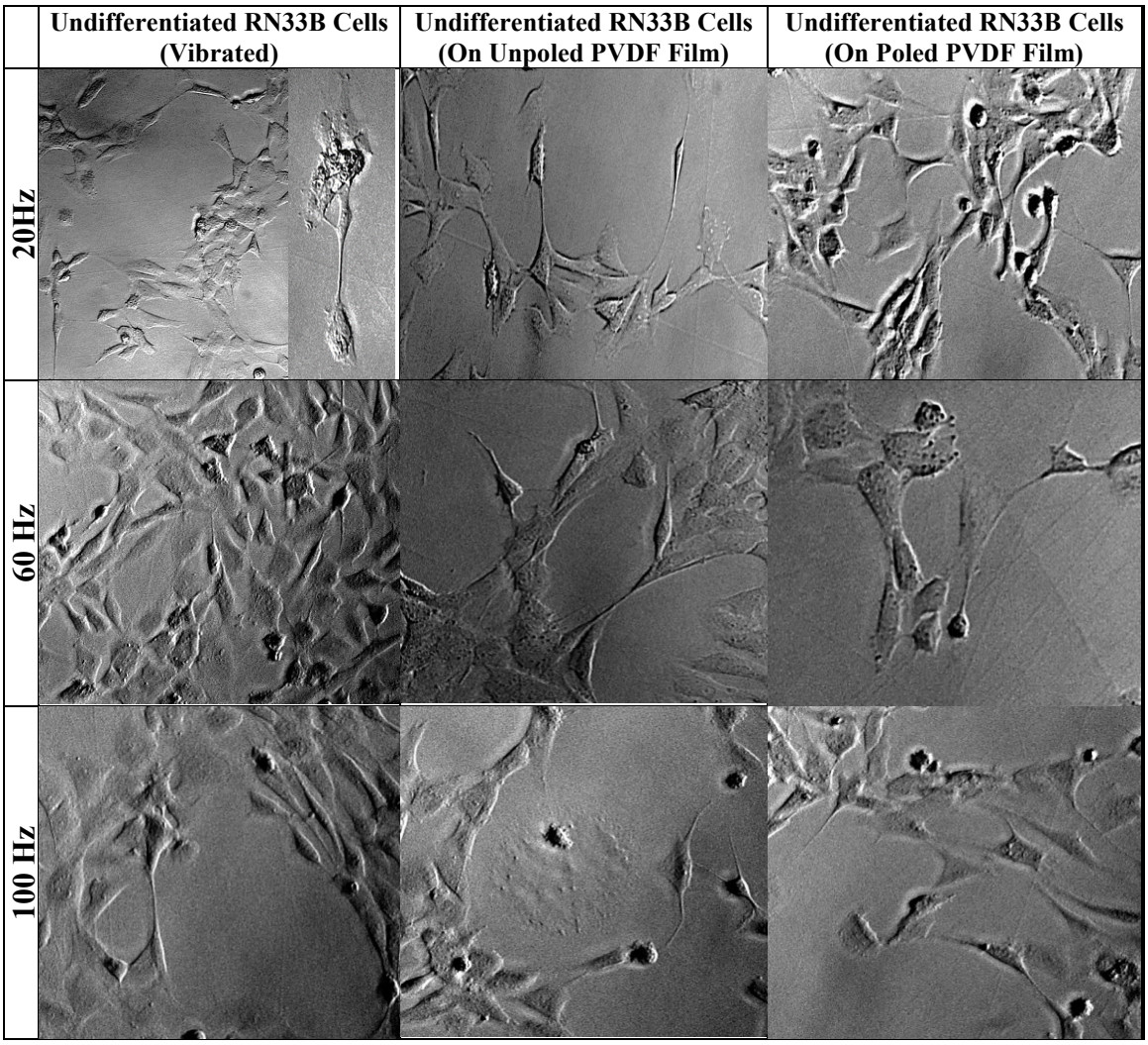

Figure 2.16: Undifferentiated RN33B cells that were vibrated on TCPS, vibrated on unpoled PVDF films or vibrated on poled PVDF films. 20x magnification. Evidence of neurite formation was strongest in cells vibrated on poled PVDF films.

Figure 2.17 shows differentiated RN33B (neurite-shaped) cells in three different conditions, vibrated cells on TCPS, and cells when seeded on (unpoled and poled) PVDF films and subjected to vibration. These images demonstrate that neurite growth is enhanced by electrical stimulation and piezoelectric stimulation.

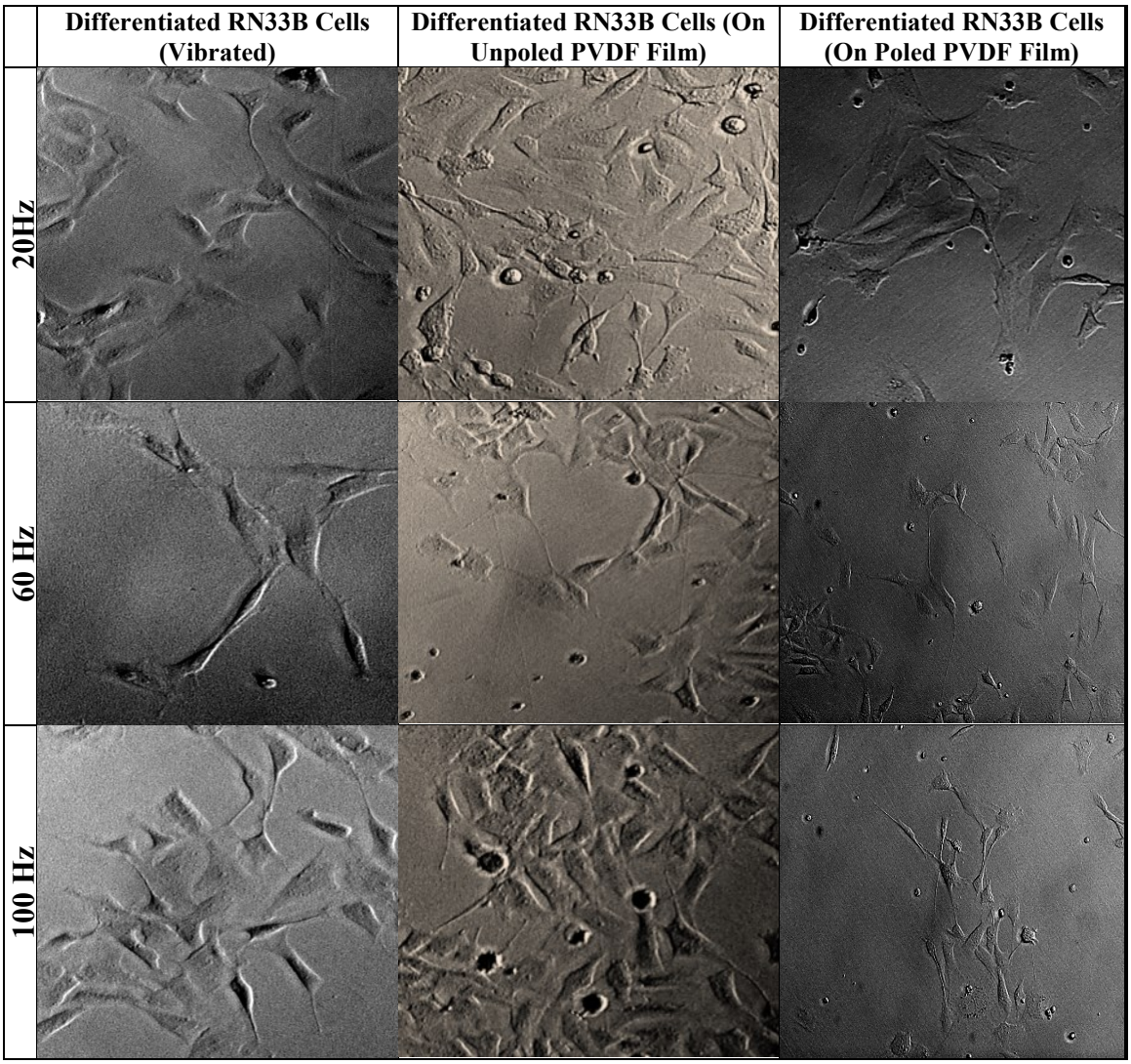

Figure 2.17: Differentiated RN33B cells that were vibrated on TCPS, vibrated on unpoled PVDF films, or vibrated on poled PVDF films. 20x magnification. Evidence of neurite formation was apparent in cells vibrated on TCPS, unpoled or poled PVDF.

Figures 2.18 and 2.19 the neurite extension of the same undifferentiated and differentiated RN33B cells when seeded on TCPS, unpoled or poled PVDF films respectively. Although these results did not show statistically significant differences, certain trends were observed.

For undifferentiated cells, vibration and not piezoelectricity resulted in the highest neurite length. Cells seeded on TCPS had the highest neurite extension (223 ± 118 µm) at 20 Hz.

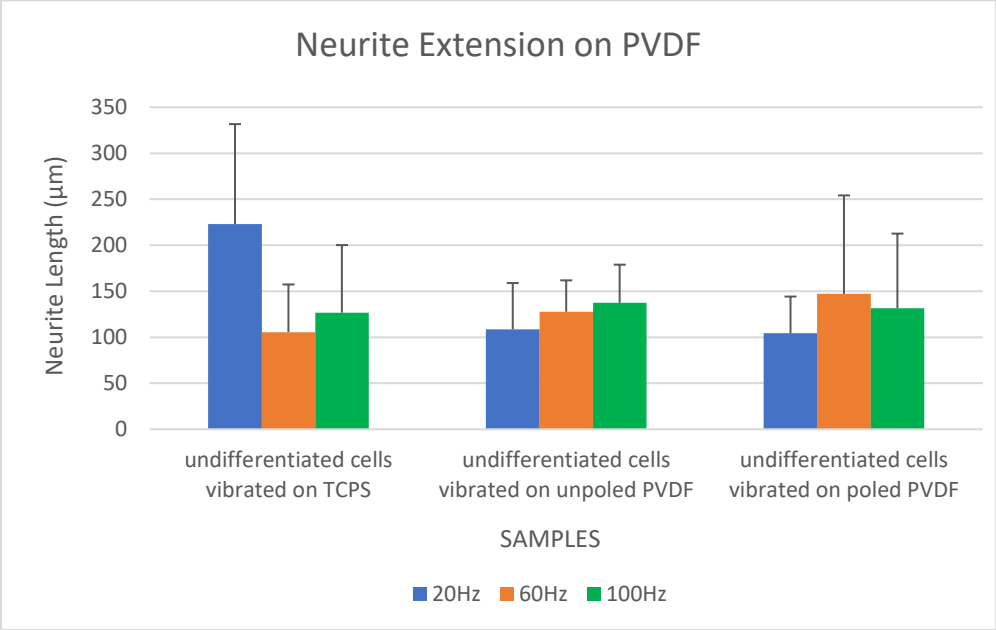

Figure 2.18: Undifferentiated RN33B neurite extension when seeding on TCPS, unpoled or poled PVDF films. Error bars show standard deviation.

For differentiated cells, vibration also resulted in the highest neurite length, but only when cells were seeded on unpoled PVDF, not TCPS. When seeded on unpoled films, the highest neurite extension occurred at 100 Hz (176 ± 78 µm).

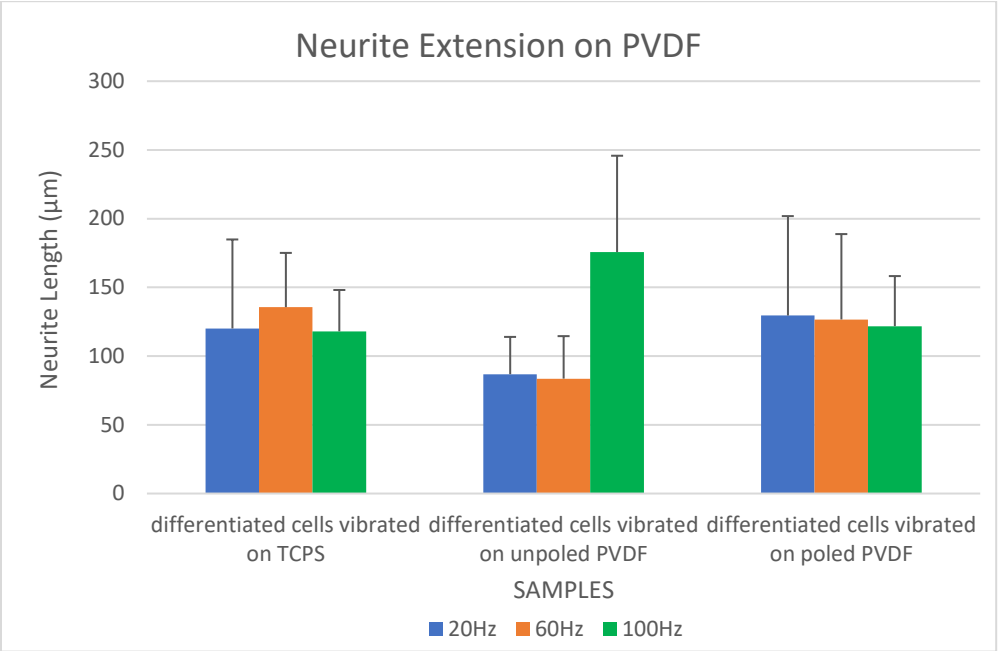

Figure 2.19: Differentiated RN33B neurite extension when seeded on TCPS, unpoled or poled PVDF films. Error bars show standard deviation.

2.4 DISCUSSION

2.4.1 The Effect of Mechanical Vibration on Cell Fate

As shown in the images, mechanical vibration significantly enhanced osteogenesis for hMSCs seeded on poled or unpoled PVDF membranes. Vibration on any substrate enhanced MC3T3-E1 mineralization. This suggests that vibration alone is sufficient to direct MC3T3-E1 cells to fully differentiate, but not sufficient for hMSCs, which are less differentiated than MC3T3-E1 pre-osteoblasts. Vibration in addition to PVDF was sufficient to differentiate hMSCs, regardless of poling state, which suggests that vibration plus a charged substrate are necessary to differentiate the hMSCs. Sate N. et al. reported similar findings, which suggested that an applied vibration induced cytomorphological changes of bone cells [12]. These changes in cellular structures are considered essential

events for bone cells detecting and transducing the external mechanical signals, and thus regulating the biological behavior of bone cells (e.g., adhesion, proliferation and differentiation) [13, 14].

2.4.2 The Effect of Polarization State on Cell Fate

Comparing the images in Figures 2.8-2.13, it is apparent that the piezoelectric PVDF films display increased red staining at earlier time points, indicating increased osteogenic activity in hMSCs and MC3T3-E1 cells. Previous in vivo and in vitro studies have indicated that poled and piezoelectric biomaterials containing piezoelectric films are biocompatible and promote bone formation around implants. Therefore, the development of biocompatible materials that mimic bone and its behavior could represent a powerful therapeutic tool [15, 16, 17]. The surface polarization state has been shown to influence cell adhesion, proliferation and differentiation. Many tissues are subjected to varying mechanical loads and those with piezoelectric properties result in charges that can stimulate a cell response, hence the use of polymer-based electroactive materials capable of mimicking mechanical and electrical biological cues has emerged as a novel approach for tissue engineering applications. For orthopedics in particular, the correct microenvironment is crucial for prosthesis osseointegration. In addition, bone exhibits piezoelectric properties, and it has been suggested that piezoelectric and streaming electrical potentials in bone may act as signals in mechanotransduction [18]. In addition, a recent study demonstrated that the surface charge of the poled PVDF films (positive or negative) influenced the hydrophobicity of the samples, leading to variations in the conformation of adsorbed extracellular matrix proteins, which ultimately modulated the stem cell adhesion on the

films and induced their osteogenic differentiation, a phenomenon that can also happen with some other cells, like pre-osteoblasts [19].

2.4.3 The Effect of Mechanical Vibration on Cell Proliferation

Figures 2.14 and 2.15 show that the mechanical stimulation reduced cell proliferation of both hMSCs and MC3T3-E1 cells when they were seeded on unpoled PVDF membranes. These results confirm the well-established fact that cell-cycle progression and differentiation are two mutually exclusive processes [20] and that increases in cell differentiation is generally accompanied by a parallel reduction in cell growth [21]. The arrest of cell growth in those two types of cells (as confirmed by MTS assay) when stimulated by mechanical vibration, combined with the positive Alizarin stain results is further evidence that this stimulus was triggering osteogenic differentiation of hMSCs and MC3T3-E1 cells. In addition, it has been demonstrated that cell differentiation causes cells to switch off genes required for proliferation [22]. Thus, it is possible that the results presented here show that when the cells start to differentiate under vibration, they switch off somatic genes associated with division.

Li et al. subjected hMSCs to oscillatory fluid flow and showed an increase in intracellular calcium mobilization as well as cell proliferation [23], while another study by Riddle et al. illustrated that fluid shear stresses enhanced hMSC proliferation in part due to calcium signaling. Ghazanfari et al. [24] demonstrated cyclic tensile strain can also increase MSC proliferation. In contrast, there are many conflicting studies that have mentioned that the mechanical stimulation has no effect on cell proliferation [25, 26, 27] or decreasing cell proliferation [28, 29, 30]. These mixed findings of mechanical stimulation's effect on cell

proliferation can most likely be explained by the diversity of conditions of each study design, including different cell types, culture conditions, and vibration protocols.

2.4.4 The Effect of Polarization State on Cell Proliferation

Figures 2.14 and 2.15 show that cell proliferation on poled PVDF films was higher than the cell proliferation on unpoled PVDF samples, suggesting that cell proliferation was improved due to the piezoelectric effect.

Previous investigations have demonstrated the influence of polarization of electroactive PVDF on biological responses of different cell types. Ashutosh K. D. et al. demonstrated that the application of an electric field enhanced cell proliferation and cell spreading on biomaterial surfaces when they remained within a narrow window of voltage/frequency of electrical stimulation [31]. In another study, C. Ribeiro et al. showed that MC3T3-E1 osteoblasts exhibited higher adhesion and proliferation in the presence of poled β-PVDF films and showed an increase in cell proliferation under dynamic conditions [32, 33].

Cell proliferation and cell growth are both cell fate processes, dependent on protein and DNA synthesis within the cell. It has been shown by Bourguignon et al. that protein and DNA synthesis are enhanced in the presence of an optimized electric field [34]. It is possible that the enhancement of protein and DNA synthesis is due to the effect of electric fields on the internal function of the cell. In a recent study by Schminnelpfeng et al., it was shown that low frequency electrical stimulation enhanced the cellular proliferation via secondary messenger dependent processes [35]. As far as the molecular mechanism of cell proliferation is concerned, an electrical signal is expected to activate extracellular signaling molecules during field application of 5 to 10 min after the first incubation stage. The

extracellular signaling molecules can be bound to cell surface receptor proteins and signals can be further transferred via molecular switch mechanisms to intracellular signaling proteins [36]. In a cell specific manner, the intracellular signaling pathway enables the electric field-induced signals to reach the target proteins.

2.4.5 The Effect of Mechanical Vibration on Neurite Growth

First, it is necessary to note the effect of mechanical vibration alone as a factor in neurite growth, as shown in Figures 2.16 and 2.17, which show vibrated cells seeded on TCPS and unpoled PVDF films. In each of these cases, the vibration increased neurite growth. Few studies have investigated effect of vibration on neural cells in culture, in addition, a detailed mechanism of the response to vibration stimulation has not yet been described; however, one study in the field of nano-vibration, showed significant vibratory enhancement of neurite growth after several days at 10 kHz, and indicated that enzymes could be activated by this stimulation [37]. These results suggest that the oscillation of membrane proteins or the cell membrane itself could be a biological signaling factor. Further, as was described in the Background section, certain studies have postulated that the cell membrane acts as a piezoelectric body, and it is possible that the vibration induced an "auto-piezoelectric" effect on the cells. Additionally, several studies have shown that mechanical force activates signaling pathways and regulates cell function, leading to morphological changes or cell–cell/cell–matrix interactions [38].

2.4.6 The Effect of Poling State on Neurite Growth

Figures 2.16 and 2.17 show images of vibrated cells that are seeded on poled PVDF films. In these images, it can be seen that piezoelectric stimulation enhanced neurite growth and

increased neurite alignment. This result is supported by the literature. Udina E. et al. showed that outgrowth from both dorsal root ganglion cells (DRGs) *in vitro* and spinal sensory nerves *in vivo* was enhanced by electrical stimulation on PVDF films vibrated at 20 Hz due to release of cyclic adenosine monophosphate (cAMP) [39]. Cyclic AMP is a second messenger used for intracellular signal transduction, such as transferring into cells the effects of hormones that cannot pass through the plasma membrane. In addition, cAMP binds to and regulates the function of ion channels such as the HCN channels and several other cyclic nucleotide-binding proteins [39].

Another potential main player in the enhanced neurite formation is calcium. Direct evidence that voltage-gated Ca^{2+} channels play a major role in electric field galvanotropism (0.1-1.0 mV/μm uniform DC electric fields) was shown in mouse neuroblastoma cells, whose neurite extension and growth cone elongation toward the cathode correlated directly with cathode-directed elevation in $[Ca]_i$ and depolarization [40, 41]. Many studies have demonstrated how electric fields, both endogenous and exogenous, can affect neuronal morphology and growth [42, 43]. The results in this study suggest that this may have been a factor; the neuronal-like cells that resulted from the hMSCs vibrated at 100 Hz showed extensive Alizarin red staining, which is a calcium stain.

2.5 CONCLUSIONS

The aim of this chapter was to investigate the effect of oscillating electric fields on a variety of mesenchymal tissues- hMSCs, bone, and nerve cells by seeding them on poled and unpoled PVDF membranes and vibrating them at 20, 60, and 100 Hz. The results of this study indicated significant increases in osteogenic activity for both of the former cell types under the effect of mechanical vibration and piezoelectricity. MTS assays of hMSCs and MC3T3-E1 cells verified that proliferation of both cell types was enhanced due to the piezoelectric effect of poled PVDF films and reduced in response to mechanical stimulation. Neurite imaging of undifferentiated and differentiated RN33B cells illustrated increases in neurite growth under the effect of both mechanical and electrical stimulation. This study better defines some of the stimulation parameters optimal for neural and osteogenic differentiation and has already resulted in unexpected and new findings not yet reported in the literature, such as the morphological changes observed in mesenchymal stem cells stimulated at 100 Hz towards a neuronal like morphology.

REFERENCES

1. Bacakova L, Filova E, Parizek M, Ruml T, Svorcik V. Modulation of cell adhesion, proliferation and differentiation on materials designed for body implants. Biotechnol Adv 2011; 29:739–767.
2. Martins P, Lopes AC, Lanceros-Mendez S. Electroactive phases of poly (vinylidene fluoride): Determination, processing and applications. olProg Pym Sci 2014; 39:683–706.
3. Sencadas V, Ribeiro C, Bdikin IK, Kholkin AL, Lanceros-Mendez S. Local piezoelectric response of single poly (vinylidene fluoride) electrospun fibers. Phys Status Solidi A 2012; 209:2605–2609.
4. Ribeiro C, Sencadas V, Ribelles JLG, Lanceros-M_endez S. Influence of processing conditions on polymorphism and nanofiber morphology of electroactive poly (vinylidene fluoride) electrospun membranes. Soft Mater 2010; 8:274–287.
5. Y.-S. Lee and T. L. Arinzeh, Tissue Eng. Part A, 2012, 19–20, 2063–2072.
6. H.-S. Huag, S.-H. Chou, T.-M. Don, W.-C. Lai and L.-P. Cheng, Polym. Adv. Technol., 2009, 20, 1082–1090.
7. N. Weber, Y. S. Lee, S. Shanmugasundaram, M. Jaffe and T. L. Arinzeh, Acta Biomater., 2010, 6, 3550–3556.
8. https://en.wikipedia.org/wiki/Hilton%27s_law Access date: 3 April 2018
9. Savio Lau-Yuen Woo, and Joseph Addision Buckwalter, Injury and Repair of the Musculoskeletal Soft Tissues Savannah, Georgia, June 18-20, 1987.
10. https://en.wikipedia.org/wiki/Mesenchymal_stem_cell Access date: 3 April 2018
11. Evan Y. Snyder and Cathryn A. Sundback, Neural Precursor Cell Lines Promote Neurite Branching, The International journal of neuroscience · February 2009.
12. Sato, N. et al. Osteoblast mechanoresponses on Ti with different surface topographies. J Dent Res 88, 812–816 (2009).
13. Huang, H., Kamm, R. D. & Lee, R. T. Cell mechanics and mechanotransduction: pathways, probes, and physiology. Am J Physiol Cell Physiol 287, C1–11 (2004).
14. Klein-Nulend, J., Bacabac, R. G. & Bakker, A. D. Mechanical loading and how it affects bone cells: the role of the osteocyte cytoskeleton in maintaining our skeleton. Eur Cell Mater 24, 278–291 (2012).
15. Baxter FR, Bowen CR, Turner IG, Dent ACE. Electrically active bio- ceramics: A review of interfacial responses. Ann Biomed Eng 2010; 38:2079–2092.
16. Beloti MM, De Oliveira PT, Gimenes R, Zaghete MA, Bertolini MJ, Rosa AL. In vitro biocompatibility of a nov el membrane of the composite poly(vinylidene-trifluoroethylene)/barium titanate. J Biomed Mater Res Part A 2006; 79:282–288.
17. Costa R, Ribeiro C, Lopes AC, Martins P, Sencadas V, Soares R, Lanceros-Mendez S. Osteoblast, fibroblast and in vivo biological response to poly (vinylidene fluoride) based composite materials. J Mater Sci: Mater Med 2013; 24:395–403.
18. Fukada E, Yasuda I. On the piezoelectric effect of bone. J Phys Soc Japan 1957; 12:1158–1162.
19. Jenita Parssinen, Henrik Hammar, Rolle Rahikainen, Vitor Sencadas, Clarisse Ribeiro, Sari Vanhatupa, Susanna Miettinen, Senentxu Lanceros-Mendez, Vesa P. Hytonen:

Enhancement of adhesion and promotion of osteogenic differentiation of human adipose stem cells by poled electroactive poly (vinylidene fluoride). University of Tampere 33014, Finland,2014.

20. Lee KW, Kim HJ, Lee YS, Park HJ, Choi JW, Ha J, et al. Acteoside inhibits human promyelocytic HL-60 leukemia cell proliferation via inducing cell cycle arrest at G0/G1 phase and differentiation into monocyte. Carcinogenesis 2007;28(9):1928.
21. Franceschi R. The developmental control of osteoblastspecific gene expression: role of specific transcription factors and the extracellular matrix environment. Critical Reviews in Oral Biology & Medicine 1999;10(1):40.
22. Chamley-Campbell, J., Campbell, G.R., and Ross, R. The smooth muscle cell in culture. Physiol. Rev. 59, 1, 1979.
23. Li YJ, Batra NN, You LD, Meier SC, Coe IA, Yellowley CE et al. Oscillatory fluid flow affects human marrow stromal cell proliferation and differentiation. J Orthop Res 2004;22(6):1283-1289.
24. Riddle RC, Taylor AF, Genetos DC, Donahue HJ. MAP kinase and calcium signaling mediate fluid flowinduced human mesenchymal stem cell proliferation. Am J Physiol 2006;290:C776-C84.
25. Ghazanfari S, Tafazzoli-Shadpour M, Shokrgozar MA. Effects of cyclic stretch on proliferation of mesenchymal stem cells and their differentiation into smooth muscle cells. Biochem. Biophys Res Commun 2009; 388:601-605.
26. Angele P, Yoo JU, Smith C, Mansour J, Jepsen KJ, Nerlich M et al. Cyclic hydrostatic pressure enhances the chondrogenic phenotype of human mesenchymal progenitor cells differentiated in vitro. J Orthop Res 2003;21(3):451-457.8. 8.
27. Thomas GP, el Haj AJ. Bone marrow stromal cells are load responsive in vitro. Calcif Tissue Int 1996; 58:101-108.
28. Simmons CA, Matlis S, Thornton AJ, Chen SQ, Wang CY, Mooney DJ. Cyclic strain enhances matrix mineralization by adult human mesenchymal stem cells via the extracellular signal-regulated kinase (ERK1/2) signaling pathway. J Biomech 2003;36(8):1087-1096.
29. Hamilton DW, Maul TM, Vorp DA. Characterization of the response of bone marrow-derived progenitor cells to cyclic strain: implications for vascular tissue-engineering applications. Tissue Eng 2004; 10:361-369.
30. Zhao F, Chella R, Ma T. Effects of shear stress on 3-D human mesenchymal stem cell construct development in a perfusion bioreactor system: Experiments and hydrodynamic modeling. Biotechnol. Bioeng. 2007;96(3):584-595.
31. Ashutosh Kumar Dubey, Shourya Dutta Gupta, Bikramjit Basu, Optimization of electrical stimulation parameters for enhanced cell proliferation on biomaterial surfaces, Department of Materials Science and Engineering, Indian Institute of Technology, Kanpur 208016, Uttar Pradesh, India, 2011.
32. C. Ribeiro, J. A. Panadero, V. Sencadas, S. Lanceros- Mendez, M. N. Tamano, D. Moratal, M. Salmeron- Sanchez and J. L. Gomez Ribelles, Biomedical Materials, 2012, 7.
33. C. Ribeiro, S. Moreira, V. Correia, V. Sencadas, J. G. Rocha, F. M. Gama, J. L. Gomez Ribelles and S. Lanceros-Mendez, RSC Adv., 2012, 2, 11504–11509.

34. Bourguignon GJ, Bourguignon LYW. Electric stimulation of protein and DNA synthesis in human fibroblasts. FASEB J 1987;1: 398–402.
35. Schimmelpfeng J, Dertinger H. The action of 50 Hz magnetic and electric fields upon cell proliferation and cyclic AMP content of cultured mammalian cells. Bioelect Bioenerg 1993; 30:143–150.
36. Alberts B, Johnson A, Lewis J, Raff M, Roberts K, Walter P, Molecular Biology of the Cell, 4th ed. New York: Garland Science; 2002.
37. Ito, Y., T. Kimura, K. Nam, A. Katoh, T. Masuzawa, and A. Kishida. Effects of vibration on differentiation of cul- tured pc12 cells. Biotechnol. Bioeng. 108(3):592–599, 2011.
38. Wang N, Tytell JD, Ingber DE. 2009. Mechanotransduction at a distance: Mechanically coupling the extracellular matrix with the nucleus. Nat Rev Mol Cell Biol 10:75–82.
39. Udina, E., M. Furey, S. Busch, J. Silver, T. Gordon, and K. Fouad. Electrical stimulation of intact peripheral sen- sory axons in rats promotes outgrowth of their central projections. Exp. Neurol. 210(1):238–247, 2008.
40. Zheng, J. Q., and M. M. Poo. Calcium signaling in neuronal motility. Annu. Rev. Cell Dev. Biol. 23:375–404, 2007.
41. Bedlack, Jr., R. S. M. Wei, and L.M. Loew. Localized membrane depolarizations and localized calcium influx during electric field-guided neurite growth. Neuron 9(3):393–403, 1992.
42. Ghasemi-Mobarakeh, L., M. P. Prabhakaran, M. Morshed, M. H. Nasr-Esfahani, H. Baharvand, S. Kiani, S. Al-Deyab, and S. Ramakrishna. Application of conductive polymers, scaffolds and electrical stimulation for nerve tissue engineering. J. Tissue Eng. Regenerative Med. 5(4): E17–E35, 2011.
43. McCaig, C. D., B. Song, and A. M. Rajnicek. Electrical dimensions in cell science. J. Cell Sci. 122(23):4267–4276, 2009.

CHAPTER 3: THE EFFECT OF STATIONARY ELECTRIC FIELDS ON CELLS

3.1 INTRODUCTION

Polarized, static piezoelectric PVDF films produce a stationary electric field at their surfaces; however, when these films are placed in cell culture media, it is expected that free ions within the media will attach to the oppositely charged surfaces of the piezoelectric PVDF films. It is also expected that although the stationary charge is cancelled out by these cell media ions, oscillating fields are not cancelled by vibratory motion. Previous studies have demonstrated that piezoelectric PVDF provides bioactive electrically charged surfaces for a variety of applications. Schneider GB et al. showed that surface charge is a critical factor for osteoblast attachment and spreading [1]. In addition, neurite lengthening and branching are promoted in neuronal cells cultured in piezoelectric PVDF substrates [2]. These studies open the door for the use of biomaterials with piezoelectric properties in different medical applications.

Mouse preosteoblasts, hMSCs, and rat neurons were seeded on tissue culture polystyrene (TCPS) and three kinds of PVDF film surfaces: 1) unpoled films with no surface charge; 2) poled films with cells cultured on the positively charged side of the sample; and 3) poled films with cells cultured on the negatively charged side of the sample. The same methods described in Chapter 2 were employed to observe how the stationary electric field affects cell differentiation and growth, see Figure 3.1.

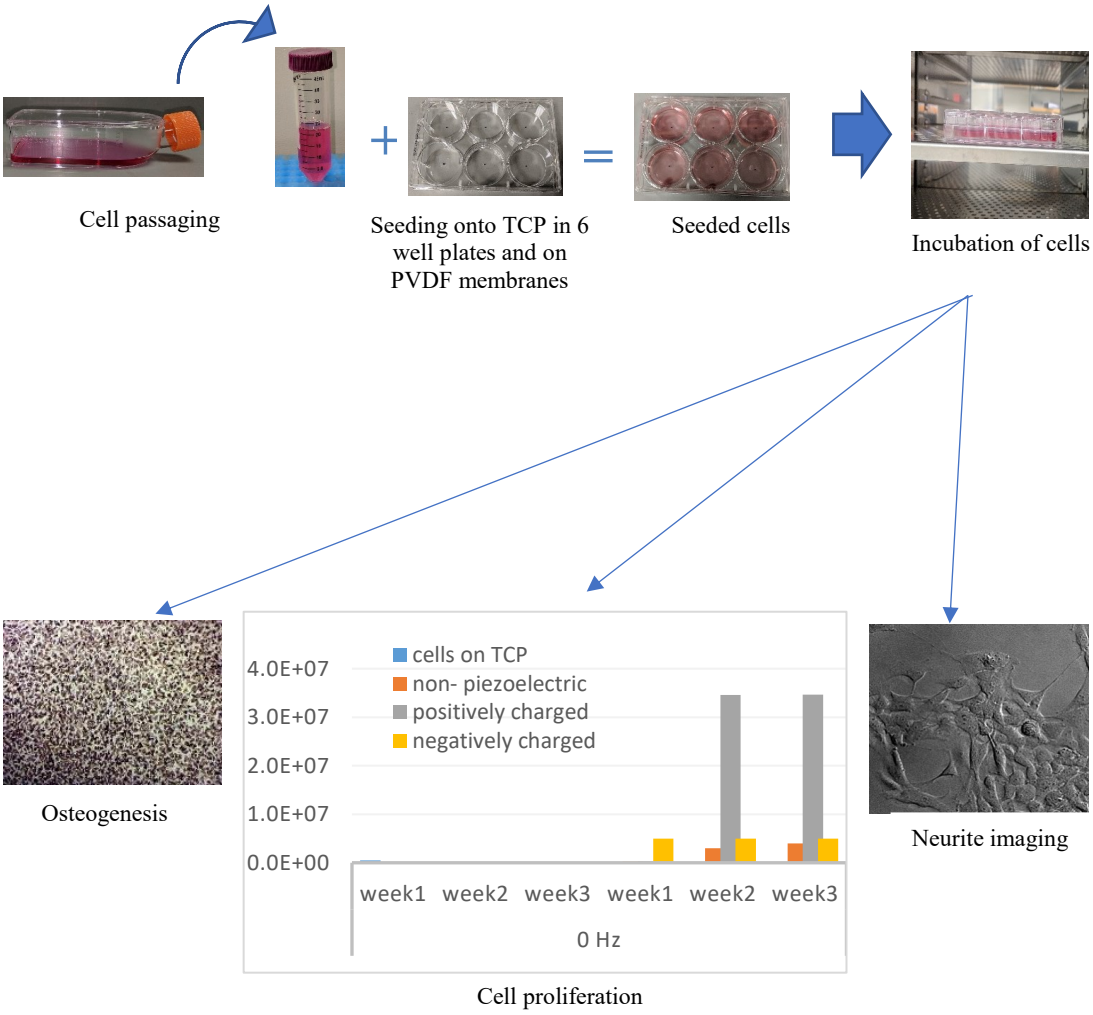

Figure 3.1: Schematic of the experimental design of this chapter.

3.2 MATERIALS AND METHODS

3.2.1 Tissue Culture

Human mesenchymal stem cells (hMSCs isolated from normal adult human bone marrow and reported to differentiate down many different lineages including chondrogenic, osteogenic, adipogenic and neural [3] were obtained from the Texas A&M Health Science Center College of Medicine Institute for Regenerative Medicine at Scott & White. MC3T3-

E1 pre-osteoblasts (a cell line of mouse (Mus musculus) calvaria preosteoblast cells, commonly used for studies concerning bone differentiation and development) were obtained from ATCC. hMSCs and MC3T3-E1 cells were cultured in Minimum Essential Medium (MEM alpha nucleosides) (was obtained from Thermofisher Scientific company) with 15% Fetal Bovine Serum (FBS) and 1% Penicillin/Streptomycin (P/S) (were obtained from Sigma Aldrich company) (growth media), at 37ºC in humidified air containing 5% CO_2. The media was changed three times a week.

RN33B (a neuronal cell line derived from medullary raphe cells that retain many properties of mature CNS neurons) spindle-shaped cells were obtained from ATCC and cultured in Dulbecco's Modified Eagle's Medium (DMEM)/Nutrient Mixture F-12 Ham with 10% Fetal Bovine Serum (FBS) and 1% Penicillin/Streptomycin (P/S), at 33ºC in 95% humidified air containing 5% CO. The medium was changed three times a week. To differentiate RN33B cells towards into neurite-shaped cells, 175 cm^2 tissue culture flasks of 75% confluent cells were incubated at 37ºC in humidified air containing 5% CO_2. The cells required about 2 weeks to differentiate.

3.2.2 Poly (vinylidene fluoride) PVDF Film Preparation

PVDF films (obtained from Kureha Corporation) were prepared identically to those described in Chapter 2 with the modification that these films were not vibrated. PVDF films (unpoled and poled) with a thickness of 0.03-0.04 mm were obtained from Kureha Corporation with the positive and negative surfaces marked. The films were cut into small square sheets (1 cm x 1 cm) and sterilized by immersing 3 times in fresh 70% ethanol for 30 min. Then, the samples were washed 5 times for 5 min in sterile PBS to eliminate any

residual ethanol. Finally, the samples were exposed to UV light for 2 hrs (1 hr. each side). The film samples were glued to 6-well tissue culture polystyrene plate (TPCS) by using liquid tissue adhesion glue, Vetbond, as described in Chapter 2 (Figure 2.4).

hMSCs, MC3T3-E1, and RN33B (spindle and neurite-shaped) cells were seeded directly onto well plates, unpoled PVDF films, or onto either the positive or negative surface of poled PVDF films. The cells were seeded at densities of $2x10^3$ cells/cm^2, $25x10^3$ cells/cm^2 and $1x10^4$ cells/cm^2 for each cell type respectively, then incubated for three weeks.

3.2.3 Alizarin Red Staining of hMSCs and MC3T3-E1 Cells

To determine whether hMSCs and MC3T3-E1 cells differentiate into osteoblasts due to the surface charge of the substrate, an Alizarin red staining (ARS) assay was used. Alizarin red is an anthraquinone dye (obtained from Sigma Aldrich company) and has been widely used to evaluate calcium deposits in cell culture. The ARS staining is quite versatile because the dye can be extracted from the stained monolayer of cells and readily assayed. Since cells that have differentiated into osteoblasts form calcium deposits as a precursor to bone, positive Alizarin staining is a marker of osteogenic differentiation. Monolayers in 6-well plates (9 cm^2/well) were washed with 1.0 mL PBS and fixed in 10% (v/v) formalin (obtained from Sigma Aldrich company) at room temperature for 15 min. The monolayers were then washed twice with excess dH_2O prior to the addition of 1 mL of 40 mM ARS (pH 4.2) per well. The plates were incubated at room temperature for 20 min with gentle shaking. After aspiration of the unincorporated dye, the wells were washed four times with 1 mL dH_2O for 5 min each time. The plates were then left at an angle for 2 min to facilitate removal of excess water. Stained monolayers were visualized by phase contrast

microscopy. The cells were fixed for staining at time points: Week 1, Week 2, and Week 3.

3.2.4 MTS Assay of hMSCs and MC3T3-E1 Cells

To evaluate the effect of surface charge on hMSCs and MC3T3-E1 cell proliferation, the cells were seeded in 6-well culture plates as described in Section and incubated for three weeks. The cells were evaluated at Week 1, Week 2 and Week 3. MTS (3 - (4, 5-dymethylthiazol- 2- yl)- 5- (3- carboxymethoxyphenyl)- 2 (4- sulfopheny)- 2H tetrazolium) assay (CellTiter 96TM Aqueous One Solution Cell Proliferation Assay, Promega) was carried out to quantify cell proliferation. Assays are performed by adding CellTiter 96 ® Aqueous One Solution Reagent (1:5 w/v) directly to media in well cultures, incubating for 1–4 hours and then recording the absorbance at 492nm with a 96-well plate reader (DTX 880 Multimode Detector).

3.2.5 Neurite Imaging

Neurons were seeded in 6-well culture plates with PVDF films and incubated for a week. Incubated neurons were imaged using phase contrast microscopy. After 1 week, RN33B cells (spindle- shaped and neurite- shaped) were imaged on TCPS or on PVDF films prepared as described in Section 3.3.3. Cell morphology was evaluated for potential neurite formation. NIH ImageJ analysis of neurite outgrowth was used to measure neurite length average.

3.2.6 Statistical Analysis

Cellular metabolic activity and neurite extension were compared between the unpoled and positive (+) or negative (-) poled PVDF membranes using an analysis of variance (ANOVA). *p*-Values less than 0.05 were considered significant. Pairwise comparison between groups was performed after ANOVA using the least significant difference (LSD) method. All analyses were conducted using Microsoft Excel. Statistical significance is denoted in the figures, which are reported as mean ± standard deviation.

3.3 RESULTS

3.3.1 Alizarin Red Staining of hMSCs and MC3T3-E1 Cells

Images of ARS stained hMSCs and MC3T3-E1cells seeded with unpoled and positive (+) or negative (-) poled PVDF membranes in 6-well plates at Week 1, Week 2 and Week 3 are presented in Figures 3.2 and 3.3. These figures show qualitatively that compared to oscillating electric fields, the stationary electric field induced a more homogeneous distribution of hMSCs and MC3T3-E1 cells. There were no particularly dense areas of cells in these non-vibrated cell groups compared to the dense areas that were common when cells were subjected to vibration and oscillating electric fields. Differentiation and mineralization was observed in hMSCs seeded on positively charged PVDF films, but mineralization was not induced in all cell samples. MC3T3-E1 cells did not show any mineralization.

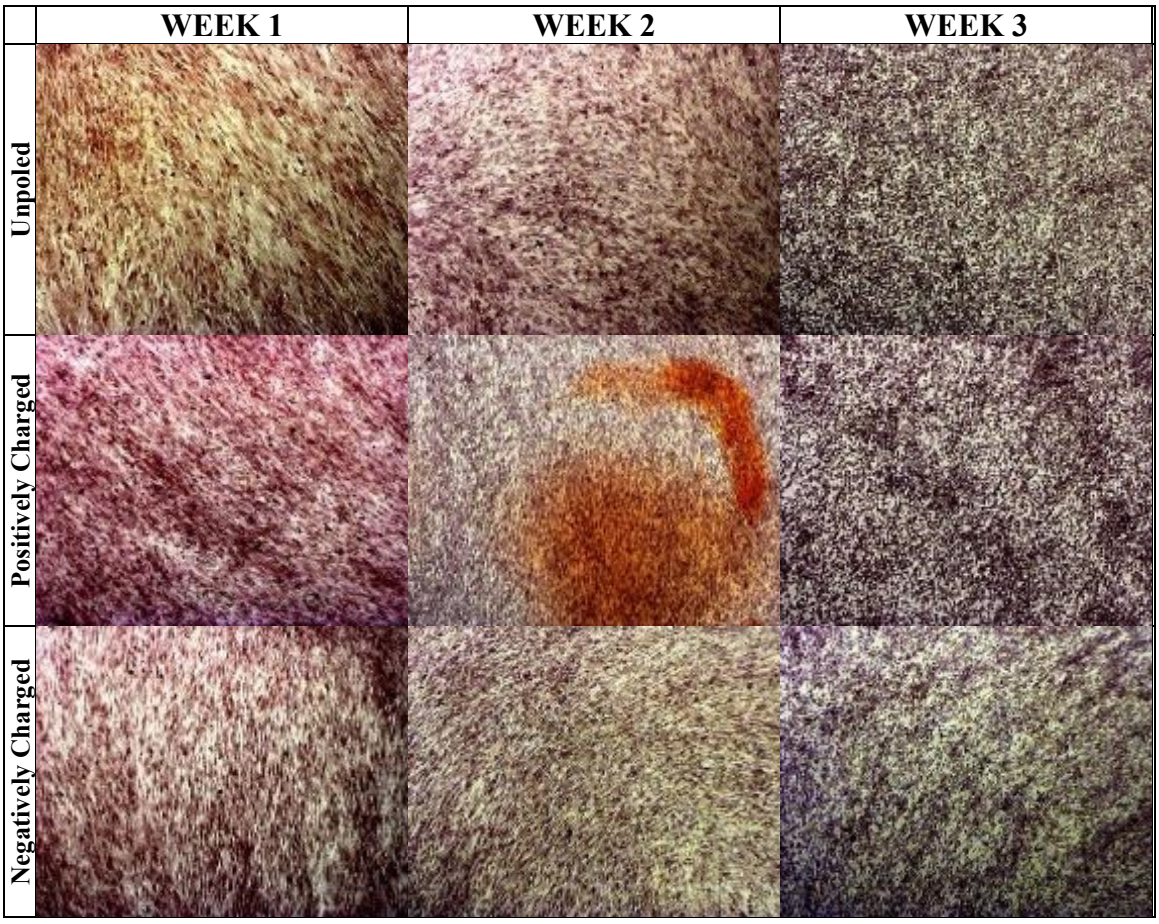

Figure 3.2: Alizarin red stained monolayers of hMSCs seeded on unpoled, positively charged, negatively charged PVDF films in 6- well plates. The cells were stained at Week 1, Week 2 and Week 3. Red stain shows mineralization.

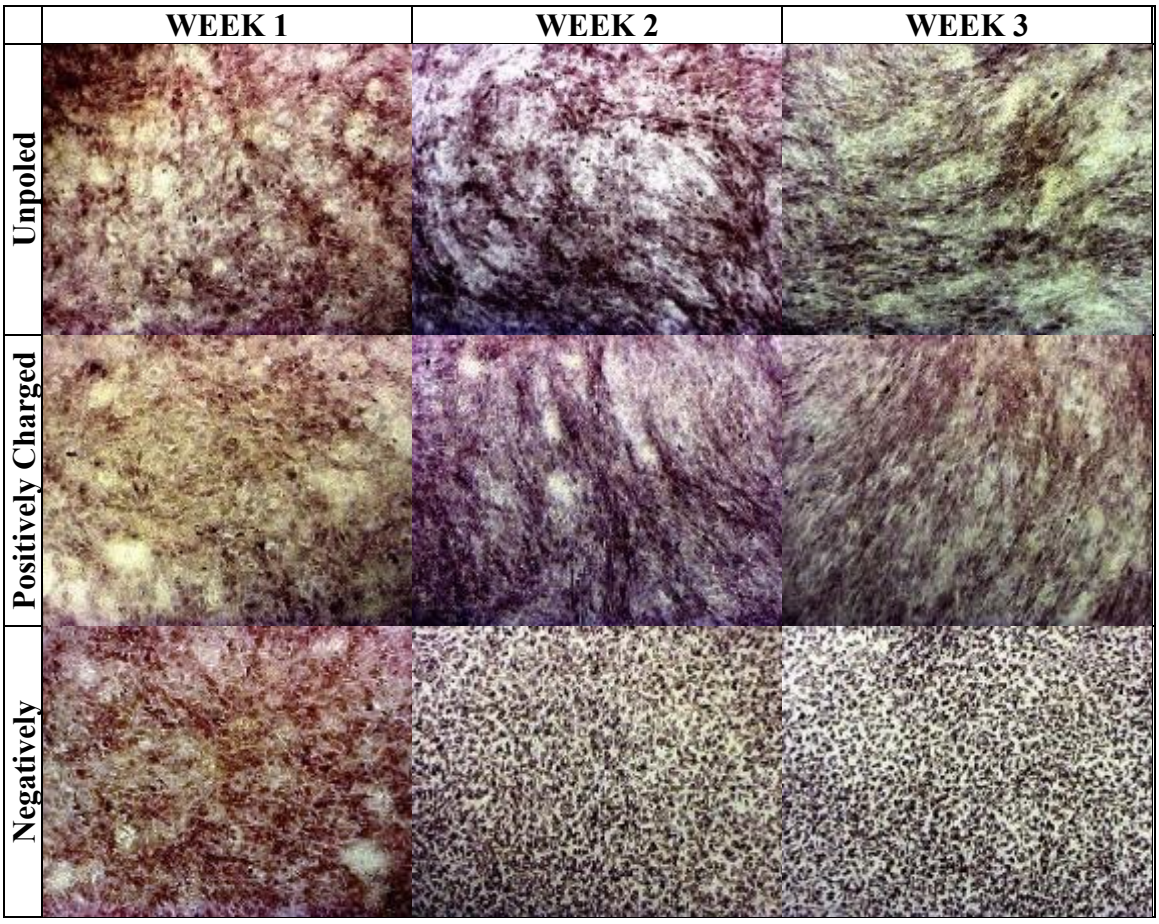

Figure 3.3: Alizarin Red Staining assays of MC3TE-E1 seeded on unpoled, positively charged, negatively charged PVDF films in 6- well plates. The cells were stained at Week 1, Week 2, and Week 3.

3.3.2 MTS Assays of hMSCs and MC3T3-E1 Cells

When seeded onto unpoled and the positive or negative surfaces of poled PVDF membranes (+) or (-), hMSCs and MC3T3-E1 cells proliferated rapidly, completely covering the surface by the first week of culture. The proliferation of both cell types appeared similar on TCPS and PVDF membranes when observed under an optical microscope.

Figures 3.4 and 3.5 show the quantified results of seeding hMSCs and MC3T3-E1 cells on the various scaffolds over the time course of the experiment. Figure 3.4 statistically shows that the experimental group with the highest number of metabolically active hMSCs were seeded on (+) poled PVDF films at Week 2 and Week 3. Figure 3.5 statistically shows the highest number of viable MC3T3-E1 cells when seeded on unpoled PVDF films at Week 2 and Week 3.

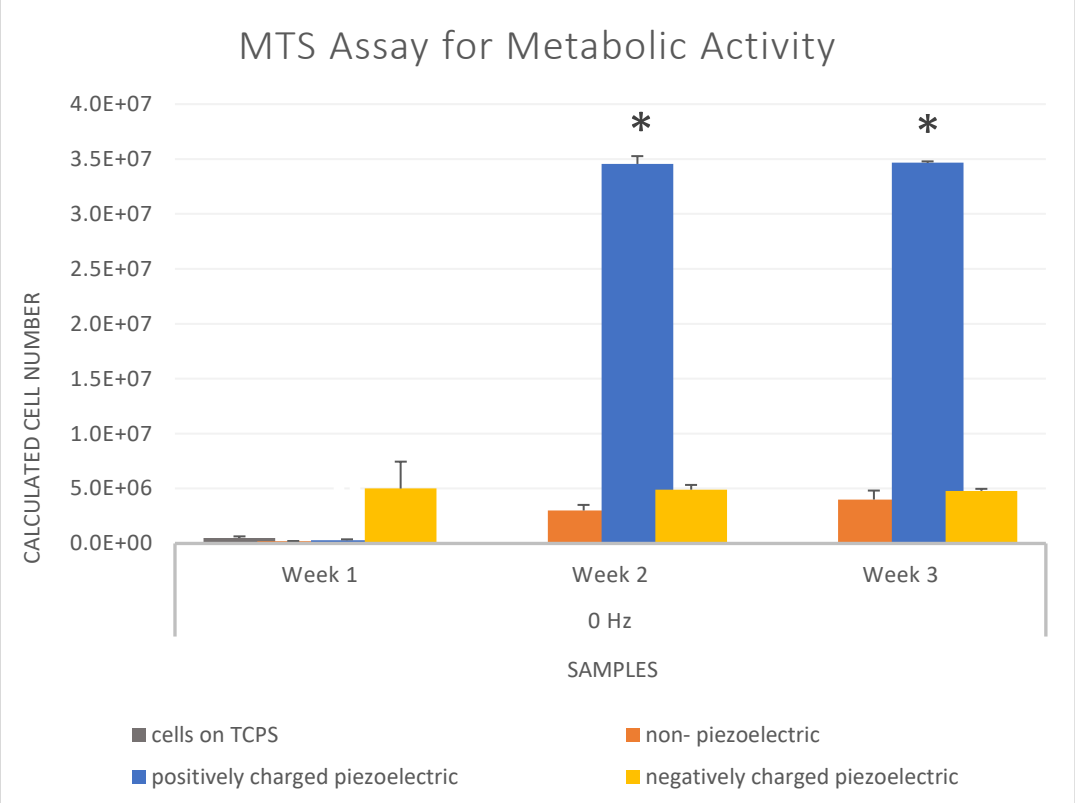

Figure 3.4: Cell proliferation of hMSCs seeded on TCPS, non-piezoelectric, and (+/-) piezoelectric PVDF films at Week 1, Week 2, and Week 3 after seeding. Positively charged piezoelectric PVDF films show statistically significant increases ($p < 0.05$) over negatively charged piezoelectric and non-piezoelectric PVDF films on corresponding days. Asterisks indicate significance. Error bars show standard deviation.

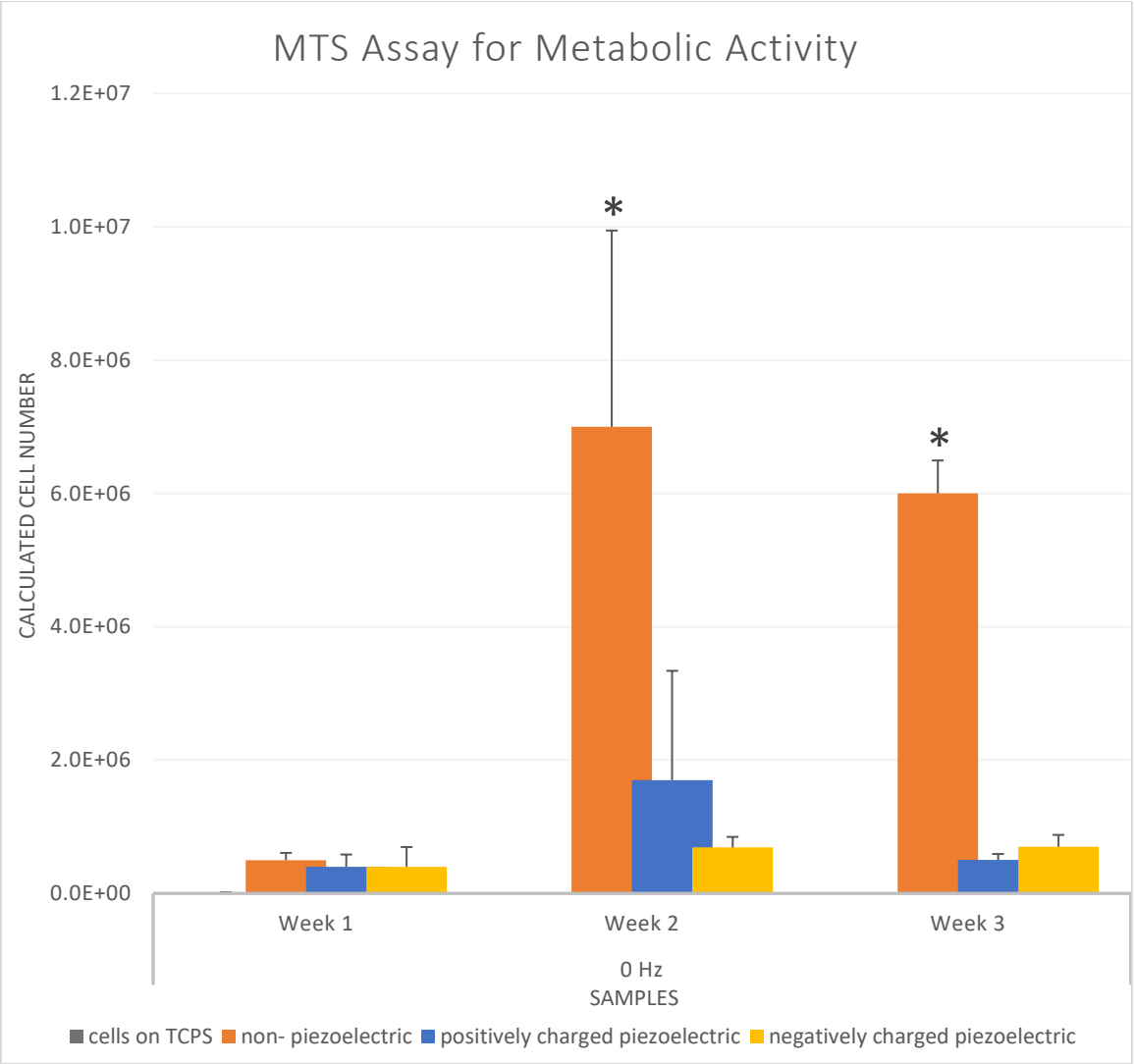

Figure 3.5: Cell proliferation of MC3T3-E1 cells seeded on TCPS, non-piezoelectric and (+/-) piezoelectric PVDF films at Week 1, Week 2, and Week 3 after seeding. Non-piezoelectric PVDF films show statistically significant increases ($p < 0.05$) over positively and negatively charged piezoelectric PVDF films on corresponding days. Asterisks indicate significance. Error bars show standard deviation.

3.3.3 Neurite Imaging

The results of this chapter indicate that in the absence of electrical stimulation, piezoelectric polymer membranes with a surface charge induce substantially higher levels of neurite outgrowth than electrically neutral membranes without surface charges as shown in Figures 3.6, 3.7 and 3.8.

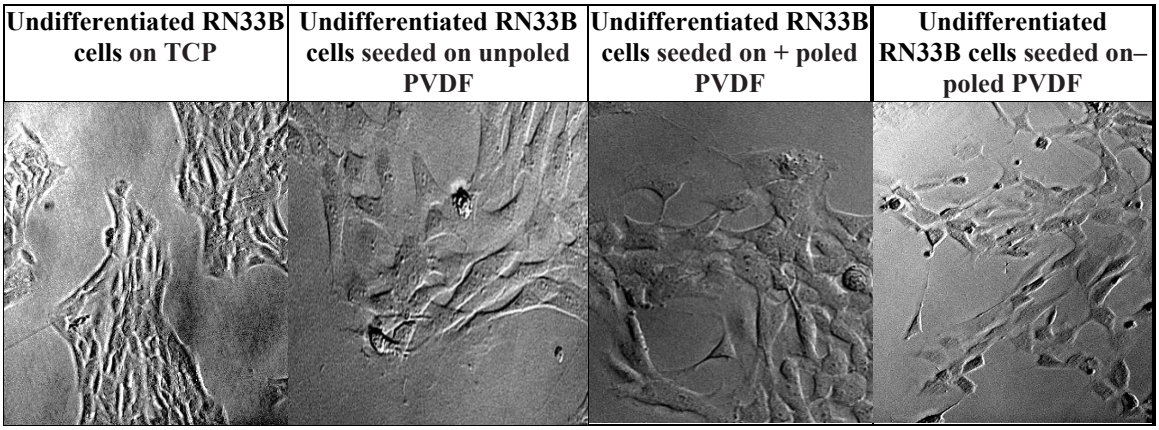

Figure 3.6: Undifferentiated RN33B cells that were seeded on TCPS, on unpoled PVDF, on (+) poled PVDF, or on (–) poled PVDF films. 20x magnification.

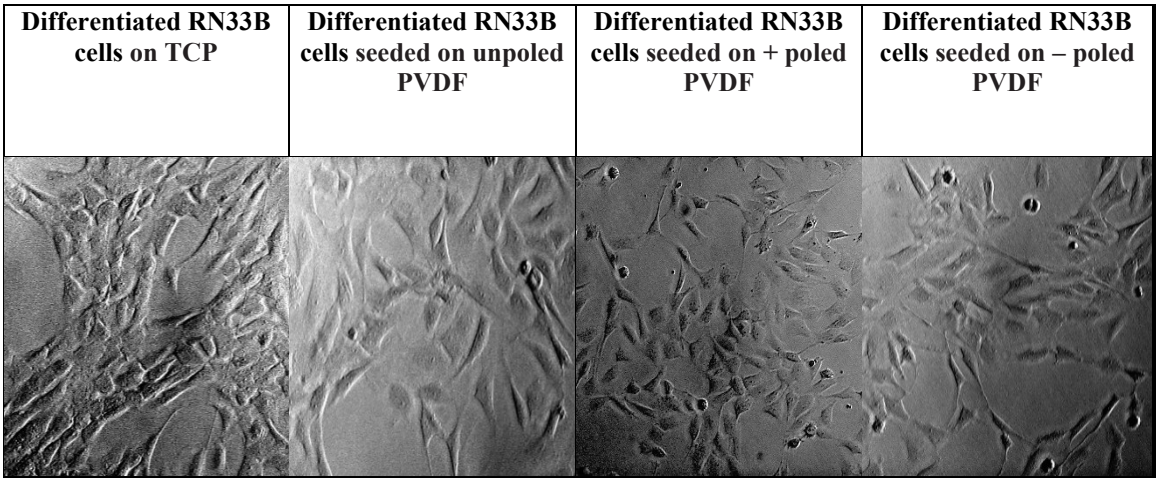

Figure 3.7: Differentiated RN33B cells that were seeded on TCPS, on unpoled PVDF films, on (+) poled PVDF, or on (–) poled PVDF films. 20x magnification.

Levels of cell attachment on poled and unpoled PVDF membranes were comparable to those on tissue culture polystyrene well plate. After a week of culture, cells with single or multiple neurites were observed on poled PVDF membranes. Neurites grew in all directions with no preferential outgrowth patterns as showed in Figures 3.6 and 3.7.

Figure 3.8 indicates undifferentiated and differentiated RN33B neurite extension when seeded on (+) poled PVDF, or on (–) poled PVDF films. Though not statistically significant, trends suggested that the undifferentiated cells preferred positively charged films whereas the differentiated cells preferred negatively charged films.

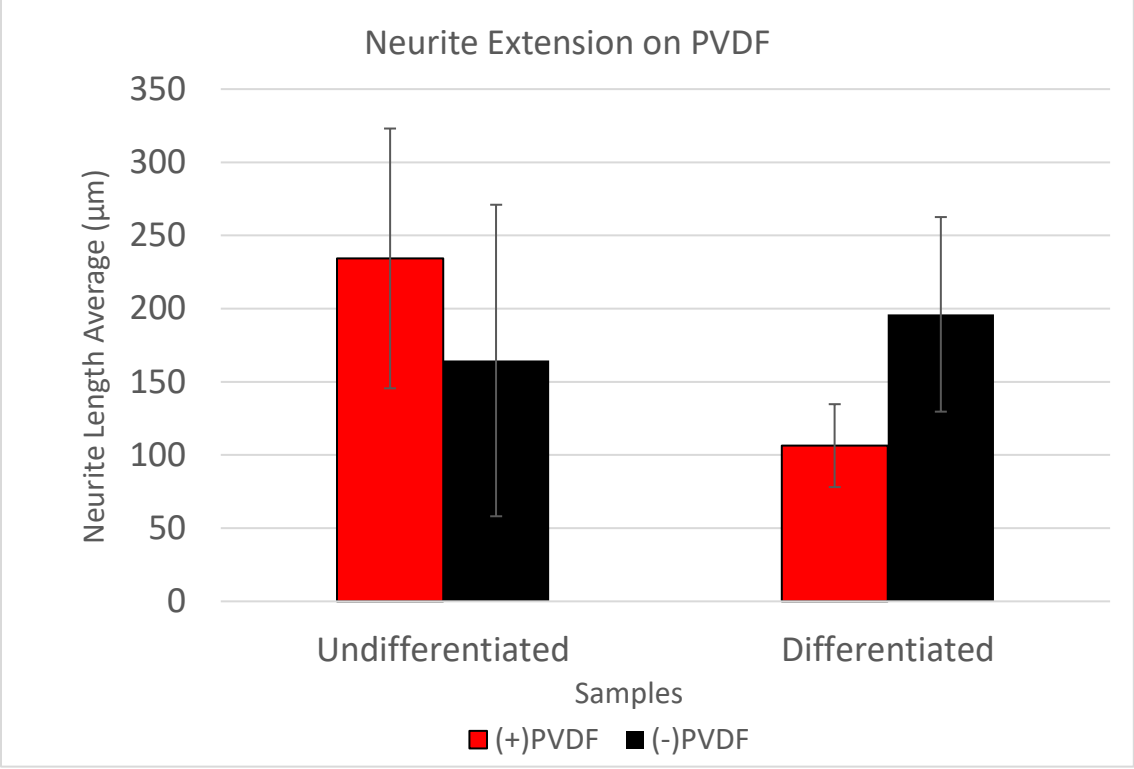

Figure 3.8: Undifferentiated and differentiated RN33B neurite extension when seeded on (+) poled PVDF, or on (–) poled PVDF films. Error bars show standard deviation.

3.4 DISCUSSION

3.4.1 Alizarin Red Staining of hMSCs and MC3T3-E1 Cells

Bone differentiation on charged PVDF membranes was not induced during the duration of this study. Conversely, during the duration of the experiments employing oscillating electric fields on poled PVDF under electromechanical stimulation, differentiation was observed. Most reports in the literature were performed in static conditions indicating only the suitability of PVDF as a biomaterial and the relevance of the (positive or negative) surface charge when the material is poled. Most of these studies do not explore the biological response to the piezoelectric effect. Based on these results, stationary conditions of piezoelectric films as biomaterials do not give a complete picture and a specific mechanical stimulus under dynamic conditions should be applied during cell culture. This dynamical mechanical stimulus can be compression, vibration or stretching of the piezoelectric material [4].

3.4.2 MTS Assays of hMSCs and MC3T3-E1 Cells

Recently, surface charge has been described as an important parameter for cell attachment and proliferation. In particular, it has been shown that positively and negatively charged surfaces support higher cell attachment than neutral surfaces and induce cell adhesion and proliferation in a cell type-dependent manner [5, 6, 7]. For instance, on a layer-by-layer polyelectrolyte with different surface charges, negatively charged surfaces supported higher attachment of C2C12 skeletal muscle cells than positively charged surfaces [8]. It has been shown that MC3T3-E1 osteoblasts exhibited higher adhesion and proliferation in the presence of (+) poled β-PVDF films and showed an increase in cell proliferation under

static and dynamic conditions [9]. This was confirmed by the experiments described in this chapter, where MC3T3-E1 cells trended towards a preference for positively charged surfaces. Conversely, hMSCs trended towards a preference for negatively charged surfaces.

The results from this chapter showed that under stationary (non-vibrating) conditions, hMSCs cell proliferation on charged PVDF membranes was higher than cell proliferation on unpoled PVDF membranes. Whereas MC3T3-E1 cells preferred the unpoled membranes. The mechanisms by which surface charge and piezoelectric properties affect the responses of different cell types has been investigated; however, to date, not a single mode of action has been identified. A factor of likely importance is the preferential adsorption of proteins and other molecules onto surfaces of different electrical states [10]. C. Ribeiro et al. demonstrated that the polarization of a PVDF electroactive crystalline phase affects the hydrophobicity/hydrophilicity of the film [11]. If the material is too hydrophobic, ECM molecules are adsorbed in a denatured and rigid state. Therefore, binding sites on these molecules are less accessible to cell adhesion receptors, and further, their conformation is inappropriate for binding to cells [12]. A protein bound in a denatured state may also be more tightly associated with the substrate compared to a non-denatured protein. Proteins with such strong surface interactions likely provide different types of mechanical cues than proteins with less pronounced surface interactions. Optimal protein adhesion only occurs on moderately hydrophilic surfaces (around 40–60º water contact angle), [13] whereas highly hydrophilic surfaces are known to bind adsorbed cell adhesion-

mediating molecules with relatively weak forces, which could lead to the detachment of these molecules during culture.

The surface properties of PVDF are influenced by its crystalline phase, not only because of the different arrangement of crystal lamellae that leads to a different roughness and surface topography, but also due to a different surface energy leading to a highly hydrophobic material in the case of unpoled *β*-PVDF and to a more hydrophilic one in the case of *α*-PVDF. The reason for these differences is related to the different ordering of the permanent dipoles along the polymer chains in different crystalline phases [14].

Jenita Pearssinen et al. confirmed that and (+) poled β-PVDF films were found to be the most hydrophilic of these materials, with a contact angle of 31.8º, which is lower than that measured for (-) pole" β-PVDF surfaces (51.1º) [15]. Therefore, the (-) poled β-PVDF films provided the most optimal surface hydrophobicity/hydrophilicity to promote protein adhesion, which modulates stem cell adhesion to PVDF films and leads to an increase in the growth of cells on that type of films. The results of this chapter confirmed these findings with the hMSCs. Furthermore, this chapter's results extend these findings by showing that positively charged surfaces are capable of inducing osteodifferentiation and osteogenesis in hMSCs.

3.4.3 Neurite Imaging

Since neurite outgrowth was observed on charged PVDF films but not on tissue culture polystyrene, it suggests that neurite outgrowth was induced by the surface charges of the films. These results suggest that local electrical charges stimulate neurite outgrowth.

The mechanism by which piezoelectric activity enhances neurite outgrowth is unknown. It is possible that piezoelectric activity increases the synthesis or secretion of extracellular matrix molecules required for neurite outgrowth [16]. Thus, the secreted molecules may form preferential pathways for neurite outgrowth. Differences in the levels of cell attachment on poled and unpoled films were not correlated with neurite growth; cell attachment densities appeared the same for both. Both poled and unpoled films have the same chemical compositions and differ only in orientation of the internal molecular structure and ability to generate transient charges, making them ideal for distinguishing cell responses to surface differences in field effects. Valentini et al. showed that the chemical compositions and adhesion profiles were indistinguishable between poled and unpoled PVDF or P(VDF-TrFE) [16]. It is important to note that these materials do not contain any potentially ionizable surface groups that may contribute to local charge generation.

Therefore, it is possible to conclude the enhancement of neurite growth is due to the influence of piezoelectric activity rather than to changes in the surface structure, chemical composition, or adhesive nature of the PVDF film. Valentini et al. [17] described the use of electrically charged and uncharged polytetrafluoroethylene channels to repair transected sciatic nerves in adult mice and showed that regeneration of nerves in both types of electrically charged channels contained significantly more myelinated axons than nerves in uncharged channels. Aebischer et al. constructed piezoelectric nerve guidance channels from PVDF tubes to study their effect in a transected mouse sciatic nerve model [18]. They compared poled PVDF channels to unpoled PVDF channels after 4 and 12 weeks of

implantation. In all animals, the proximal and distal nerve stumps were connected by a continuous nerve cable. Similar to the Aebischer study, nerves regenerated in poled channels had a higher number of myelinated axons than those regenerated in unpoled channels at both time periods. This study concluded that piezoelectric nerve guidance channels induce peripheral nerve regeneration and provide a tool to investigate the influence of electrical activity on nerve regeneration.

3.5 CONCLUSIONS

The aim of this chapter was to explore the effect of stationary electric fields on a variety of mesenchymal tissues—hMSCs, bone, and nerves cells by seeding them on TCPS and three kinds of PVDF film surfaces: unpoled films with no surface charge, poled films with cells cultured on the positively charged side of the sample, and poled films with cells cultured on the negatively charged side of the sample. The same methods that were used in investigating the effect of oscillating electric fields on cells were employed to observe how a stationary electric field would affect cells differentiation and growth. The results showed a more homogeneous distribution of hMSCs and MC3T3-E1 cells seeded on (-) poled PVDF films but did not induce osteogenesis for any of the cell types. MTS assays of hMSCs and MC3T3-E1 cells indicated that the highest number of viable hMSCs were those that were seeded on (-) poled PVDF films while the highest number of viable MC3T3-E1 cells were obtained when seeding on (+) poled PVDF films. Neurite imaging verified that charged piezoelectric PVDF membranes induce neurite outgrowth more than electrically neutral membranes.

REFERENCES

1. Schneider GB, English A, Abraham M, Zaharias R, Stanford C, Keller J. The effect of hydrogel charge density on cell attachment. Biomaterials 2004; 25:3023–3028.
2. Lee YS, Collins G, Livingston Arinzeh T. Neurite extension of primary neurons on electrospun piezoelectric scaffolds. Acta Biomater 2011; 7:3877–3886.
3. https://en.wikipedia.org/wiki/Mesenchymal_stem_cell Access date: 3 April 2018
4. Ribeiro, C.; Sencadas, V.; Correia, D.M.; Lanceros-Méndez, S. Piezoelectric polymers as biomaterials for tissue engineering applications. Colloids Surf. B Biointerfaces **2015**, 136, 46–55.
5. H.-S. Huag, S.-H. Chou, T.-M. Don, W.-C. Lai and L.-P. Cheng, Polym. Adv. Technol., 2009, 20, 1082–1090.
6. I. F. Amaral, A. L. Cordeiro, P. Sampaio and M. A. Barbosa, J. Biomater. Sci., Polym. Ed., 2007, 18, 469–485.
7. G. B. Schneider, A. English, M. Abraham, R. Zaharias, C. Stanford and J. Keller, Biomaterials, 2004, 25, 3023–3028.
8. L. Ricotti, S. Taccola, I. Bernardeschi, V. Pensabene, P. Dario and A. Menciassi, Biomed. Mater., 2011, 6, 031001.
9. C. Ribeiro, S. Moreira, V. Correia, V. Sencadas, J. G. Rocha, F. M. Gama, J. L. Gomez Ribelles and S. Lanceros-Mendez, RSC Adv., 2012, 2, 11504–11509.
10. Baxter FR, Bowen CR, Turner IG, Dent ACE. Electrically active bioceramics: A review of interfacial responses. Ann Biomed Eng 2010; 38:2079–2092.
11. Ribeiro C, Panadero JA, Sencadas V, Lanceros-M_endez S, Tama~no MN, Moratal D, Salmer_on-S_anchez M, Ribelles JLG. Fibronectin adsorption and cell response on electroactive poly (vinylidene fluoride) films. Biomed Mater 2012; 7:035004.
12. Bacakova L, Filova E, Parizek M, Ruml T, Svorcik V. Modulation of cell adhesion, proliferation and differentiation on materials designed for body implants. Biotechnol Adv 2011; 29:739–767.
13. van Wachem PB, Beugeling T, Feijen J, Bantjes A, Detmers JP, van Aken WG. Interaction of cultured human endothelial cells with polymeric surfaces of different wettabilities. Biomaterials 1985; 6:403–408.
14. Lovinger A J 1982 *Developments in Crystalline Polymers* (London: Elsevier).
15. Jenita P€arssinen, Henrik Hammar_en, Rolle Rahikainen, Vitor Sencadas, Clarisse Ribeiro, Sari Vanhatupa, Susanna Miettinen, Senentxu Lanceros-M_endez, Vesa P. Hyt€onenEnhancement of adhesion and promotion of osteogenic differentiation of human adipose stem cells by poled electroactive poly (vinylidene fluoride), 2014.
16. Robert F. Valentini, Terrence G. Vargo, Joseph A. Gardella Jr.and Patrick Aebischer, Electrically charged polymeric substrates enhance nerve fibre outgrowth in vi&O,Bafullo NY, 1991
17. Valentini, R.F., Sabatini, A.M., Dario, P. and Aebischer, P., Polymer electret guidance channels enhance peripheral nerve regeneration in mice, Brain Res. 1989,480,300-304
18. Aebischer, P., Valentini, R.F., Dario, P., Domenici, C. and Galletti, P.G., Piezoelectric guidance channels enhance regeneration in the mouse sciatic nerve after axotomy, Brain Res. 1967, 438, 165-168.

CHAPTER 4: CORRELATING CELL RESPONSES TO THE ELECTROMECHANICAL RESPONSE OF POLY (VINYLIDENE FLUORIDE) FILMS SUBJECTED TO VIBRATION WHILE SUBMERGED IN FLUID

4.1 INTRODUCTION

Materials like metals, alloys and ceramics have been replaced by polymers in multiple applications, including aerospace and automotive industries, sensors, actuators, and tissue engineering. When compared to inorganic materials, polymers present attractive properties. They are light in weight, inexpensive, mechanically and electrically tough, and some are biodegradable and/or biocompatible [1, 2, 3]. There are benefits and drawbacks to both natural and synthetic polymers used for tissue engineering purposes. Natural polymers have ligands that promote cell attachment, viability, and in some cases, differentiation. They possess inherent microarchitectural cues reminiscent of the native tissues that cells originate from. Unfortunately, natural polymers often have batch-to-batch variability and can cause an immune response when implanted. Finally, natural polymers can be difficult to process and often possess poor mechanical and electrical properties [4]. Thus, a variety of synthetic polymers such as poly (glycolic acid) (PGA) [5,6], poly (lactic acid) (PLA) [7, 8], poly (lactic-co-glycolic acid) (PLGA) [9, 10], and poly (ethylene glycol) (PEG) [11, 12] have been extensively investigated as materials or scaffolds for tissue engineering [13]. It has been demonstrated that for certain cells and tissues, the behavior of electroactive materials can be exploited for scaffold development, resulting in scaffolds capable of providing stimuli necessary for specified tissue regeneration. This capability has stimulated a strong increase in the development of smart materials for tissue engineering

applications [14]. In a piezoelectric material, an electrical response due to a mechanical input or vice versa can be observed (Figure 4.1). The direct piezoelectric effect (dij) describes the conversion of mechanical energy into electrical energy whereas the inverse piezoelectric effect (eij) concerns the conversion of electrical energy into mechanical energy. In this type of smart material, a certain anisotropy in its structure is required. For synthetic polymers that are non-crystalline or semi-crystalline and are originally isotropic, they are typically subjected to a poling procedure (like corona poling) to meet this requirement [15].

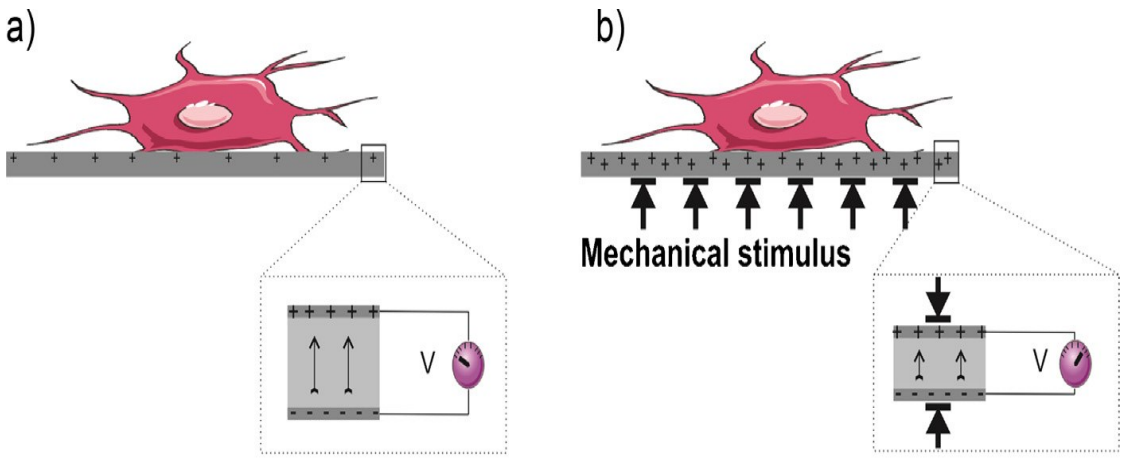

Figure 4.1: Schematic of the piezoelectric effect and a cell seeded on a piezoelectric film (the film is drawn in grey) (a) without and (b) with a mechanical stimulus which causes a variation of film electrical potential which influences the cell response as well [15].

Currently, PVDF is the most common piezoelectric polymer used to study the piezoelectric effect in tissue engineering applications, due to its sizeable piezoelectric response. It can be effectively used as a substrate for cell stimulation prior to the cells' implantation, due to both the polymer's large piezoelectric response and physicochemical stability. Because

it is a non-degradable material, PVDF can only be implanted in applications that do not require a degradable scaffold. Such applications may include the use of PVDF films as nerve guides.

Neurons were cultured directly on electrically charged PVDF membranes to investigate if local electrical charges enhance nerve fiber outgrowth in vitro [16, 17]. The investigators calculated that the poled PVDF membranes generated 2–3 mV when vibrated at 1200 Hz and it was concluded that an enhanced neural outgrowth process was induced by the piezoelectric output of the films, while the unpoled PVDF membranes showed no output.

In addition to neural cells, PVDF films have been used to study the effect of piezoelectricity on bone cells. Osteoblasts were seeded on PVDF films and examined under static and dynamic conditions. The dynamic culture was performed in a home-made bioreactor, where the mechanical stimulation was carried out by placing the culture plate on a vertical vibration module at a frequency of 1 Hz. This study showed that an oscillating electric field enhances osteoblast growth and proliferation. However, this study did not attempt to decouple the mechanical stimulation and response from the electrical stimulation and response, which is important since vibration alone is known to stimulate osteoblast activity [18]. Further, this study did not explore multiple frequencies, nor correlate the mechanical input to the electromechanical output. Low magnitude high frequency vibration has been demonstrated to positively affect cells, with differing responses at low (< 20 Hz), medium (40-60 Hz), and high (> 80 Hz) frequencies. Additionally, several studies that evaluated the cell response to vibrated PVDF films did not fix these films to the culture plates, nor

did the studies measure the motion of the films to determine whether the amplitude of the vibration input matched the actual vibration of the PVDF films.

In this chapter, these relationships are explored. In all experiments, PVDF films were fixed to the bottom of 6-well plates, seeded with cells, and submerged in cell media. Films were not allowed to freely float within the well plate in the media, as it was expected that the media would dampen the vibration imparted to the films. Attaching the film to the well ensured that the maximum vibratory input was translated to the PVDF film and minimized damping due to media. The actual displacement of the films under each loading condition was measured, as were the films' mechanical properties.

4.2 MATERIALS AND METHODS

4.2.1 Displacement and Acceleration

The displacement of the PVDF films was measured as a function of applied vibration using a laser interferometer (Keyence LK-G10). Films were prepared as previously described for cell culture, briefly, they were glued into 6-well plates and submerged in cell culture media. A stand was reconfigured for the interferometer such that it could be inserted below the well plates in the Bose Electroforce device (Figure 4.2). The laser light from the interferometer was directed upwards and focused on the edges of the film, away from the glue. The vibration frequencies (20, 60, and100 Hz) were selected to capture the low, medium, and high frequency ranges for reasons discussed in previous chapters. To ensure that all cells received an acceleration of 0.3g, peak-to-peak displacements of 0.37, 0.04, and 0.014 mm applied for the vibration frequencies of 20, 60, and 100Hz, respectively, according to the relation below:

$$a = \frac{D(2\pi f)^2}{g}$$

where a is acceleration, D is zero-to-peak displacement, f is vibration frequency, and g is the acceleration of gravity Measurements were obtained from media alone, from unpoled films submerged in media, and from poled films submerged in media. Measured displacement data from the interferometer was directly recorded on computer for comparison with applied displacement data. All data was normalized by subtracting a base measurement (vibration measurements with no well plates mounted) from the measurements taken with well plates mounted.

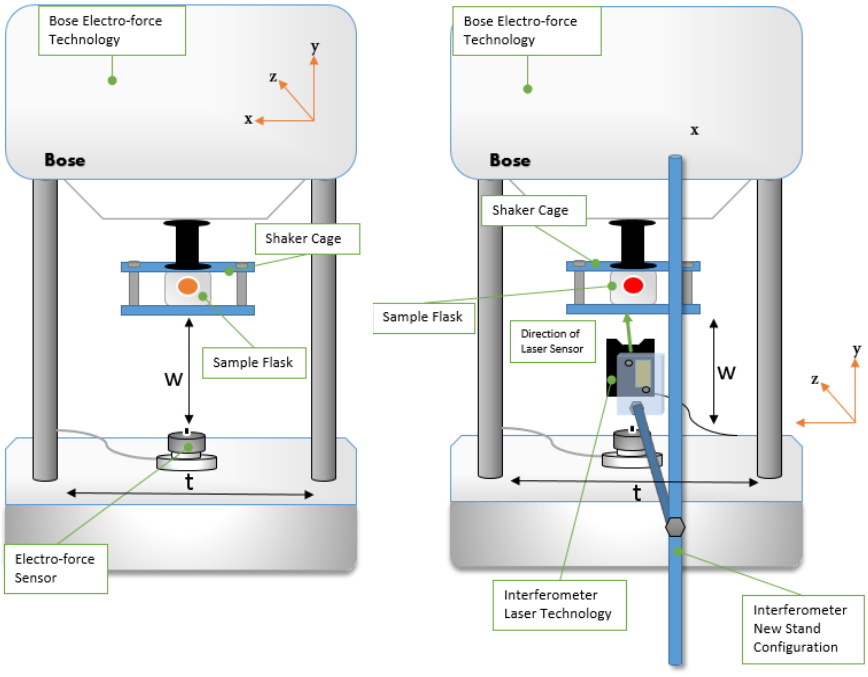

Figure 4.2: Experimental set-up. Left schematic shows the set-up for cell stimulation. Right schematic shows the set-up to measure PVDF film displacement with an interferometer. W is 11.5 cm and t is 20.5 cm.

4.2.2 PVDF Young's Modulus

The elastic moduli (E), also known as Young's moduli of poled and unpoled PVDF films scaffolds were determined by performing both tensile using a Bose Electroforce 3100 with a 1 Newton load cell (Figure 4.3). PVDF films were cut to (1x3) cm and were (0.03-0.05) mm in thickness. The force measurements obtained from the Bose Electroforce device were converted into stress using the cross-sectional area of the films. PVDF films were clamped at either end using the flat knurled face tension grips of the Bose Electroforce device. The films were tested in uniaxial strain applied at a rate of 6 mm/min. WinTest® 7 software was used for system control and force data acquisition. The data was collected and used to calculate the elastic modulus from the slope in the linear portion of the stress-strain curve.

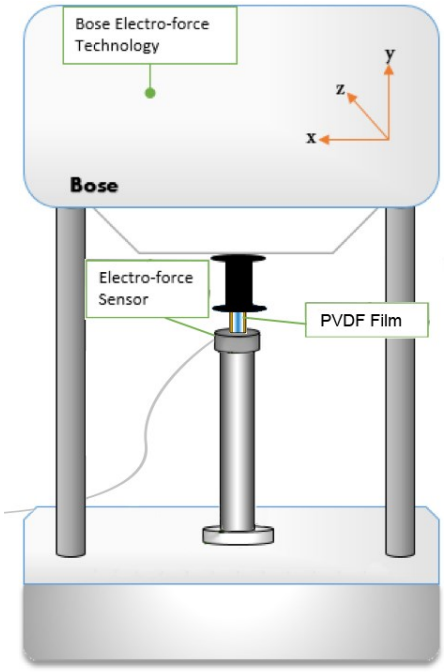

Figure 4.3: Bose Electroforce set-up for tensile testing.

4.3 RESULTS

4.3.1 Displacement and Acceleration

The recorded displacement data was processed and used to determine applied acceleration, and subsequently to approximate voltages delivered to the cells. All film displacements and accelerations were below the values delivered by the Bose Electroforce device (Figures 4.4- 4.6). Media displacements were also below, except for displacements occurring at 60 Hz. Unpoled PVDF films displaced more than poled PVDF films.

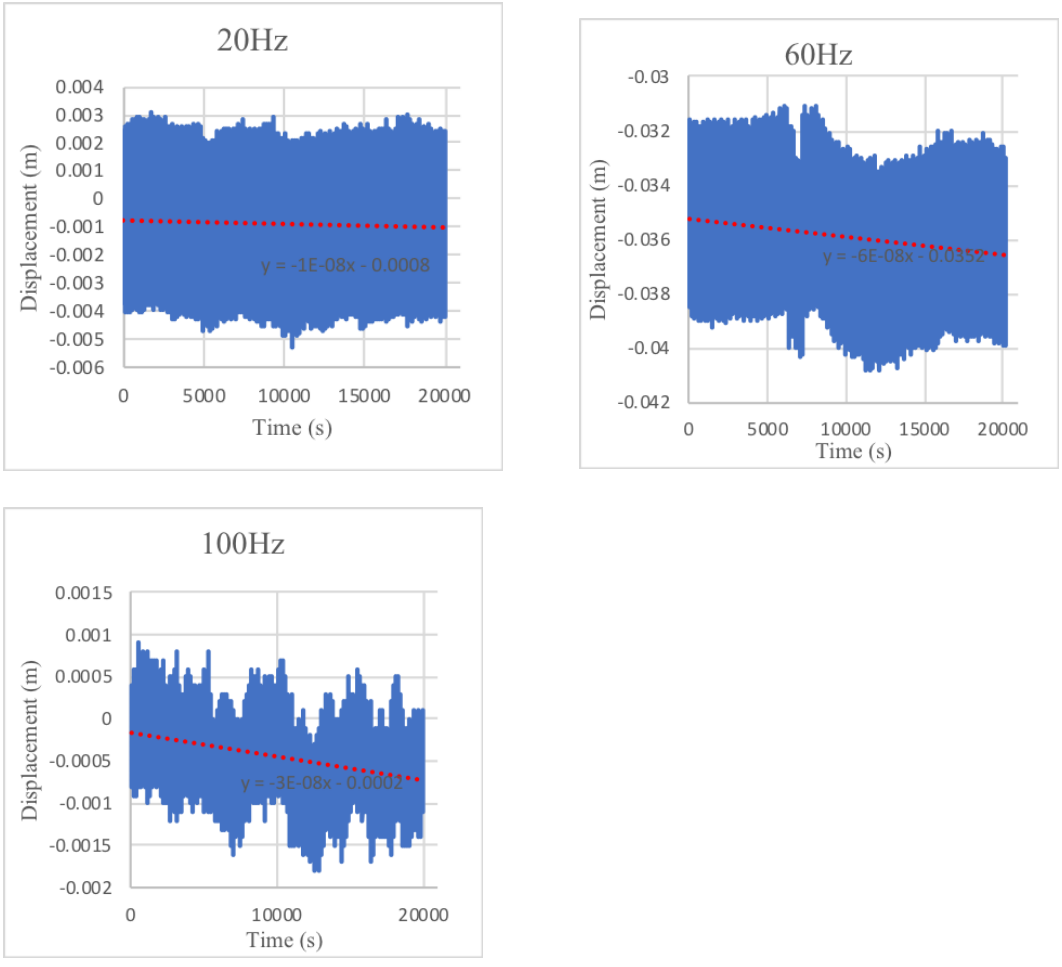

Figure 4.4: Representative measurements of the displacement of cell culture media while subjected to experimental vibrations.

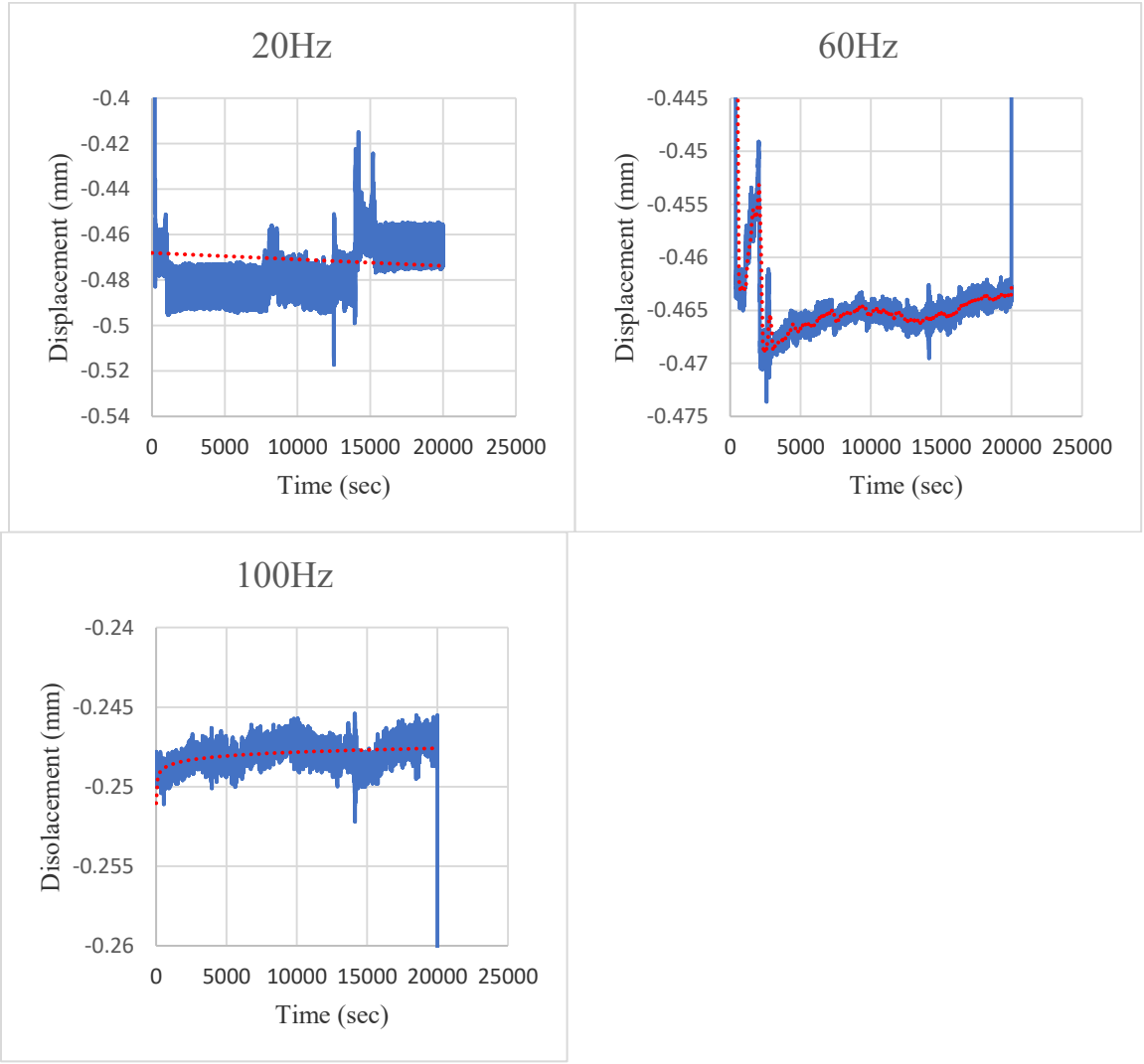

Figure 4.5: Representative measurements of the displacement of unpoled PVDF films submerged in cell culture media while subjected to experimental vibrations.

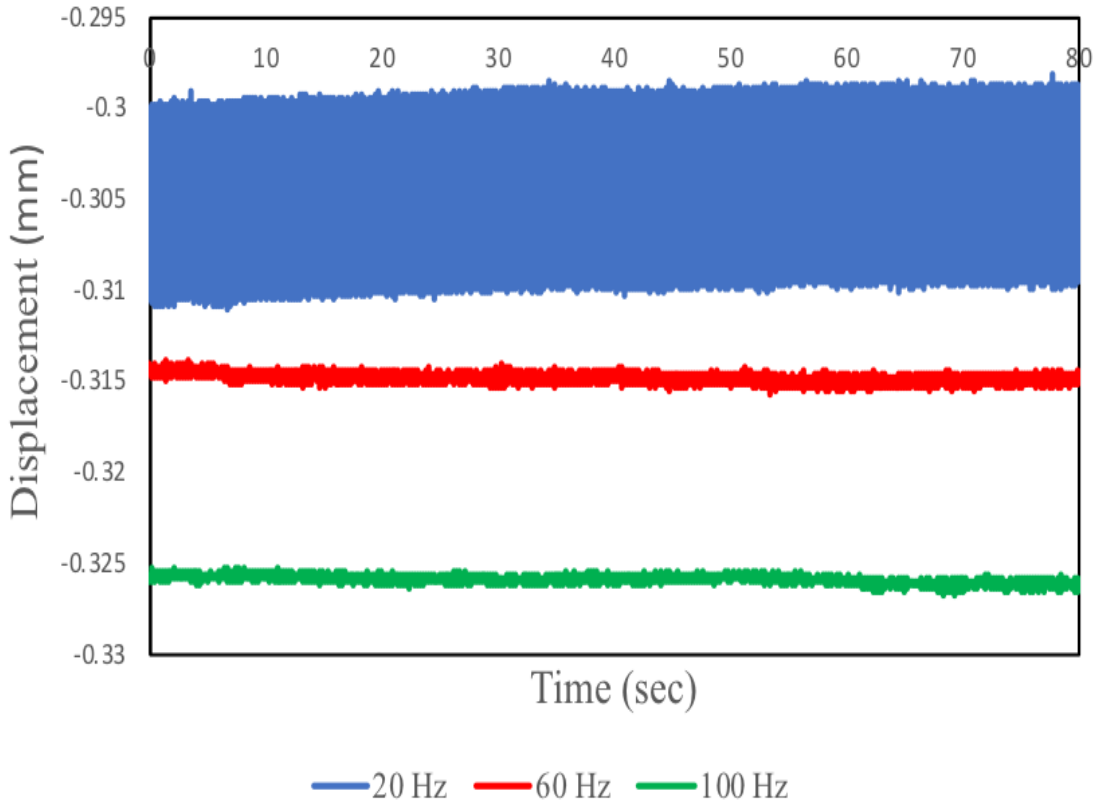

Figure 4.6: Representative measurements of the displacement of poled PVDF films submerged in cell culture media while subjected to experimental vibrations.

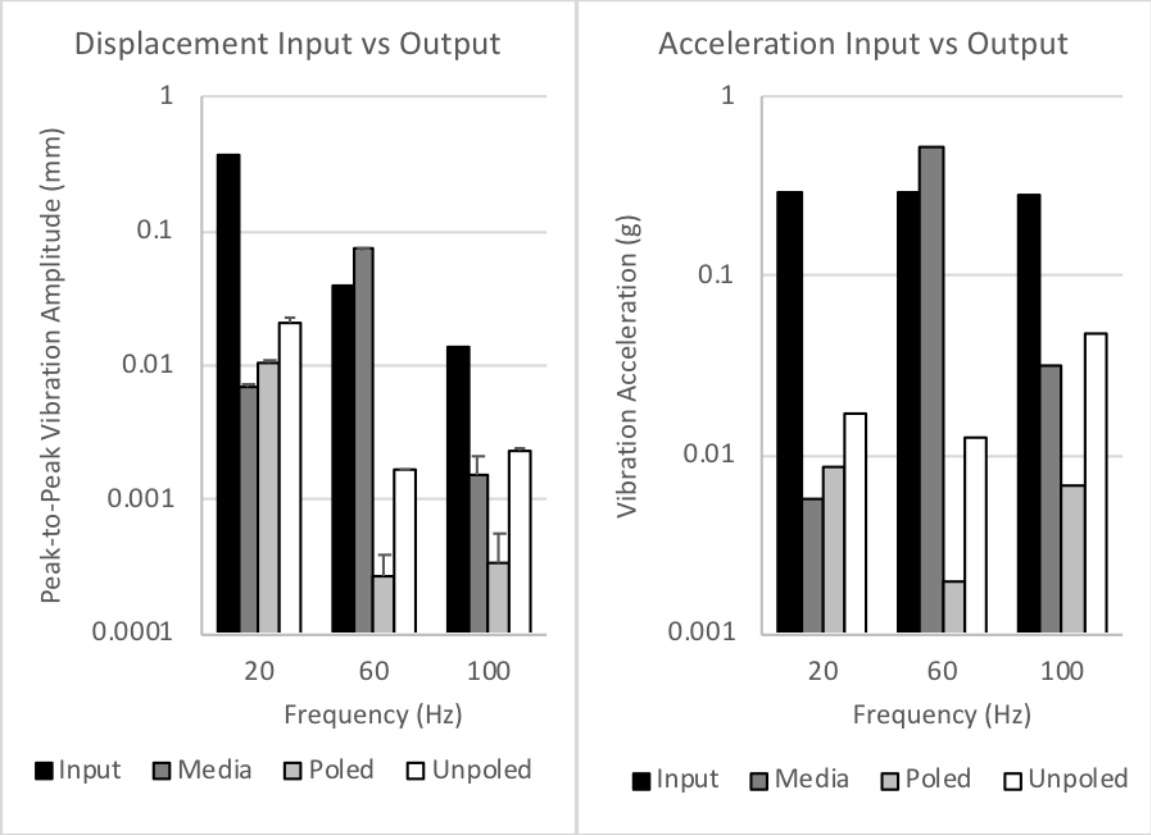

Figure 4.7: Semi-log graphs comparing the applied and actual displacements (left) and accelerations (right) received by the cell culture media and the PVDF films.

Song et al. determined the voltage output of various PVDF films using both measurements and simulations [19]. Their data was a good fit to their simulation, and by interpolating their linear equation:

$$\text{PVDF Voltage} = 3.0007a - 0.0201$$

where a is applied acceleration, it is possible to approximate the voltage delivered to cells (Table 4.1). Accelerations are reported in the table assuming the PVDF films are subjected to the accelerations imparted by the media, and assuming the PVDF films are only subjected to accelerations due to their own movement.

Table 4.1: Voltage delivered to cells based on actual accelerations.

Frequency (Hz)	Media (mV)	PVDF (mV)
20	0	5.6
60	1,587	0
100	75	0.05

4.3.2 PVDF Young's Modulus

The Young's moduli for poled PVDF films was higher than that of unpoled PVDF films (Figure 4.8). Stiffer poled PVDF films had moduli of 20 kPa while unpoled films had moduli of 70 kPa.

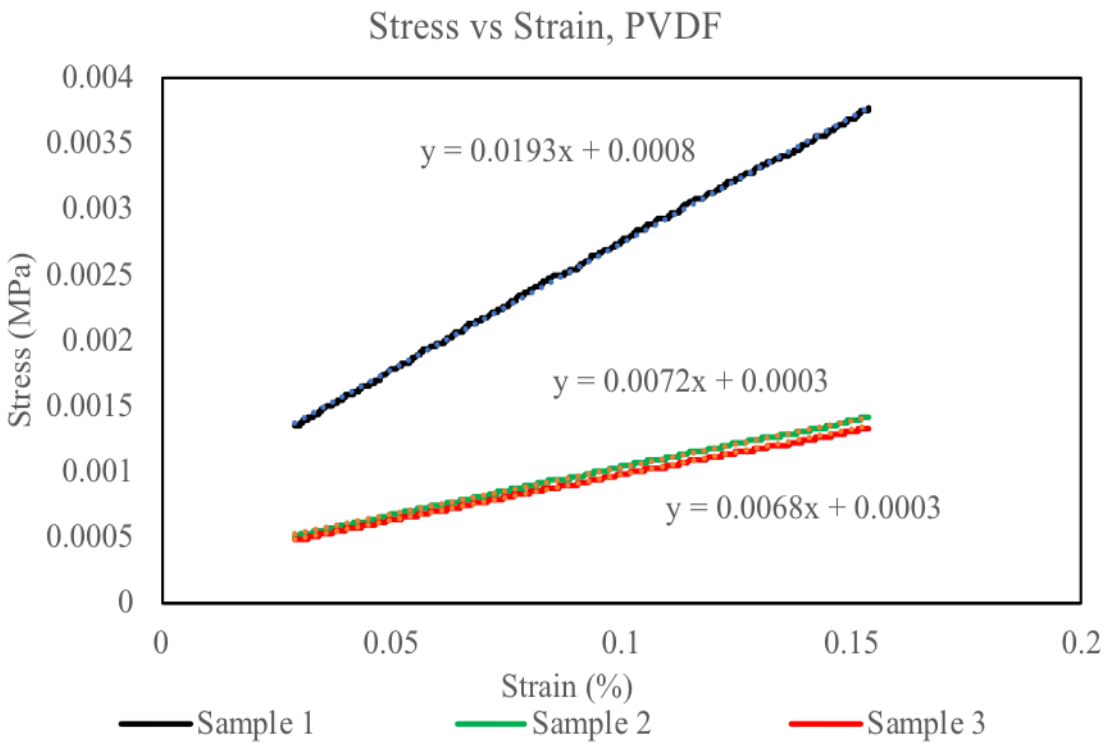

Figure 4.8: Stress strain curves of representative PVDF films. Samples 1 is poled, samples 2 and 3 are unpoled.

4.4 DISCUSSION

When vibrating the well culture plates that contained media with PVDF films at 20, 60, and 100 Hz, actual media displacements were 2%, 185%, and 11% of well displacements, respectively. The 185% increase in media displacement suggests that 60 Hz may have been at or near the natural frequency for the 2 mL of fluid in the 6-well plates. This may be changed by adding more or less media to alter the natural frequency, which is a function of weight and stiffness. The 20, 60, and 100 Hz vibrations resulted in actual film displacements of poled films by 3%, 1%, and 2% of well displacements and unpoled films by 6%, 4%, and 17%, respectively. This in turn resulted in accelerations that were reduced by the same amount since acceleration is directly related to zero-to-peak vibration distance. There were differences in displacements achieved by the unpoled compared to the poled PVDF. These can likely be explained by the difference in stiffness between the unpoled and poled PVDF. The stiffer poled PVDF displaced less, which is expected. Since the poling process involved stretching to align the semicrystalline molecules of the PVDF films, it follows that this would result in an elastically stiffer substrate. It also follows that given the same vibration input, these stiffer films would displace less.

Using the displacement values, it was possible to calculate theoretical voltages generated by the PVDF films (Table 4.1). Voltage values were calculated assuming that the acceleration of the media applied an oscillatory pressure to the PVDF films (Media column) and assuming that the movement of the films itself were the only mechanical input received by the films. Although these values are theoretical and should be measured to corroborate them, it is important to note that for 100 Hz the theoretical voltage calculated

was 75 mV. This value is close to the 70 mV depolarization threshold that excitable cells such as neurons and myofibers experience during action potentials [20]. Thus, it may explain the morphological change from mesenchymal stem cells to neural cells that was observed for cells stimulated at 100 Hz.

4.5 CONCLUSIONS

The main goal of this chapter was to characterize the environment that the cells experienced during the vibration experiments. The results point to an answer for some of the more surprising results, such as the morphological changes observed in 100 Hz stimulated mesenchymal stem cells. It may be that that there is an optimal range of electromechanical loading that permits precise control of cell fate. The successful vibratory measurements lead to important conclusions: the liquid media has a significant impact on the piezoelectric output of the PVDF, and by simply changing the amount of media in the experiments it may be possible to get vastly different results.

REFERENCES

1. H. Alexander, J.B. Brunski, S.L. Cooper, L.L. Hench, R.W. Hergenrother, A.S.Hoffman, J. Kohn, R. Langer, N.A. Peppas, B.D. Ratner, S.W. Shalaby, S.A.Visser, I.V. Yannas, Biomaterials Science, in: B.D. Ratner, A.S. Lemons (Eds.),Academic Press, San Diego, 1996, Chapter 1.2.
2. P. Fattahi, G. Yang, G. Kim, M.R. Abidian, Adv. Mater. 26 (2014) 1846–1885.
3. J. Jordan, K.I. Jacob, R. Tannenbaum, M.A. Sharaf, I. Jasiuk, Mater. Sci. Eng. A393 (2005).
4. H.S. Yoo, T.G. Kim, T.G. Park, Adv. Drug Deliv. Rev. 61 (2009) 1033–1042.
5. E.D. Boland, T.A. Telemeco, D.G. Simpson, G.E. Wnek, G.L. Bowlin, J. Biomed.Mater. Res. B 71 (2004) 144–152.
6. E.D. Boland, G.E. Wnek, D.G. Simpson, K.J. Pawlowski, G.L. Bowlin, J.Macromol. Sci. A: Pure Appl. Chem. 38A (2001) 1231–1243.
7. G. Khang, J.M. Rhee, P. Shin, Y.K. In, B. Lee, J.L. Sang, M.L. Young, B.L. Hai, I.Lee, Macromol. Res. 10 (2002) 158–167.
8. J. Yuan, J. Shen, I.K. Kang, Polym. Int. 57 (2008) 1188–1193.
9. S.W. Kang, W.G. La, B.S. Kim, J. Biomater. Sci. Polym. Ed. 20 (2009) 399–409.
10. H.J. Shao, C.S. Chen, I.C. Lee, J.H. Wang, T.H. Young, Artif. Organs 33 (2009)309–317.
11. J.A. Beamish, J. Zhu, K. Kottke-Marchant, R.E. Marchant, J. Biomed. Mater.Res. A 92 (2010) 441–450.
12. J. Zhu, Biomaterials 31 (2010) 4639–4656.
13. X. Liu, P. Ma, Ann. Biomed. Eng. 32 (2004) 477–486.
14. R. Ravichandran, S. Sundarrajan, J.R. Venugopal, S. Mukherjee, S.Ramakrishna, Macromol. Biosci. 12 (2012) 286–311.
15. T. Furukawa, IEEE Trans. Electr. Insul. 24 (1989) 375–394.
16. R.F. Valentini, T.G. Vargo, J.A. Gardella Jr., P. Aebischer, Biomaterials 13(1992) 183–190.
17. R.F. Valentini, T.G. Vargo, J.A. Gardella, P. Aebischer, J. Biomater. Sci. Polym.Ed. 5 (1994) 13–36.
18. C. Ribeiro, S. Moreira, V. Correia, V. Sencadas, J.G. Rocha, F.M. Gama, J.L.Gomez Ribelles, S. Lanceros-Mendez, RSC Adv. 2 (2012) 11504–11509.
19. Song, J., Zhao, G., Li, B. and Wang, J., 2017. Design optimization of PVDF-based piezoelectric energy harvesters. *Heliyon*, *3*(9), p.e 00377.
20. https://en.wikipedia.org/wiki/Threshold_potential Access date: 3 April 2018

CHAPTER 5: CONCLUSIONS AND FUTURE DIRECTIONS

This dissertation aimed to probe the response of a variety of mesenchymal tissues, namely, mesenchymal stem cells, osteoblasts, and neurons, to piezoelectric substrates. Though within the literature there are studies that evaluate the effect of frequency while stimulating cells with piezoelectric oscillating electric fields, the majority of these employ random vibration. The results presented here demonstrate that random vibration misses certain responses. The morphological change observed from mesenchymal stem cell to neural-type cell was not observed at any other frequency, and to date has not been reported in the literature. To better design tissue engineering constructs using electroactive materials, it is necessary to know the optimal stimulation parameters that will permit the control growth and differentiation for a variety of tissues. This study better defines some of these parameters and has already resulted in unexpected and new findings not yet reported in the literature.

5.1 KEY FINDINGS

5.1.1 The Effect of Oscillating Electric Fields on Cells

Poled and unpoled poly (vinylidene fluoride) (PVDF) membranes were seeded with MC3T3-E1 mouse pre-osteoblasts, hMSCs, and RN33B rat neurons, then vibrated at 20, 60, and 100 Hz. At weeks 1, 2, and 3, bone formation was assessed with alizarin red staining and cell proliferation was assessed with MTS assays. RN33B neurons were evaluated with neurite imaging one week after vibration. Alizarin red staining of hMSCs and MC3T3-E1 cells indicated significant increases in osteogenic activity for both cell types when subjected to oscillating electric fields due to piezoelectricity. For MC3T3-E1s,

vibration alone was an osteogenic input. MTS assays of hMSCs and MC3T3-E1 cells showed that the proliferation of both cell types was enhanced due to the piezoelectric effect of poled PVDF films but was reduced when vibrated on tissue culture plastic or unpoled PVDF films. For 100 Hz vibrations, hMSC morphology changed to neural-like cells. Neurite imaging of undifferentiated and differentiated RN33B cells illustrated increases in neurite growth due to both mechanical and electrical stimulation.

5.1.2 The Effect of Stationary Electric Fields on Cells

The same methods that were used in investigating the effect of oscillating electric fields on cells were employed to observe how the stationary electric field affects cells differentiation and growth and at the same time points. As described above, MC3T3-E1, hMSCs, and RN33B cells were seeded on TCPS and three kinds of PVDF film surfaces: unpoled films with no surface charge, poled films with cells cultured on the positively charged side of the sample, and poled films with cells cultured on the negatively charged side of the sample. Alizarin red staining of hMSCs and MC3T3-E1 cells showed that stationary electric fields resulted in more homogeneous distributions of hMSCs and MC3T3-E1 cells when these cells were seeded on (-) poled PVDF films but did the negative surfaces did not induce osteogenesis. MTS assays of hMSCs and MC3T3-E1 cells indicated that the highest number of viable hMSCs cells were achieved when cells were cultured on (-) poled PVDF films while the highest number of viable MC3T3-E1 cells occurred on (+) poled PVDF films. Interestingly, (+) poled PVDF films were able to initiate osteogenesis in hMSCs, but the result was inconsistent. The neurite imaging study verified that stationary poled piezoelectric PVDF membranes did not induce neurite outgrowth.

5.1.3 Characterizing the Electromechanical Response

There are many different options for the integration of PVDF films into the cell culture environment. For this application, cells were cultured within a six well culture plate. The cells were introduced via a liquid media and actuated with a steady vibratory load. PVDF as a piezoelectric material, can utilize physical actuation to induce a voltage. It is the combination of this actuation and electronic stimuli that has been implicated in directing cell fate. In order to understand how the PVDF responds to the actuation, the movement of the cell media and the PVDF films were measured. The PVDF films were fixed to the well plate to prevent them from freely floating within the media, which may have dissipated the vibration imparted to the films. This vibratory study of displacement illustrated that cell media has a significant impact on the piezoelectric output of the PVDF. Further, theoretical calculations from this study suggests that the voltage delivered by the PVDF films may be very close to physiologic ranges of the depolarization excitable cells undergo during action potentials. This may explain the change in morphology of the MSCs to neuronal.

5.2 FUTURE DIRECTIONS

5.2.1 Establishing that Piezoelectric Stimulation Can Drive MSC Morphology towards Neurons

Poled PVDF membranes will be seeded with human mesenchymal stem cells hMSCs and vibrated at a 100 Hz for 24 hours. After 1, 3, 5, 7, and 14 days, cultures will be immunolabelled for an MSCs marker (DJ 3) [1], a neural stem cell marker (nestin), and a neuron marker (NeuN, tau, neurofilaments). Parallel cultures of human neural cells and human neural stem cells as positive and negative controls for the staining will be

maintained. If the hMSCs are indeed differentiating into neurons, it is likely they will first differentiate into neural stem cells. These NSCs may differentiate into neurons or other neural cells (astrocytes or oligodendrocytes). If the staining is negative for all of these, that would indicate that the hMSCs turned into something else, and the direction of investigation will depend on the results.

5.2.2 Examine the Effect of Oscillating Electric Fields on Non-Vibrated Cells

Cells will be stimulated with DC and AC electrical stimulation via electrodes directly inserted into the media. Although the films will not be vibrated with the Electroforce, it is expected that the cultured cells on the piezoelectric films will experience vibration and strain due to the inverse piezoelectric effect. However, since they will not experience the combined vibration of the weight of the media, a different result is expected. It is expected that neurites will grow towards the cathodes and away from the anodes. It is also expected that increased osteogenic and myogenic differentiation will be observed, as well as alignment with the electrical field.

5.2.3 Measure the Electric Field Delivered by PVDF Films

To confirm whether the theoretical values determined by the vibration at 100 Hz are correct, it is necessary to directly measure the voltages generated by the vibrating PVDF films. This will be achieved by mounting PVDF films in 6-well plates and submerging them as before. Then, leads will be attached to PVDF films to measure voltages. The leads will be attached at three locations on the PVDF film; the center location where the film is glued, near the periphery of the glue, and at the edge of the PVDF film where there is no

glue. Three data sets will be recorded for each loading configuration to establish reproducibility.

5.2.4 *In Vivo* Model Development

There are studies that show that by crossing a spinal lesion with an oscillating current using percutaneous leads, voluntary motion can be re-established [2]. With PVDF, there is no need for percutaneous leads and a vibration input can be applied on the outside of the skin. Thus, it may be possible to use PVDF both as a nerve guide and as a functional scaffold that returns function during vibration. This can be first explored using a peripheral denervation model, where the peroneal nerve is transected. PVDF films seeded with MSCs or neural stem cells and primed 24 hours at 100 Hz would then be rolled and placed over either end of the nerve transection. This would be performed in a mouse or rat model, and the animal monitored for functional return. After the study's end, animals would be sacrificed for histology. Two groups would be followed – in one group, the animals would receive no further stimulation. In the stimulation group, animals would be fitted with a portable vibration device that would deliver a set amount of daily vibration. Otherwise, animals would be retrieved to have vibration applied. Results from this study would be used to direct the experimental design for a spinal transection study.

5.3 SUMMARY

The work in this dissertation revealed that PVDF membranes stimulated mesenchymal stem cells, osteoblasts, and neurons towards differentiation especially under dynamic conditions. Piezoelectric PVDF membranes that are dynamically stimulated induce MSC and osteoblast proliferation and differentiation towards osteogenic lineages, as well as induce neurite growth in neurons. The morphological changes observed from mesenchymal stem cell to neural-type cells at 100 Hz was not observed at any other frequency, and to date has not been reported in the literature. The analysis of actual displacement illustrated that cell media has a significant impact on the piezoelectric output of the PVDF. In addition, theoretical calculations from this study suggests that the voltage delivered by the PVDF films may be very close to physiologic range of the depolarization excitable cells undergo during action potentials, which may explain the morphological changes of the MSCs towards a neuronal appearance. Piezoelectric PVDF membranes hold promise for applications in bone and neural tissue engineering and offer a novel finding in MSCs differentiation studies.

REFERENCES

1. https://www.ncbi.nlm.nih.gov/pmc/articles/PMC3887673/ Access date: 3 April 2018
2. Harkema, Susan, Yury Gerasimenko, Jonathan Hodes, Joel Burdick, Claudia Angeli, Yangsheng Chen, Christie Ferreira et al. "Effect of epidural stimulation of the lumbosacral spinal cord on voluntary movement, standing, and assisted stepping after motor complete paraplegia: a case study." *The Lancet*377, no. 9781 (2011): 1938-1947.